HOKKAIDO UNIVERSITY

Title	Studies on physiological functions and regulatory mechanisms of a newly identified murine testis-specific long noncoding RNA, Start
Author(s)	大塚, 海
Degree Grantor	北海道大学
Degree Name	博士(生命科学)
Dissertation Number	甲第14608号
Issue Date	2021-06-30
DOI	https://doi.org/10.14943/doctoral.k14608
Doc URL	https://hdl.handle.net/2115/96815
Type	doctoral thesis
File Information	Kai_Otsuka.pdf

Hokkaido University Collection of Scholarly and Academic Papers : HUSCAP

Doctoral Dissertation

Studies on physiological functions and regulatory mechanisms of a newly identified murine testis-specific long noncoding RNA, *Start*

新規同定されたマウス精巣特異的な長鎖非コード RNA「*Start*」の

生理機能ならびに分子基盤解析

Kai OTSUKA

Graduate School of Life Science, Hokkaido University

2021. 06

CONTENTS

Abbreviations.....**1**

General Abstract **3**

General Introduction **5**

Chapter1 .....**9**

Chapter2 .....**46**

Chapter3 .....**68**

General Discussion.....**85**

Acknowledgements.....**90**

References **91**

Abbreviations

Ar, androgen receptor

BrU, 5-Bromo-2′-Uridine

ceRNA, competing endogenous RNA

CRISPR/Cas9, clustered regularly interspaced short palindromic repeat/ Cas9

DIG, digoxigenin

dpp, days postpartum

Dox, Doxycycline

ELISA, enzyme-linked immunosorbent assay

eRNA, enhancer-RNA / enhancer-derived RNA

FSH, follicle-stimulating hormone

GnRH, gonadotropin-releasing hormone

GSP, gene-specific primer

HPG_axis, hypothalamus–pituitary–gonadal axis

H3K27ac, H3 lysine 27 acetylation

H3K4me1, H3 lysine 4 mono-methylation

KD, knockdown

KO, knockout

LH, luteinizing hormone

lncRNA, long noncoding RNA

miRNA, microRNA

nt, nucleotide(s)

OE, Overexpression

qRT-PCR, quantitative reverse transcription-polymerase chain reaction

RACE, rapid amplification of cDNA ends

RNA-seq, RNA-sequencing

RPKM, reads per kilo-base of exon per million-mapped reads

RT-PCR, reverse transcription-polymerase chain reaction

S.D., standard deviation

shRNA, short-hairpin RNA

TK, thymidine kinase

General Abstract

Long noncoding RNAs (lncRNAs) are a class of noncoding RNAs that are composed of more than 200 nucleotides (nt). The testis carries a number of lncRNAs that are assumed to be indispensable for male reproduction, but their functions are poorly understood. Here, I reported the presence of a newly identified testis-specific RNA, Steroidogenesis activating lncRNA in testis (*Start*), and showed evidence which provided the physiological significance and molecular mechanism. *Start* was found in both nuclei and the cytosol in germlines and Leydig cells, but there was no expression in Sertoli cells. Based on RNA-sequencing (RNA-seq) and quantitative reverse transcription-polymerase chain reaction (qRT-PCR) results in *Start*-knockout (KO) mice and qRT-PCR in Leydig cell lines overexpressing *Start*, I concluded that *Start* regulated a subset of steroidogenic genes in Leydig cells. Indeed, serum testosterone was significantly reduced in *Start*-KO male. Intriguingly, by *in vitro* studies, I found that both cytosolic *Start* and its target genes could be targeted by the microRNA (miRNA) pathway in a Leydig cell line. This result led me to conclude that *Start* regulates steroidogenesis via the miRNA pathway. In addition, I also noticed that expression of two Protease, Serine (*Prss*)/ Testis specific serine protease (*Tessp*) genes in the testis was decreased by *Start*-KO. Consistently, reporter assays revealed that a 5.4-kb genome sequence encompassing *Start* could act as an enhancer for the two *Prss/Tessp* genes, and demonstrated that the transcriptional level of *Start* was positively correlated with the enhancer activity. Collectively, I concluded that *Start* is a multi-functional testis-specific lncRNA, which regulates steroidogenesis in the cytosol of Leydig cells via the miRNA pathway, and also activates transcription of adjacent *Prss/Tessp* genes in germ cell nuclei via its enhancer function.

General Introduction

The testis consists of germ cells and somatic cells including Sertoli cells and Leydig cells, and play extremely important roles in the male reproductive system for spermatogenesis and steroid synthesis. Spermatogenesis takes places in seminiferous tubules with a nutritious support of nursing Sertoli cells and generates haploid spermatozoa from diploid spermatogonia [1-5]. On the other hand, steroidogenesis is mainly driven by Leydig cells that reside outside of seminiferous tubules. Leydig cells mainly release testosterone as a final steroid product, and the secreted testosterone is received by the hypothalamus and pituitary [6-11]. The pituitary governs secretion of luteinizing hormone (LH) depending on the amount of testosterone secretion and eventually controls testosterone production in Leydig cells, forming a feedback system termed as the hypothalamus-pituitary-gonadal axis (HPG_axis). Once steroidogenesis in Leydig cells is disturbed, diagnostic defects appear in male reproductive context [12,13]. Thus, these two distinct functions, namely spermatogenesis and steroidogenesis, must be orchestrated precisely to guarantee quality of male reproductive trails throughout lifespan; however, regulatory mechanisms lying on those two functions are still not well uncovered.

lncRNAs are a class of noncoding RNAs which are longer than 200 nt in length. They act as gene regulators at various levels including transcription, post-transcription and translation, without being translated [14-18]. A number of studies have reported that lncRNAs play roles in lots of biological process *in vivo*, although their physiological functions in male reproduction still remain elusive. According to an increasing number of transcriptomic analyses, the testis expresses many more lncRNAs than any other tissues, suggesting their significance in testis-specific functions [19,20]. For a last decade, several studies have attempted to reveal their contribution to spermatogenesis, but only few of them could partially describe their significance [20-23]. In terms of functions of lncRNAs in steroidogenesis, much less studies have been published [24,25]. Moreover, they mainly focused only on a profiling of lncRNAs that are available in Leydig cells, not on the physiological function of each transcript. Therefore, functional investigation for each testis lncRNA in steroidogenesis along with spermatogenesis is strongly desired to describe the mechanism underlying the male reproductive

system in-depth. To reveal functions of testis lncRNAs, our group has attempted and successfully identified several novel transcripts in mouse [23,26-28]. Intriguingly, two of these noncoding transcripts were found to be transcribed at the gene cluster which is specifically activated in the testis.

The mouse *Prss/Tessp* gene locus is located at 110,795-110,870 kb of mouse chromosome 9. This locus consists of six serine-protease genes that are specifically or dominantly expressed in the testis [29-31]. Of six, *Prss42/Tessp-2* and *Prss43/Tessp-3* are known to be essential for complete progression of meiosis, implying the significance of this locus in male reproduction. In addition, our previous studies identified two lncRNAs, *lncRNA-HSVIII* and *Tesra*, at intergenic regions between *Prss42/Tessp-2* and *Prss44/Tessp-4,* and *Prss44/Tessp-4* and *Prss43/Tessp-3*, respectively [27,28]. Both an enhancer flanking to *lncRNA-HSVIII* and the *Tesra* transcript are involved in *Prss42/Tessp-2* transcriptional activation synergistically in spermatocytes, suggesting the importance of these intergenic elements/factors for accurate control of protein-coding genes at the locus. However, how this locus is adequately regulated during spermatogenesis was not fully uncovered.

In chapter 1, I found the expression of a newly identified lncRNA, *Start*, which was transcribed at the intergenic region between *Prss43/Tessp-3* and *Prss45,* and the physiological significance in the murine testis. *Start* was found only in the testis, especially in germ cells and Leydig cells, and was localized both in nuclei and the cytosol. By utilizing strong advantages of KO mice and RNA-seq analyses, we identified a subset of steroidogenic genes as candidates that were regulated by *Start* in Leydig cells. Consistently, the serum testosterone level was low in KO mice, and those steroidogenic genes were responsive to *Start* overexpression (OE) in two Leydig cell lines. Thus, I concluded they were truly regulated by this lncRNA.

In chapter 2, I attempted to reveal a molecular basis of *Start* function in Leydig cells. Intriguingly, reporter gene assay revealed that knockdown (KD) of the argonaute RISC catalytic subunit 2 (*Ago2*), a major endonuclease involved in the microRNA (miRNA) pathway, rescued reporter activity decreased by including the *Start* sequence, suggesting its involvement in the miRNA pathway. Subsequently, both *Start* and its target steroidogenic genes showed negative correlation in

their expression with proteins involved in miRNA biogenesis such as *Ago2* [32-35]. Moreover, significant reduction in expression of steroidogenic genes by *Ago2* OE was recovered by *Start* OE. Collectively, *Start* and its target genes were found to be downregulated by the miRNA pathway for precise control of steroidogenesis in Leydig cells.

In chapter 3, I focused on *Start* function in germ cell nuclei, and found that expression of two *Prss/Tessp* genes was dramatically decreased in *Start*-KO testes compared to wild type males, implying *Start* function in a *cis*-regulatory mechanism. Further *in vitro* analyses revealed that a 5.4-kb genome sequence encompassing *Start* could act as an enhancer for those *Prss/Tessp* genes and the enhancer activity was positively correlated with transcriptional activity of *Start*. Collectively, the current study is the first report of a multi-functional testis-specific lncRNA which acts in both spermatogenesis and steroidogenesis, and provides its molecular basis to control such testis-specific functions precisely.

Chapter 1

A testis-specific long noncoding RNA, *Start*, is a regulator of steroidogenesis in mouse Leydig cells

Abstract

Many lncRNAs, are expressed in the testis, but their functions and overview are not well understood. The mouse *Prss/Tessp* locus contains six serine protease genes and two lncRNAs that have been suggested to play important roles in spermatogenesis. Here, I found a novel testis-specific lncRNA, *Start*, in this locus. *Start* is 1,822 nt in length and was found in both nuclei and cytosol in germ cells and Leydig cells, but there was no expression in Sertoli cells. *Start*-KO mice generated by the clustered regularly interspaced short palindromic repeat/ Cas9 (CRISPR/Cas9) system were fertile and showed no morphological abnormality in adults. However, in adult *Start*-KO testes, abnormal expression of steroidogenic genes, was revealed by RNA-seq and qRT-PCR and significant low level of the serum testosterone was shown by enzyme-linked immunosorbent assay (ELISA) analysis. This low testosterone level in adult *Start*-KO mice was thought to be compensated by enhancement of androgen receptor (Ar) expression in the pituitary and apparently normal luteinizing hormone (LH) secretion. Interestingly, at 8 days postpartum (dpp), relatively early postnatal stage, both steroidogenic gene expression and testosterone level were decreased in *Start*-KO mice, and a reduced number of Leydig cells was observed. Since OE of *Start* in two Leydig-derived cell lines resulted in elevation of the expression of steroidogenic genes, *Start* is likely to be involved in their upregulation. Collectively, my results strongly suggest that *Start* is a regulator of steroidogenesis in Leydig cells. The current study provides an insight into the overall picture of the function of testis lncRNAs.

Introduction

Testis has two main functions: spermatogenesis and androgen production. Spermatogenesis is regulated within the seminiferous tubules that contain germ cells and Sertoli cells and consists of three steps: mitosis, meiosis and spermiogenesis [1,2]. Some of the mitotically proliferating spermatogonia

enter meiosis to differentiate into haploid spermatids via primary and secondary spermatocytes, and mature spermatozoa are formed by spermiogenesis. During these processes, Sertoli cells nurse germ cells to support sperm development by releasing glial cell line-derived neurotrophic factor signaling molecules, retinoic acid, and growth factors [3-5]. Leydig cells, another type of somatic cells, reside in the interstitial regions among the seminiferous tubules and produce androgens such as testosterone [6-8]. Testosterone is a major androgen produced in the steroidogenesis pathway in Leydig cells and plays a critical role in spermatogenesis by targeting Sertoli cells [36,37]. Dysfunction of Leydig cells frequently leads to disruption of spermatogenesis due to insufficient serum testosterone [12,13].

In mammals, androgen production is precisely controlled by the HPG_axis [9-11]. The hypothalamus secretes gonadotropin-releasing hormone (GnRH) and induces the secretion of LH and follicle-stimulating hormone (FSH) from the pituitary to Leydig and Sertoli cells in the testis. Testosterone is produced and secreted in response to LH in Leydig cells for spermatogenesis and simultaneously suppresses the production and secretion of GnRH and gonadotropins in the hypothalamus and pituitary, respectively, by a negative feedback loop [10,11,38]. Moreover, steroidogenesis is known to be controlled by autocrine and paracrine factors within the testis [39,40]. While the hormonal endocrine system that is responsible for steroidogenesis in the HPG_axis has been relatively well characterized [41,42], the molecular mechanism underlying the precise control of spermatogenetic genes is unclear. The findings in previous studies suggest some pivotal roles of a novel regulator in spermatogenesis and androgen production in the testis.

Recent high-throughput studies have revealed that the testis expresses much more lncRNAs than those expressed in other tissues [19,43]. lncRNAs are noncoding RNAs that are comprised of more than 200 nt and they exhibit a wide variety of non-translational functions including gene regulation [14-18]. During meiosis, many lncRNAs are differentially transcribed [44,45], and the functions of several lncRNAs in the testis have been revealed. For instance, testis lncRNAs have been shown to function in meiotic entry in spermatogonia, activation of immune-related genes in primary spermatocytes, and regulation of postmeiotic genes [20-23]. Moreover, some studies have suggested a

function of lncRNAs in testicular somatic cells [24,26,46,47].

Our group previously identified two testis-specific lncRNAs at the *Prss/Tessp* locus located at 110,795-110,870 kb of mouse chromosome 9 [27,28]. This locus contains six *Prss* genes that are specifically or predominantly expressed in the testis and encode serine proteases (Fig. 1-1) [29-31]. Among the protein-coding genes, it has been suggested that *Prss42/Tessp-2* and *Prss43/Tessp-3* are essential for the progression of spermatogenesis and that the noncoding regions are involved in transcriptional regulation of the *Prss42/Tessp-2* gene [27,28]. Those studies indicate that there are diverse molecular species and functions of lncRNAs in the testis. However, very little evidence for *in vivo* functions of lncRNAs in spermatogenesis and steroidogenesis has been provided.

In this study, I identified a novel lncRNA, *Start*, transcribed at the *Prss/Tessp* locus. *Start* was found to be transcribed downstream of the *Prss43/Tessp-3* gene (Fig. 1-1) exclusively in the testis, especially in germline and Leydig cells. Using *Start*-deficient mice and cultured Leydig cell lines, *Start* was found to be a regulator of steroidogenesis in the testis. This is the first identification of an lncRNA finetuning the steroidogenic pathway in the testis.

Materials and Methods

Animals

The experimental procedures used in this study were approved by the Institutional Animal Use and Care Committee at Hokkaido University and by the Animal Care and Use Committee of the National Research Institute for Child Health and Development. C57BL/6Ncl mice (CLEA Japan Inc., Tokyo, Japan) and *Start*-KO mice (ICR and mixed background of C57BL/6 and DBA2, Sankyo Labo Service Corporation) were maintained on 14 hr light/10 hr dark cycles at 25℃ and given food and water ad libitum. In the analysis of *Start*-KO mice, we used male mice at 64-83 dpp as 2.5-month-old adult mice.

Reverse transcription-polymerase chain reaction (RT-PCR) analysis

Total RNAs were extracted by ISOGEN and ISOGEN II (Nippon Gene, Tokyo, Japan) for tissues and cultured cells, respectively, according to the manufacturer's instructions. After treatment with TurboDNase (Thermo Fisher Scientific, Rockford, IL, USA), the RNAs were reverse-transcribed into cDNAs with the oligo(dT) primer or random hexamer using Superscript III (Invitrogen, Carlsbad, CA, USA), according to the manufacturer's instructions. A random hexamer was used for RT-PCR to check tissue distribution (Fig. 1-3A), and oligo(dT) was used for other experiments. PCR was performed using ExTaq polymerase (Takara, Otsu, Japan) or KOD Fx Neo (Toyobo, Tokyo, Japan). For strand-specific RT, "*Start* full length" reverse and "*Start* full length" forward primers were used to synthesize *Start* sense and antisense cDNAs, respectively, and a reaction temperature of 55°C was used to avoid non-specific binding of primers. Primer sequences are shown in Table 1-1.

Rapid amplification of cDNA ends (RACE) analyses

For 5'RACE, cDNA was generated using a gene-specific primer 1 (GSP1) and total RNAs from mouse male germ cells. After purification of cDNA with a QIAquick PCR Purification Kit (Qiagen, Hilden, Germany), oligodeoxycytidine was added by terminal deoxynucleotidyl transferase (Takara). The first-round PCR was performed with an abridged anchor primer (AAP) and GSP2. For the second nested amplification, GSP3 and an abridged universal amplification primer (AUAP) were used.

For 3'RACE, cDNA was prepared by reverse transcription with oligo(dT) connected to an adaptor sequence (AP). The first-round PCR was conducted by using primers, AP and GSP4. The second nested amplification was carried out with the same adaptor primer and GSP5.

All of the PCR products were subcloned into the *Eco*RV site of a pBluescript II KS(+) vector (Stratagene La Jolla, CA, USA), which carries T nt at the end, by the TA-cloning method, and 10 subclones for each sample were sequenced. All of the primer sequences are listed in Table 1-1.

qRT-PCR

cDNAs were synthesized as described above using the oligo(dT) primer. PCR was performed by using SYBR Green PCR Master Mix for protein-coding genes (Thermo Fisher Scientific) and KOD SYBR qPCR Mix for *Start* (Toyobo). In both cases, the 7300 real-time PCR system (Applied Biosystems, Foster City, CA, USA) was used as previously described [48]. The relative expression levels were normalized to endogenous *Gapdh* or *Aip* mRNA. Primer sequences are shown in Table 1-1.

Preparation of germ cell, Sertoli cell, and Sertoli/Leydig cell fractions

Native germ cells were isolated from two adult mouse testes, and their purity was checked by marker gene expression as previously described [29,48]. Sertoli cells were obtained from 11-day-old testes for primary culture as previously described [26,49]. The Sertoli/Leydig cell fraction was obtained from 6-month-old testes by using a discontinuous Percoll gradient (20%, 37%, and 53%) as previously described [27].

Cytosolic and nuclear extraction from germ cells

Subcellular fractions were obtained by using NP-40 lysis buffer (10 mM Tris HCl [pH 7.5], 10 mM NaCl, 3 mM $MgCl_2$, 0.5% NP 40) containing 1× proteinase inhibitor cocktail (Roche Molecular Biochemicals, Mannheim, Germany) as previously described [27,50]. The nuclear fraction was collected as a pellet after centrifugation, and the supernatant was used as the cytosolic fraction.

***In situ* hybridization**

The RNA probes to detect *Start* were prepared as follows. The full length of *Start* was amplified by RT-PCR with mouse testis cDNA and a primer pair of *Start* full length (Table 1-1) using KOD Fx Neo and was subcloned into the *Eco*RV site of a pBluescript II KS+ vector (pBlue-Start). After the sequence had been confirmed, the full length was cut out by *Eco*RI and *Hin*dIII digestion, blunted by

T4 DNA polymerase (Takara), and inserted into the blunted *Pst*I site of a pGEM-3Zf(+) vector. The resulting plasmid was linearized with *Apa*I and *Not*I digestion for synthesizing sense and antisense RNA probes, respectively. Digoxigenin (DIG)-labeled RNA probes were synthesized using a DIG RNA labeling kit (Roche Molecular Biochemicals) with SP6 RNA polymerase for a sense probe and T7 RNA polymerase for an antisense probe.

In situ hybridization with the Tyramide Signal Amplification Plus system (PerkinElmer, Waltham, MA, USA) was performed according to the procedure reported previously [27,51]. Briefly, adult mouse testes were fixed for 3 h at 4°C with 4% paraformaldehyde in phosphate buffered saline (PBS). After washing with PBS, each testis was dissected into two pieces with a razor blade under a dissecting microscope. The two pieces of testis were dehydrated, embedded in paraffin, and cut into 7-μm-thick sections. The sections were hybridized with 2 ng/μl of the DIG-labeled RNA probe overnight at 45°C. After washing, the sections were incubated with an anti-DIG-horseradish peroxidase antibody (1:500 dilution; Roche Molecular Biochemicals) for 30 min at room temperature. The reaction with tyramide-Cy3 (1:50 dilution in 1X Plus Amplification Diluent (PerkinElmer), followed by 1:100 dilution with distilled water) was performed at room temperature for 20 min. To detect nuclei, the sections were incubated with 10 μg/ml Hoechst 33258 at room temperature for 10 min. The samples were mounted with a Fluoro-KEEPER Antifade Reagent (Nacalai Tesque, Kyoto, Japan) and observed under an LSM 5 LIVE confocal microscope (Carl Zeiss, Oberkochen, Germany).

Generation of *Start*-KO mice

sgRNA sequences were designed by CRISPRdirect (https://crispr.dbcls.jp/) [52]. sgRNAs were synthesized and purified by using a CUGA7 gRNA Synthesis Kit (Nippon Gene) according to the manufacturer's instructions. The selected sequences were *Start* sgRNA-UP (AGTACTTCCCTAGGTAAATGAGG) and *Start* sgRNA-DOWN (GTAACATCCTGTCATATTGCGGG), in which proto-spacer adjacent motif (PAM) sequences are underlined. Oligo DNA sequences used for sgRNA synthesis are listed in Table 1-1.

For injection, oocytes were collected from F1 hybrid (C57BL/6 x DBA/2) BDF1 female mice that were superovulated by standard procedures [53] and fertilized *in vitro* with sperms from male mice of the same genetic background. CAS9 protein (100 ng/μl; Nippon Gene) and sgRNAs (250 ng/μl each) were microinjected into the cytoplasm of fertilized oocytes. The oocytes were cultured in KSOM medium overnight, and embryos at the two-cell stage were transferred to pseudo-pregnant ICR female mice on the next day.

Spermatogenetic cell count by Giemsa-staining

Testes from wild type and *Start*-KO mice were washed with PBS, and tunica albuginea were removed. The tissues were soaked into 1% sodium citrate solution for 15 min to be washed, and the ice-cold mixture of ethanol and acetic acid (1:1; fixation liquid) was added for fixation. Then, seminiferous tubules were torn into pieces in 60%-diluted fixation liquid and filtered through a paper towel. The cells were fixed and washed again with fixation liquid, collected by centrifugation at 6,000 rpm, and suspended in fixation liquid.

Collected testicular cells were spread onto a slide and stained with 5% Giemsa/phosphate buffer solution (pH 7.3) for 10 min at room temperature. The slides were observed under a light microscope and the number of each cell type was counted.

RNA-seq analysis

RNA-seq analysis was performed as previously described [23,54]. In brief, total RNAs were isolated from a wild-type testis and *Start*-KO testis (line #2) of mice at the age of 2.5 months using ISOGEN according to the manufacturer's protocol. The RNAs were treated with TurboDNase to completely remove genome DNA, and the quality of the RNA samples was evaluated by electrophoresis and BioAnalyzer (Agilent Technologies, Palo Alto, CA, USA) with RNA6000 nano tip. cDNA synthesis was performed with 500 ng RNA from each sample by using a TruSeq Stranded mRNA Sample preparation kit (Illumina, San Diego, CA, USA) according to the manufacturer's

protocol. The resulting cDNA library was validated using BioAnalyzer with DNA1000 Chip and quantified using NEBNext Library Quant Kit for Illumina (NEB, Ipswich, MA, USA). A total of 101-cycles single-end sequencing was performed using HiSeq1500 (Illumina) in the rapid mode. After conversion to fastq format, reads were mapped to the mouse reference genome, mm10, with Bowtie2 software. The expression level of each gene was calculated as gene-specific Reads Per Kilobase of exon per Million mapped reads (RPKM). Total reads, mapping rates, and accession numbers are summarized in Table 1-2.

Testosterone measurement

A blood sample from each mouse was collected into a microtube and kept on ice for 1-2 hr until it became clotted. The sample was then centrifuged at 2,000g for 10 min at 4°C. The supernatant was collected as serum and quickly frozen by liquified nitrogen. The serum from adult mice was diluted 10 or 20 times with milli-Q water and used for enzyme-linked immunosorbent assay (ELISA) analysis, and that from 8 dpp mice was used after 3.3 times dilution. Serum testosterone concentration was measured by using a Cayman Testosterone EIA kit (Cayman Chemical, Ann Arbor, MI, USA) according to the manufacturer's instructions.

Morphological observation of testes

Wild-type and *Start*-KO mice were euthanized, and their body weights were measured. Then testes were isolated and their weights were measured. The testes were fixed with Bouin's solution at room temperature for 2 days, dehydrated, embedded in paraffin, and sectioned at 7 μm in thickness. The sections were stained with hematoxylin and eosin and observed under a light microscope.

Plasmid constructs for OE

The full length of *Start* was amplified and inserted into a pBluescript II KS+ vector as described above. The *Start* sequence was obtained by *Eco*RI and *Hind*III digestion from this vector, and the

fragment was blunted by T4 DNA polymerase and inserted into the *Eco*RV site of a pCAG-Hyg vector (Fujifilm Wako Pure Chemicals). Constructs with insertion of the *Start* sequence in both directions were obtained.

Cell culture and transfection

Mouse Leydig cell lines, TM3 and MA-10, were kindly provided from Dr. Takashi Yazawa at Asahikawa Medical University. TM3 cells were cultured in Dulbecco Modified Eagle Medium (DMEM)/F12 containing 2.5% fetal bovine serum, 5% horse serum, 100 U/ml penicillin, 100 μg/ml streptomycin, and 292 μg/ml L-glutamine (Invitrogen, Carlsbad, CA, USA). After coating a 3.5-cm dish with 0.1% gelatin, before use, 2.0×10^5 cells were spread in the dish one day before transfection. The next day, 6.0 μl PEI Max (Polyscience, Warrington, PA, USA) was mixed with 200 μl Opti-MEM (Thermo Fisher Scientific) and 2 μg DNA in that order. The mixture was added to the dish after 20-min incubation. Selection was done with the medium containing 250 μg/ml of hygromycin for 8 days.

MA-10 cells were cultured in DMEM/F12 containing 15% horse serum, 100 U/ml penicillin, 100 μg/ml streptomycin, and 292 μg/ml L-glutamine on a dish coated with 0.1% gelatin. One-tenth of confluent cells in a 6-cm dish was spread in a 3.5-cm dish one day before transfection. The next day, 24.0 μl PEI Max was mixed with 200 μl Opti-MEM and 8 μg DNA in that order. The mixture was added to the dish after 20-min incubation. Selection was done with the medium containing 100 μg/ml of hygromycin for 8 days.

Statistical analysis

Results are presented as the mean value ± standard deviation (S.D.) of at least three independent experiments. The data were statistically analyzed by Student's t-test, Welch's t-test or one-way analysis of variance (ANOVA) followed by the Tukey HSD test. A *P* value less than 0.05 was considered statistically significant. All statistical calculations were done by R software (Ver. 3.5.0; https://cran.ism.ac.jp/bin/windows/).

Results

Cloning and characterization of a testis-specific lncRNA, *Start*

Previously, our group revealed the presence of two testis-specific lncRNAs at the mouse *Prss/Tessp* locus and we suggested significant roles of these noncoding regions. In this study, I searched for other lncRNAs and found by RT-PCR that a 1,418-bp sequence was transcribed in an intergenic region between *Prss43/Tessp-3* and *Prss45/TESPL* genes in the testis (Fig. 1-2A). I then determined the 5'- and 3'-ends of this transcript by RACE analyses. In 3'RACE, two bands were specifically amplified by the second PCR (marked as "a" and "b" in Fig. 1-2B), and 10 subclones from each were sequenced. It was found that all subclones contained the same sequence for each band. Due to stronger band intensity, a cytosine from band "a" was determined to be a major transcriptional termination site (Fig. 1-2C). In 5'RACE, two bands were detected by the second PCR (marked as "c" and "d" in Fig. 1-2D), and 10 subclones were checked for each band. For band "c", three different sequences were detected, but the subclones from band "d" contained a single sequence. Because band "d" was more intense than band "c", a guanine from band "d" was determined to be a major transcriptional start site (Fig. 1-2E). Note that the transcriptional start site was within the primer sequence used for the initial RT-PCR amplifying the 1,418-bp product (Fig. 1-2A). Consequently, this transcript was defined to be a single-exon structure of a 1,822-nt sequence with a poly(A) tail at its 3' end. Based on the function reported here, I named this transcript *Start*.

RT-PCR was performed using 8 tissues to examine the tissue specificity of *Start*, and a positive band was only observed in the testis (Fig. 1-3A). During the first wave of spermatogenesis, qRT-PCR showed that *Start* expression was significantly elevated from 7 dpp to 14 dpp and remained at high levels thereafter (Fig. 1-3B). I then separated testicular cells into three fractions, germ cells, Leydig/Sertoli cells and Sertoli cells, and performed RT-PCR. As shown in Fig. 1-3C, *Start* was

expressed in both germ cells and Leydig cells but not in Sertoli cells. To investigate the subcellular localization, germ cells were separated into nuclear and cytosolic fractions. RT-PCR showed more dominant localization in the cytosol, but the positive band was also found in the nucleus (Fig. 1-3D). These results indicated that *Start* is a germ cell and Leydig cell-specific lncRNA and is activated during sperm development.

To further determine the localization of *Start*, we performed *in situ* hybridization by the highly sensitive tyramide signal amplification method [51]. Antisense and sense probes for *Start* were hybridized with adult testis sections and the signal was detected as red fluorescence. Consistent with results shown in Fig. 1-3C, a strong signal was detected in Leydig cells, mostly in the cytosolic region, by the antisense probe, while few signals were seen in the section hybridized with the sense probe (Figs 1-4A and B). In the seminiferous tubules, many more red dots were observed with the antisense probe (Figs 1-4C-E) than with the sense probe (Fig. 1-4F). At seminiferous epithelial stages II-IV and VI-VII (Figs 1-4C and D), the signals were found in all types of spermatogenetic cells including spermatogonia (SG), primary spermatocytes at the early and mid-pachytene stages (ePS and mPS), and round and elongating spermatids (RS and ES, respectively). Consistent with the results of RT-PCR shown in Fig. 1-3D, more signals were present in the cytosol of these cell types. At stage X, most of the spermatogenetic cells were stained in a cytosol-predominant manner as in earlier stages (Fig. 1-4E), but late pachytene spermatocytes (lPS) appeared to contain more signals in the nuclei than did other types of germ cells. Collectively, the results showed that *Start* was dominantly present in the cytosol of Leydig cells and all types of spermatogenetic cells, though transcripts were also localized in the nucleus. Noticeably, Leydig cells carried the strongest signals among all cell types, suggesting that *Start* plays an important role in Leydig cells.

Generation of *Start*-KO mice and morphological phenotype in adult testis

To reveal the physiological role of *Start*, I generated *Start*-KO mice by the CRISPR/Cas9 system using two guide RNAs designed at the 5'- and 3'-flanking sequences of *Start* (Fig. 1-5A).

Injection of the guide RNAs and CAS9 protein into fertilized eggs resulted in the generation of four founder mice that had a deletion of *Start*, and two KO lines, lines #1 and #2, were successfully established by mating with wild-type mice. These KO mice contained 2,222-bp (#1) and 2,208-bp (#2) deletions, which meant that #1 contained 5 and 9 nt longer deletions than #2 at the 5' and 3' regions, respectively (Figs. 1-5A and B). These two lines were used in this study.

Both #1 and #2 lines of *Start*-KO mice were fertile, and I observed morphology of the adult testis by collecting testes from 2.5-month-old wild-type and *Start*-KO mice. The testis weight normalized to body weight was not significantly different between wild-type and KO mice (Fig. 1-5C), and observations of testis sections stained with hematoxylin and eosin did not show any morphological difference (Fig. 1-5D). To evaluate the population of spermatogenetic cells, testicular germ cells were spread onto a slide and stained with Giemsa solution, and the number of each cell type was counted. However, no difference was found in any types of cells between wild-type and KO mice (Fig. 1-5E). In addition, the number of sperms collected from the cauda epididymis was not different between two genotypes in KO adult mice (Fig. 1-5F). Therefore, the adult *Start*-KO testis appeared to be morphologically normal.

Increased expression of testicular steroidogenic genes and decreased serum testosterone level in *Start*-KO adult mice

Subsequently, we attempted to detect differentially expressed genes between wild-type and *Start*-KO mice. Total RNA was purified from whole testes of a 2.5-month-old mice from the same litter and used for RNA-seq analysis. The resultant reads, mapping rate to the mouse cDNA library, and fastq accessions in the NCBI SRA database are summarized in Table 1-2. Interestingly, the steroidogenic acute regulatory protein (*Star*) gene encoding a protein to trigger steroidogenesis was found to be upregulated by 2.3-fold in the *Start*-KO testis (Fig. 1-6A). Furthermore, we search for differently expressed genes by focusing on steroidogenic pathway, and found that expression levels of other genes including cytochrome P450, family 11, subfamily a, polypeptide 1 (*Cyp11a1*), cytochrome

P450, family 17, subfamily a, polypeptide 1 (*Cyp17a1*), hydroxy-delta-5-steroid dehydrogenase, 3 beta and steroid delta-isomerase 1 (*Hsd3b1*), and hydroxysteroid (17-beta) dehydrogenase 3 (*Hsd17b3*) showed 1.3-1.6-fold increases in the *Start*-KO testis (Fig. 1-6A). qRT-PCR for these genes using four sets of wild-type and KO mice confirmed that *Star* and *Hsd3b1* genes were significantly upregulated in the *Start*-KO testis (Fig. 1-6B). I then measured testosterone concentration in serum. Surprisingly, ELISA analysis showed that the testosterone level was significantly reduced in KO mice (Fig. 1-6C). This is inconsistent with the increase of steroidogenic gene expression, but the results suggested that *Start* participates in regulation of the steroidogenesis pathway in Leydig cells.

Notably, an ELISA assay and qRT-PCR indicated that the LH level in the feedback system and *Lhb* mRNA expression in the pituitary were not significantly different between adult wild-type and *Start*-KO mice (Figs. 1-6D and E). qRT-PCR showed that *Ar* expression in the pituitary of KO mice was dramatically elevated (Fig. 1-6F), suggesting that a low testosterone level was compensated by AR upregulation in *Start*-KO mice. Presumably, the upregulation of *Star* and *Hsd3b1* in *Start*-KO testes did not result from the feedback system but from a secondary or indirect effect of the *Start* deficiency.

Effect of *Start* deficiency at a younger age

To evaluate more direct effects of *Start* deficiency on steroidogenesis, I investigated *Start*-KO mice at 8 dpp, when the feedback loop via the HPG_axis is not completely matured [55-57]. I first conducted morphological observation by preparing cross-sections of testes of wild-type and *Start*-KO mice from the same litter and staining them with hematoxylin and eosin. As shown in Fig. 1-7A, no significant differences were observed within the seminiferous tubules, whereas more interstitial regions containing few cells were observed in the *Start*-KO testis than in the wild-type testis (see regions encircled in red). Indeed, the number of interstitial cells in randomly selected areas (0.25 mm^2) in the sections was significantly smaller in *Start*-KO testes at 8 dpp than in wild-type testes (Fig. 1-7B). In contrast, no significant change was observed in interstitial cells between KO and wild-type

mice at 2.5 months of age (Fig. 1-7B). Since interstitial cells mainly consist of Leydig cells but also contain small populations of other types of cells [58,59], I investigated whether the altered number of interstitial cells reflected the Leydig cell population by examining the expression of insulin-like 3 (*Insl3*), a marker gene for Leydig cells [60,61]. By qRT-PCR, *Insl3* expression was found to be significantly decreased in *Start*-KO testes at 8 dpp, while it was not altered at 2.5 months of age (Fig. 1-7C). These results indicated that the number of Leydig cells was decreased in *Start*-KO mice at 8 dpp and strongly suggested a physiological role of *Start* in Leydig cell differentiation.

Next, I investigated the expression of steroidogenic genes in wild-type and *Start*-KO testes at 8 dpp. My qRT-PCR indicated that expression levels of *Star* and *Hsd3b1* genes were significantly low in *Start*-KO testes (Fig. 1-7D), in contrast with the results for *Start*-KO mice at 2.5 months of age. Serum testosterone level was also found to be lower in *Start*-KO mice than in wild-type mice at 8 dpp (Fig. 1-7E). Collectively, the results showed that steroidogenic genes were downregulated in the testis and that the testosterone level was decreased in *Start*-KO mice at 8 dpp.

Activation of steroidogenic genes by *Start* in Leydig cell lines

To determine how *Start* regulates steroidogenic genes in Leydig cells, I utilized two mouse Leydig cell lines, TM3 and MA-10 [62,63], to perform *Start* OE. The antisense sequence of *Start* was overexpressed as a negative control. Strand-specific RT-PCR confirmed successful OE of *Start* and its antisense transcript in both cell lines (Figs 1-8A and C). In TM3 cells, *Star* gene expression was significantly increased by *Start* OE (Fig. 1-8B), and in MA-10 cells, not only *Star* but also *Cyp17a1*, *Hsd3b1*, and *Hsd17b3* genes were significantly upregulated by *Start* (Start_OE, Fig. 1-8D). These results supported the notion that *Start* acts as an activator of steroidogenic genes in Leydig cells, as shown by results for 8-day-old mice (Fig. 1-7). Based on these results, I concluded that *Start* activates a subset of genes involved in steroidogenesis in Leydig cells.

Discussion

In the present study, I identified a novel testis-specific lncRNA, *Start*, that is encoded with *lncRNA-HSVIII* and *Tesra* at the mouse *Prss/Tessp* locus [27,28]. Interestingly, these three lncRNAs are all expressed in germ cells and Leydig cells, suggesting some integrated mechanism for their transcriptional activation. Given that several protein-coding genes at this locus have been suggested to participate in the progression of meiosis and that lncRNAs have been suggested to be involved in gene regulation in germ cells and Leydig cells [27-29], the *Prss/Tessp* locus is thought to be responsible for multiple testis functions including spermatogenesis.

While various transcriptomic data have indicated differential expression of many lncRNAs and mRNAs in the testis and suggested their testis-specific functions such as spermatogenesis and androgen synthesis [44,64], only a few studies have shown the phenotype of KO mice for lncRNAs. *Tsx*, an X-linked lncRNA, is expressed in meiotic germ cells, and its deletion resulted in a reduction of testis size and an increase in apoptotic cells due to meiotic arrest at pachynema, although mutant males were fertile [65]. *Tslrn1*, a testis-specific lncRNA, was found to be involved in the formation of spermatozoa since the number of sperm was significantly reduced in KO mice [66]. In the case of *1700121C10Rik*, which encodes two testis-specific lncRNAs, the KO mice were fertile and showed no obvious phenotype [67]. These findings confirmed some physiological roles of the lncRNA in germ cells and suggested that such roles were compensated by lncRNAs or protein-coding genes and that multiple lncRNAs share common physiological roles. In contrast, results of *in vivo* evaluation of the functions of lncRNAs in Leydig cells have not been reported. The current study showed that a testis-specific lncRNA, *Start,* was involved in Leydig cell differentiation before puberty and in activation of steroidogenic genes in the testis. Thus, this is the first evidence for *in vivo* biological functions of an lncRNA in Leydig cells.

In general, lncRNAs regulate the expression of their target genes at various levels depending on their subcellular localization [68,69]. In germ cells, *Start* was mainly localized in the cytosol of most

meiotic cells and in both the cytosol and nucleus at the late pachytene stage, suggesting some roles of *Start* in transcriptional and posttranscriptional gene regulation, as was observed for other lncRNAs in previous studies [70-72]. In contrast, in Leydig cells, *Start* was mostly localized in the cytosol, suggesting its function in posttranscriptional regulation such as mRNA stability and translation. In the case of regulation of mRNA stability, lncRNAs are known to form double-strand RNAs with their target mRNAs and induce molecular events leading to RNA degradation or stabilization [73-75]. In translational regulation, lncRNAs generally interact with miRNAs to block their function, resulting in enhancement of the translation of miRNA-targeted mRNAs [76-78]. These findings suggest various functions of cytosolic lncRNAs, and *Start* may regulate target genes through such a mechanism. Elucidation of the detailed molecular mechanism by which *Start* controls the expression of steroidogenic genes will be described in the next chapter.

My current data indicated a decrease in the number of interstitial cells, including Leydig cells, in *Start*-KO mice at 8 dpp. Expression of the *Insl3* gene, a Leydig cell marker, was found to be suppressed in *Start*-KO mice at 8 dpp, while OE of *Start* did not affect *Insl3* expression in MA-10 cells (Fig. 1-9A). These findings led to the conclusion that the number of Leydig cells was decreased by deletion of *Start* at 8 dpp. In contrast, neither the number of interstitial cells nor *Insl3* expression was altered in *Start*-KO adult testes. This might reflect the difference between fetal and adult Leydig cells. It is known that fetal and adult Leydig cells are differentiated by distinct regulatory mechanisms and their gene expression profiles are different [79,80]. No difference in hydroxy-delta-5-steroid dehydrogenase, 3 beta- and steroid delta-isomerase 6 (*Hsd3b6*) gene expression, a marker for adult Leydig cells [81], between wild-type and *Start*-KO testes by a qRT-PCR result (Fig. 1-9B) supports the notion that *Start* only affects fetal Leydig cells. Therefore, our data suggest that *Start* is involved in the differentiation of fetal Leydig cells but not that of adult Leydig cells. Given that terminally differentiated fetal Leydig cells do not proliferate [82,83], *Start* is likely to play a role in the middle of the differentiation process.

The present study provided data supporting the involvement of *Start* in the regulation of

steroidogenesis in Leydig cells. First, many *Start* transcripts were localized in Leydig cells, where steroid hormones are synthesized. Second, expression of *Star* and *Hsd3b1* genes was decreased in *Start*-KO mice at 8 dpp and in adults. Third, serum testosterone level was lower in *Start*-KO mice than in wild-type mice both in adults and at 8 dpp. Fourth, OE of *Start* in two Leydig cell lines significantly increased the expression of steroidogenic genes. Although the decreases in the gene expression and testosterone level might be partially due to the reduction in the number of Leydig cells at 8 dpp, these results strongly suggest that *Start* is a regulator of steroidogenesis in the mouse testis by controlling at least *Star* and *Hsd3b1* gene expression in Leydig cells.

Interestingly, *Star* and *Hsd3b1* gene expression was upregulated in adult *Start*-KO testes. I initially expected an increase in LH secretion caused by the low level of testosterone, but neither LH secretion nor *Lhb* mRNA expression was significantly affected by *Start* deficiency. Testosterone has been reported to either increase or decrease *Ar* expression depending on the cell type and experimental conditions [79], and *in vivo* evaluation showed that castration and testosterone injection caused an increase and decrease, respectively, in *Ar* expression in the prostate and brain [55,84]. In *Start*-KO adult mice, the low level of testosterone led to a dramatic increase in *Ar* expression in the pituitary, which probably counterbalanced the decreased feedback signal and resulted in the unaltered LH secretion. This suggests that *Star* and *Hsd3b1* genes were not enhanced by distal feedback via the HPG_axis in adults. Instead, enhancement of *Star* and *Hsd3b1* expression might be caused by autocrine signaling of the androgen-AR trail in Leydig cells. It has been reported that the expression levels of some steroidogenic genes were significantly decreased but that the expression levels of other steroidogenic genes were increased in Leydig cell-specific AR KO testes [85]. This indicates that the deficiency of autocrine signaling via AR in Leydig cells can cause a disturbance of steroidogenic gene expression. In adult *Start*-KO males, the low level of testosterone might cause a deficiency in this autocrine system and lead to secondary or indirect effects, resulting in abnormal elevation of *Star* and *Hsd3b1* expression. On the other hand, at 8 dpp, I verified more direct effects of *Start* deficiency: downregulation of *Star* and *Hsd3b1* genes. Taken together with the increased expression of

steroidogenic genes in *Start*-overexpressing TM3 and MA-10 cells, the function of *Start* is likely to be enhancement of the expression of steroidogenic genes.

Most previous studies focused on the functions of testis lncRNAs in germ cells [21-24,29,65-67,86] but not on their roles in Leydig cells [87,88]. The results of the present study shed light on the *in vivo* function of *Start*, which plays roles in the differentiation of fetal Leydig cells and in the maintenance of the steroid synthesis pathway in the testis. Thus, this report is the first report on a testis-specific lncRNA that controls the steroid synthesis pathway in Leydig cells.

Table 1-1. Oligo DNAs used in the chapter 1

Name	Forward	Reverse
[RT-PCR]		
Start 1418bp	CTGGGTTTTGGTATCCCTGA	ATCGCATATCGAGGCAAGCA
Gapdh	CATGACCACAGTCCATGCCATC	TAGCCCAAGATGCCCTTCAGTG
[RACE]		
GSP1		AAACAAAACTGGGGGTGGAG
GSP2		GATGGGTTCATCCTTCCTTG
GSP3		ATGCCCACAAAAGCCATAGA
GSP4	GAAGGCAACCTTCTCTTGCT	
GSP5	CTCGATATGCGATTGGCACC	
AAP	GGCCACGCGTCGACTAGTACGG GIIGGGIIGGGIIG	
AUAP	GGCCACGCGTCGACTAGTAC	
AP	CTGATCTAGAGGTACCGGATCC	
[qRT-PCR]		
Start	CCCACTCTTAGCCTCATGGT	CCATCACCCAGCCTGTTCGTT
Star	GGGTGGTAGTCAGGAGACAC	TTCACAGCTATGCAGTGGGA
Cyp11a1	ATGAGCCAGGAGGTCTAAGC	TCCACCCTATGGGTCCCTAA
Cyp17a1	CATGCATGAGAACGGCATCA	CATTCGAACAAGACCAGGGC
Hsd3b1	ATGAGCCACTTGTCAACTGGGA GG	TGCTGAAGCCTAAGAACTGAGAC TC
Hsd17b3	GTCACGATCGGAGCTGAATC	TCGTGTCAGGAGGAATCGTT
Aip	GAGGACGGGATCCAAAAGC	CTGTGCAGCGTCCGAAAGT
Gapdh	TGCACCACCAACTGCTTAGC	GGCATGGACTGTGGTCATGAG
Insl3	CCTGGCTATGTCATTGCAACA	TGGTCCTTGCTTACTGCGATCT
Lhb	ACTGTGCCGGCCTGTCAACG	AGCAGCCGGCAGTACTCGGA
Ar	GATGGTATTTGCCATGGGTTG	GGCTGTACATCCGAGACTTGTG
[Cloning]		
Start full length	GGGTTTTGGTATCCCTGAC	GTTGCCTGGCTTTGGGCATA
[gRNA]		
5’-gRNA	CTAATACGACTCACTATAGAGTA CTTCCCTAGGTAAATGGTTTTAG AGCTAGAAATAGCA	
3’-gRNA	CTAATACGACTCACTATAGGTAA CATCCTGTCATATTGCGTTTTAG AGCTAGAAATAGCA	

Table 1-2. Summary of RNA-seq results and accession numbers

Sample name	Total reads	Overall alignment rate	Accession number
Wild type adult testis (line #2)	28,098,634	82.17%	SRR12700727
Start-KO adult testis (line #2)	30,258,284	82.96%	SRR12700726

Figure 1-1

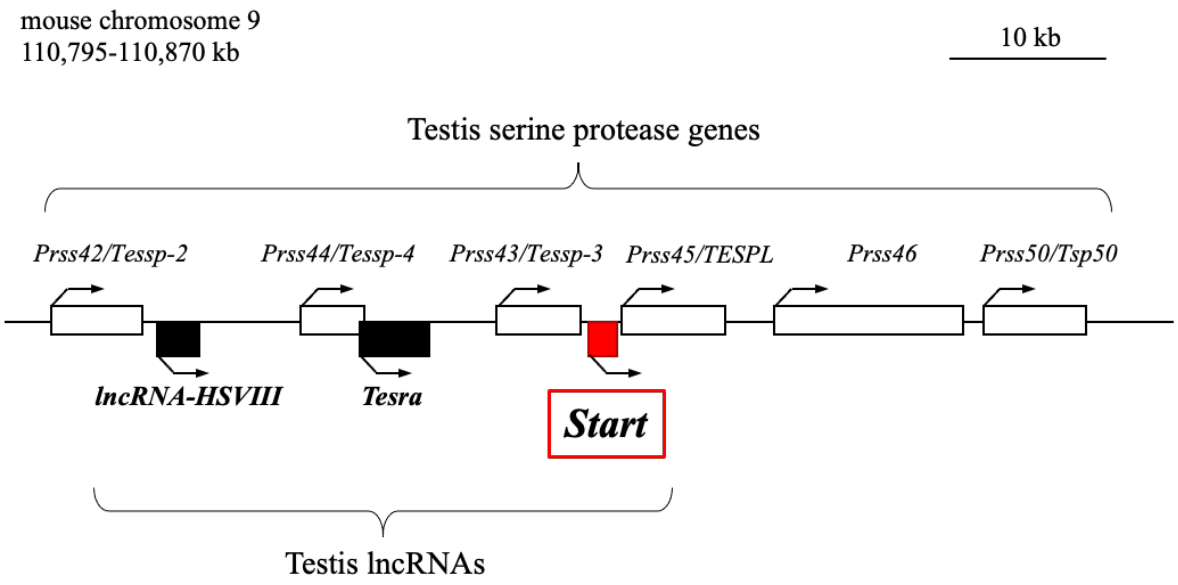


Figure 1-1. Schematic drawing of the mouse *Prss/Tessp* locus on chromosome 9. A 75-kb region corresponding to 110,795-110,870 kb of mouse chromosome 9 is shown. This region contains six genes encoding serine proteases and three lncRNAs as indicated by white and black/red boxes, respectively. *Start* is an lncRNA that was identified in this study and is indicated by a red-filled box. Bent arrows indicate the transcriptional direction of the protein-coding genes and lncRNAs.

Figure 1-2

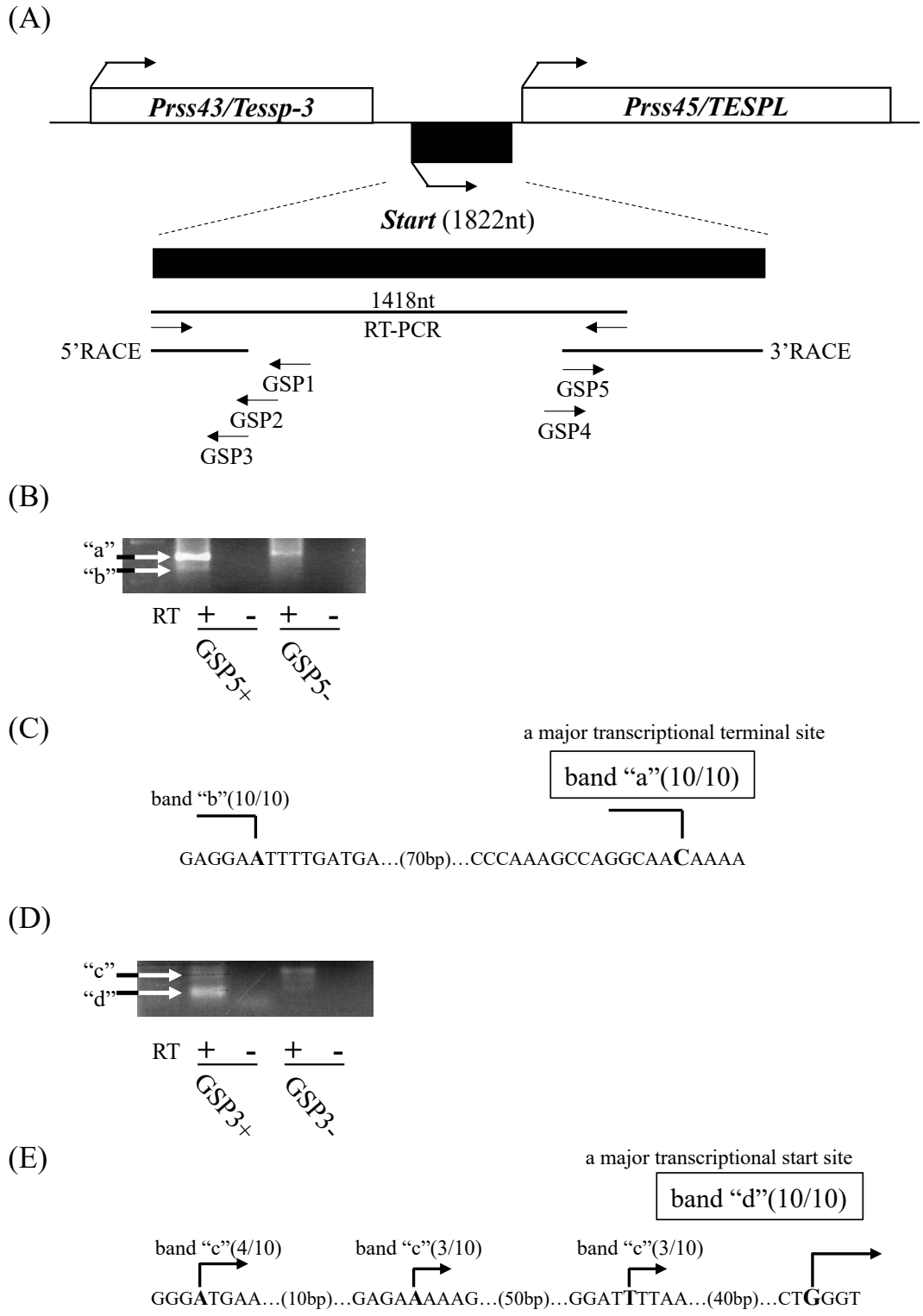

(A)
Prss43/Tessp-3
Prss45/TESPL
Start (1822nt)
1418nt
RT-PCR
5'RACE
3'RACE
GSP1
GSP2
GSP3
GSP4
GSP5
(B)
"a"
"b"
RT + - + -
GSP5+
GSP5-
(C)
a major transcriptional terminal site
band "a"(10/10)
band "b"(10/10)
GAGGAATTTTGATGA…(70bp)…CCCAAAGCCAGGCAACAAAA
(D)
"c"
"d"
RT + - + -
GSP3+
GSP3-
(E)
a major transcriptional start site
band "d"(10/10)
band "c"(4/10)
band "c"(3/10)
band "c"(3/10)
GGGATGAA…(10bp)…GAGAAAAAG…(50bp)…GGATTTTAA…(40bp)…CTGGGT

Figure 1-2. Determination of the full-length sequence of *Start*. (A) An overview of RACE analyses. Two protein-coding genes, *Prss43/Tessp-3* and *Prss45/TESPL*, and *Start* between them are drawn as in Fig. 1-1. The region transcribed into *Start* is enlarged below the drawing. A 1,418-nt sequence that was detected by the first RT-PCR and the sequences determined by 5′ and 3'RACE are indicated by horizontal lines. Positions and directions of three primers (GSP1–GSP3) for 5'RACE and two primers (GSP4 and GSP5) for 3'RACE are also shown by horizontal arrows. (B) PCR results of 3'RACE. Two bands (a and b) were obtained by the second PCR as indicated in the gel image. The result of RT-PCR using GSP5 and AP primers is represented as GSP5+, and the result without a GSP5 primer is represented as GSP5-. Reverse transcription was performed with a reverse transcriptase (RT+) or without a reverse transcriptase (RT-). White arrows indicate the specifically amplified bands. (C) Transcriptional termination sites of *Start*. Ten subclones from each band ("a" and "b") were subjected to DNA sequencing, and the number of subclones containing the same transcriptional termination site is indicated on each nucleotide in the genome sequence. Due to its stronger intensity, a cytosine from band "a" was determined to be a major transcriptional termination site. (D) PCR results of 5'RACE. Two bands ("c" and "d") were obtained by the second PCR as indicated in the gel image. Results of RT-PCR using GSP3 and AUAP primers are represented as in (B). (E) Transcriptional start sites of *Start*. Ten subclones from each band were subjected to DNA sequencing, and the number of subclones containing each transcriptional start site is shown. Due to its stronger intensity, a guanine from band "d" was determined to be a major transcriptional start site.

Figure 1-3

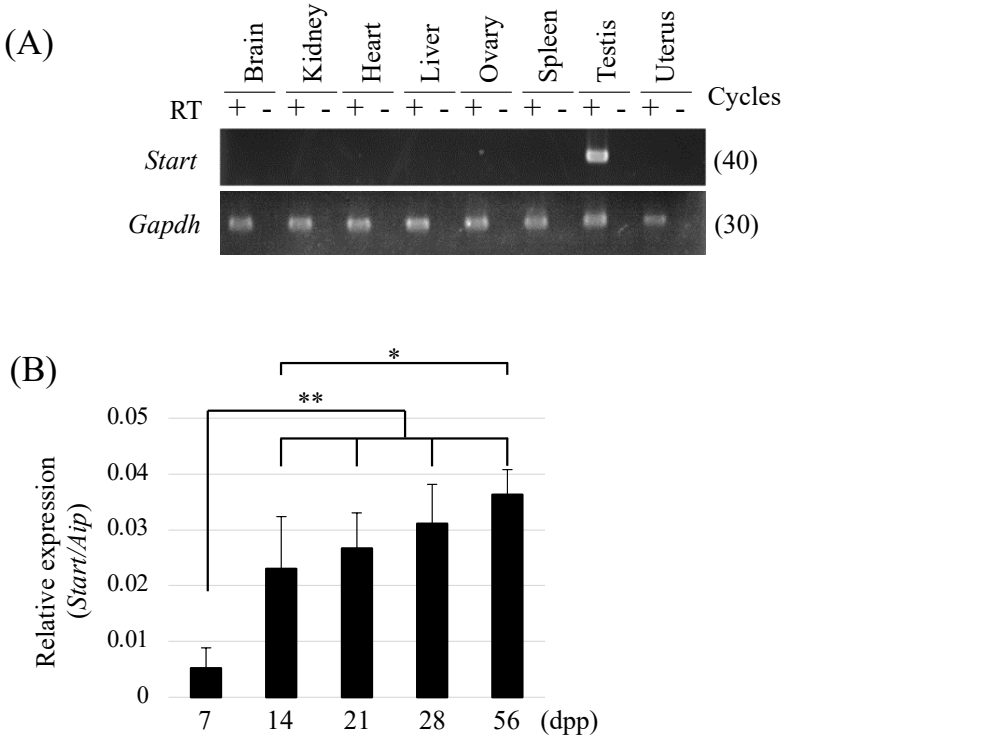

(A)
Brain
Kidney
Heart
Liver
Ovary
Spleen
Testis
Uterus
RT + - + - + - + - + - + - + - + -
Cycles
Start
(40)
Gapdh
(30)
(B)
*
**
0.05
0.04
0.03
0.02
0.01
0
Relative expression
(Start/Aip)
7
14
21
28
56
(dpp)
(C)
Germ
Leydig + Sertoli
Sertoli
RT + - + - + -
Cycles
Start
(40)
Gapdh
(20)
(D)
Nuclei
Cytosols
RT + - + -
Cycles
Start
(35)
Gapdh
(30)

Figure 1-3. Expression of the *Start* transcript. (A) Tissue specificity of *Start*. Total RNAs from eight mouse tissues, as indicated, were collected from adult wild-type mice and used for RT-PCR with a random hexamer for reverse transcription. The *Gapdh* gene was detected as an internal control. The cycle number of each PCR is shown in parenthesis. (B) *Start* expression during testis development. Mouse testes at 7, 14, 21, 28, and 56 dpp were collected, and total RNAs were purified and used for qRT-PCR. The *Aip* gene was used as an internal control to normalize the *Start* expression level. Data are presented as means ± S.D. from three independent experiments. Statistical significance was analyzed by Tukey's HSD test. * $P < 0.05$, ** $P < 0.01$. (C) RT-PCR with fractionated testicular cells. Total RNAs from germ cells, Leydig/Sertoli cells, and Sertoli cells were collected and used for RT-PCR. The *Gapdh* gene was utilized as an internal control. The cycle number of each PCR is shown in parenthesis. (D) RT-PCR for subcellular localization of *Start*. Total RNAs were purified from nuclear and cytosolic fractions of germ cells and used for RT-PCR. *Gapdh* was used to amplify a region within exon 6 as an internal control. The cycle number is indicated in parenthesis.

Figure 1-4

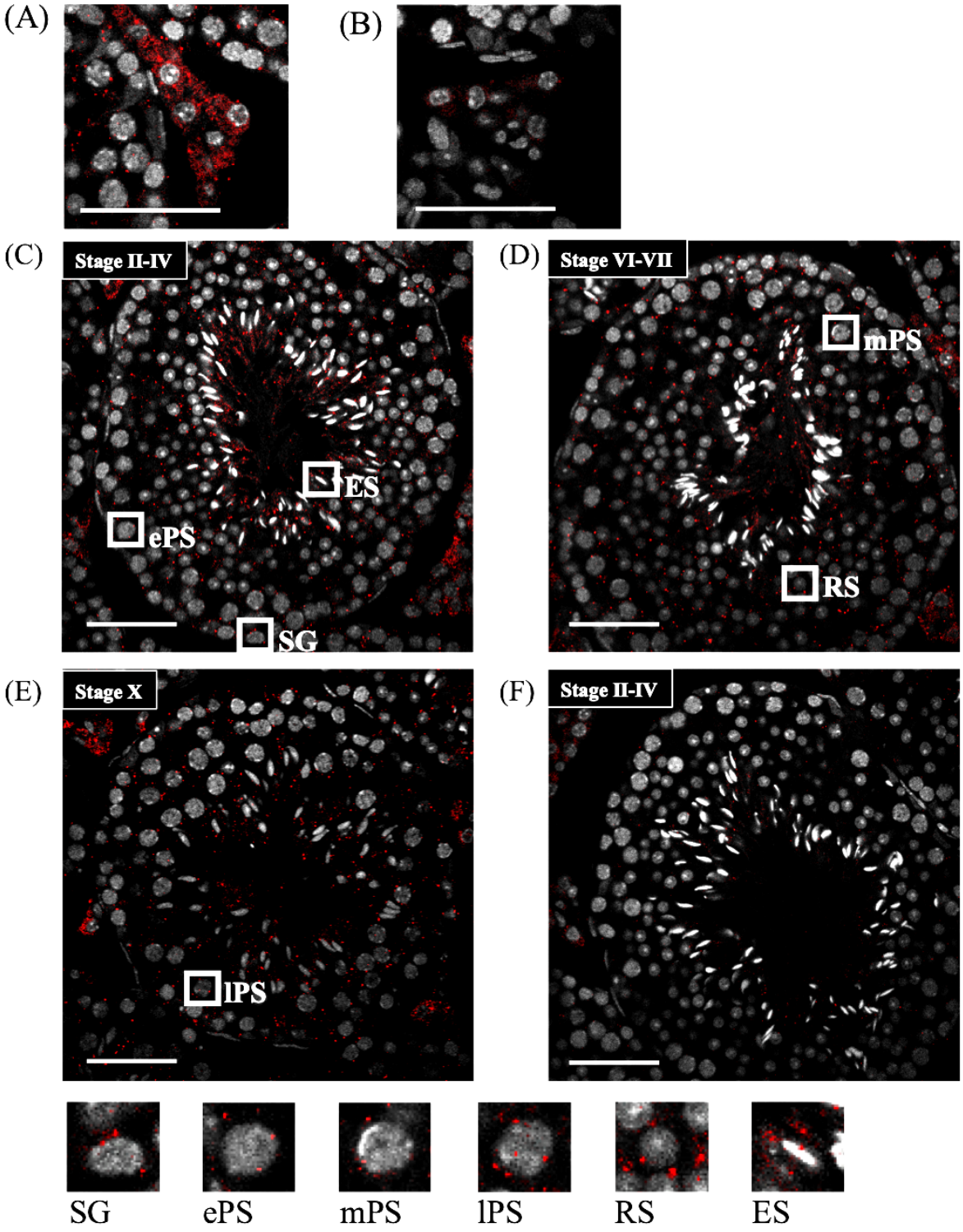

(A)
(B)
(C)
Stage II-IV
ES
ePS
SG
(D)
Stage VI-VII
mPS
RS
(E)
Stage X
lPS
(F)
Stage II-IV
SG
ePS
mPS
lPS
RS
ES

Figure 1-4. *Start* localization determined by *in situ* hybridization using the tyramide signal amplification system. (A, B) Representative images of *Start* localization in interstitial Leydig cells stained with the antisense probe (A) and sense probe (B). Staining with the sense probe was performed as a negative control. (C-E) Representative images of seminiferous tubules at seminiferous epithelial stages II-IV (C), VI-VII (D), and X (E) stained with the antisense probe. The squares indicate the cells enlarged below. As specified in (C-E), the squares emphasize a spermatogonium (SG), primary spermatocytes at the early, mid, and late pachytene stages (ePS, mPS, and lPS, respectively), round spermatid (RS), and elongating spermatid (ES). (F) An image of seminiferous tubules at stage II-VI stained with the sense probe as a negative control. In all images, red dots represent *Start* signals, and nuclei were co-stained with Hoechst 33258 (grey). Scale bars, 50 μm.

Figure 1-5

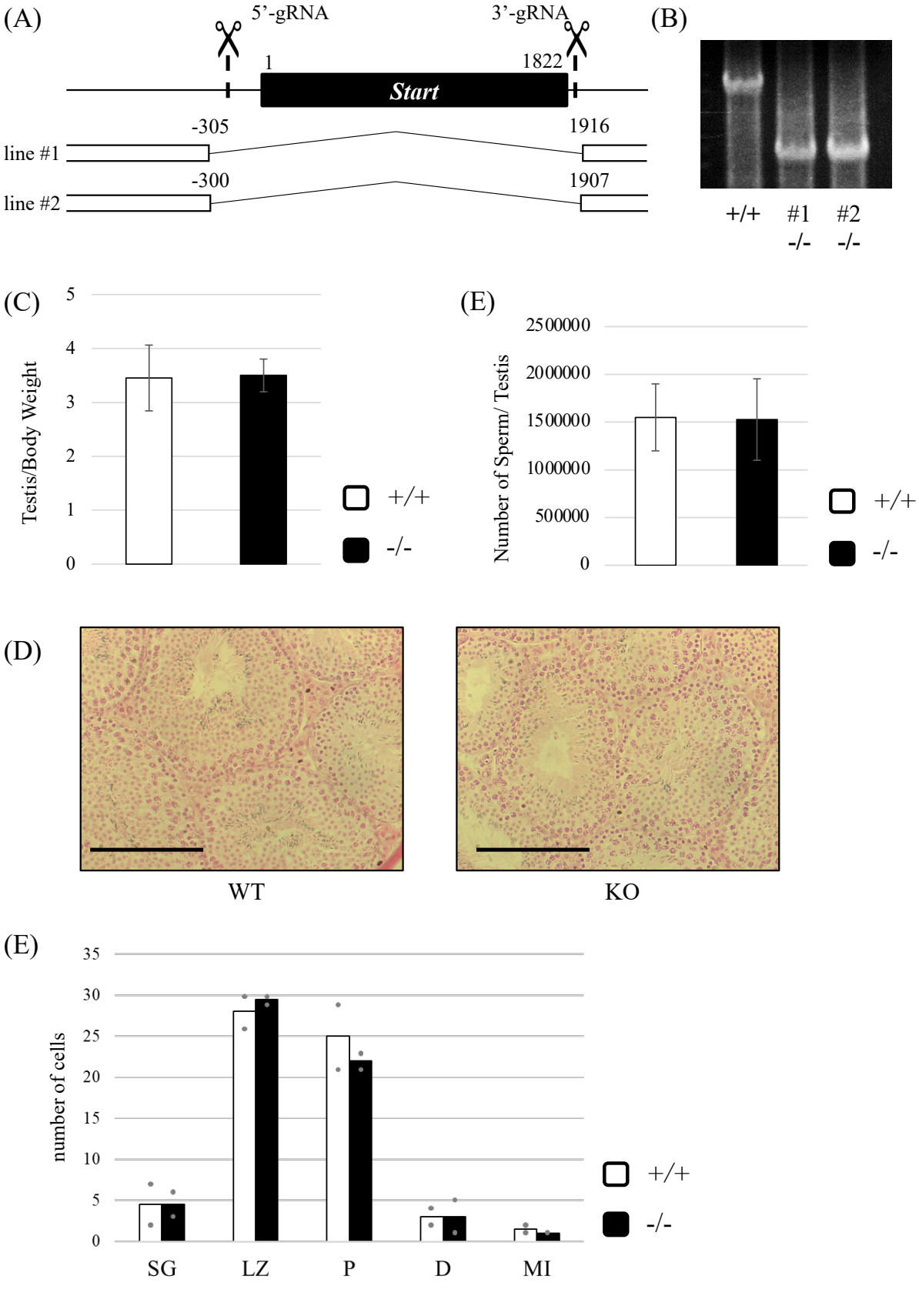

(A)
5'-gRNA
3'-gRNA
1
1822
Start
-305
1916
line #1
-300
1907
line #2
(B)
+/+
#1 -/-
#2 -/-
(C)
Testis/Body Weight
0
1
2
3
4
5
+/+
-/-
(E)
Number of Sperm/ Testis
0
500000
1000000
1500000
2000000
2500000
+/+
-/-
(D)
WT
KO
(E)
number of cells
0
5
10
15
20
25
30
35
SG
LZ
P
D
MI
+/+
-/-

Figure 1-5. Generation of *Start*-KO mice and evaluation of steroidogenic genes in adults. (A) Strategy for deletion at the *Start* locus. *Start* is a transcript of 1822 nt in length as shown by a black box. Positions of target sequences of gRNAs are indicated by dashed lines with scissor pictures. By injection of these gRNAs and CAS9 protein into fertilized eggs, two *Start*-KO lines, #1 and #2, were established. The deleted regions of the two KO lines are indicated by the number relative to the transcriptional start site of *Start*. (B) A representative result of genomic PCR for genotyping. Genome DNAs from wild-type and *Start*-KO #1 and #2 mice were subjected to PCR amplifying a 4021-bp region including the deleted region. The upper band corresponds to the wild-type locus and the lower band indicates the deleted locus. (C) Ratio of testis to body weight at 2.5 months (lines #1 and #2). Data are presented as means ± S.D. from four independent sets of wild-type and *Start*-KO littermates. Student's t-test revealed no significant difference between wild-type and KO mice. (D) Testis section at 2.5 months (line #2). Testes from 2.5-month-old wild-type and *Start*-KO littermates were fixed with Bouin's solution, dehydrated, embedded in paraffin, cut into 7-μm-thick sections, and stained with hematoxylin and eosin. No difference was observed. Scale bars, 100 μm. (E) Total testicular cells were isolated from two different sets of 2.5-month-old wild-type and *Start*-KO littermates (line #1). The cells were fixed with an ethanol and acetic acid mixture (1:1), spread on slides, and stained with Giemsa solution. The number of each cell type was counted. Average values of two sets of experiments in each genotype were obtained, and the values from each set are indicated by dots. There was no obvious difference between wild-type and *Start*-KO mice. SG: spermatogonia, LZ: leptotene/zygotene primary spermatocytes, P: pachytene spermatocytes, D: diplotene spermatocytes, MI: MI phase spermatocytes. (F) Sperm number at 2.5 months (line #2). Mature sperms were isolated from the cauda epididymis of three sets of 2.5-month-old wild-type and *Start*-KO littermates in HTF medium. After fixation with 5% formalin, the number was counted. Data are presented as means ± S.D. Student's t-test showed no significant difference.

Figure 1-6

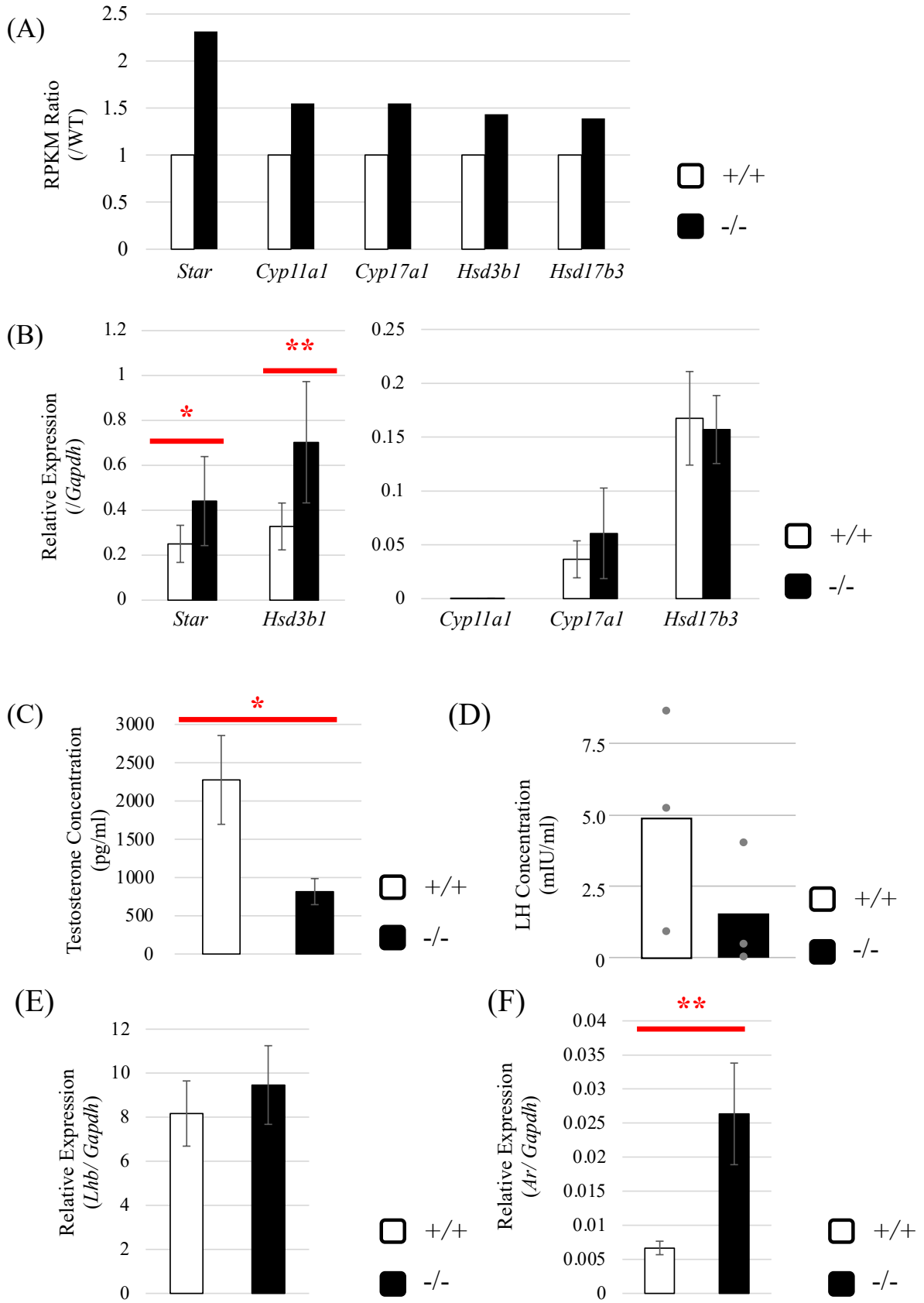

(A)
RPKM Ratio (/WT)
2.5
2
1.5
1
0.5
0
Star
Cyp11a1
Cyp17a1
Hsd3b1
Hsd17b3
+/+
-/-
(B)
Relative Expression (/Gapdh)
1.2
1
0.8
0.6
0.4
0.2
0
*
**
Star
Hsd3b1
0.25
0.2
0.15
0.1
0.05
0
Cyp11a1
Cyp17a1
Hsd17b3
+/+
-/-
(C)
Testosterone Concentration (pg/ml)
3000
2500
2000
1500
1000
500
0
*
+/+
-/-
(D)
LH Concentration (mIU/ml)
7.5
5.0
2.5
0
+/+
-/-
(E)
Relative Expression (Lhb/ Gapdh)
12
10
8
6
4
2
0
+/+
-/-
(F)
Relative Expression (Ar/ Gapdh)
**
0.04
0.035
0.03
0.025
0.02
0.015
0.01
0.005
0
+/+
-/-

Figure 1-6. Expression of steroidogenic genes, testosterone, LH and AR in *Start*-KO male

(A) Expression of steroidogenic genes in the testis at 2.5 months (line #2) by RNA-seq. The ratios of RPKM values for *Star*, *Cyp11a1*, *Cyp17a1*, *Hsd3b1*, and *Hsd17b3* in a *Start*-KO testis to those in a 2.5-month-old wild-type testis were calculated. The expression level for each gene in the wild-type is set to 1 and fold changes in a KO mouse are presented. (B) Expression of steroidogenic genes in the testis at 2.5 months (lines #1 and #2) determined by qRT-PCR. Total RNAs were purified from 2.5-month-old wild-type and *Start*-KO testes and used for qRT-PCR. The *Gapdh* gene was used as an internal control to normalize the expression level of each gene. Data are presented as means ± S.D. from four sets of wild-type and KO littermates. Statistical significance was analyzed by Welch's t-test. * $P < 0.05$, ** $P < 0.01$. (C) Serum testosterone level at 2.5 months (line #2). Serum was collected from 2.5-month-old wild-type and *Start*-KO mice, and testosterone concentration (pg/ml) was measured by ELISA. Data are presented as means ± S.D. from three sets of wild-type and KO littermates. Statistical significance was analyzed by Student's t-test. * $P < 0.05$. (D) LH level at 2.5 months (line #2). Serum was collected from 2.5-month-old wild-type and *Start*-KO mice, and LH concentration (mIU/ml) was measured by ELISA using a LH ELISA kit (CUSABIO, Wuhan, China). Data are presented as means from three sets of wild-type and KO mice. Each black dot represents an average value of triplicates from one serum sample. Statistical significance was analyzed by Welch's t-test, but no significance was detected. (E) *Lhb* expression in the pituitary at 2.5 months (lines #1 and #2). Total RNAs were purified from pituitaries of 2.5-month-old wild-type and *Start*-KO mice and used for qRT-PCR. The *Gapdh* gene was amplified as an internal control to normalize the expression level. Data are presented as means ± S.D. from four sets of wild-type and KO littermates. Statistical significance was analyzed by Student's t-test, but no significance was detected. (F) *Ar* expression in the pituitary at 2.5 months (lines #1 and #2). The cDNAs synthesized in (E) were used for qRT-PCR to amplify *Ar* mRNA. Data are presented as means ± S.D. from four sets of wild-type and KO littermates, and statistical significance was analyzed by Student's t-test. ** $P < 0.01$.

Figure 1-7

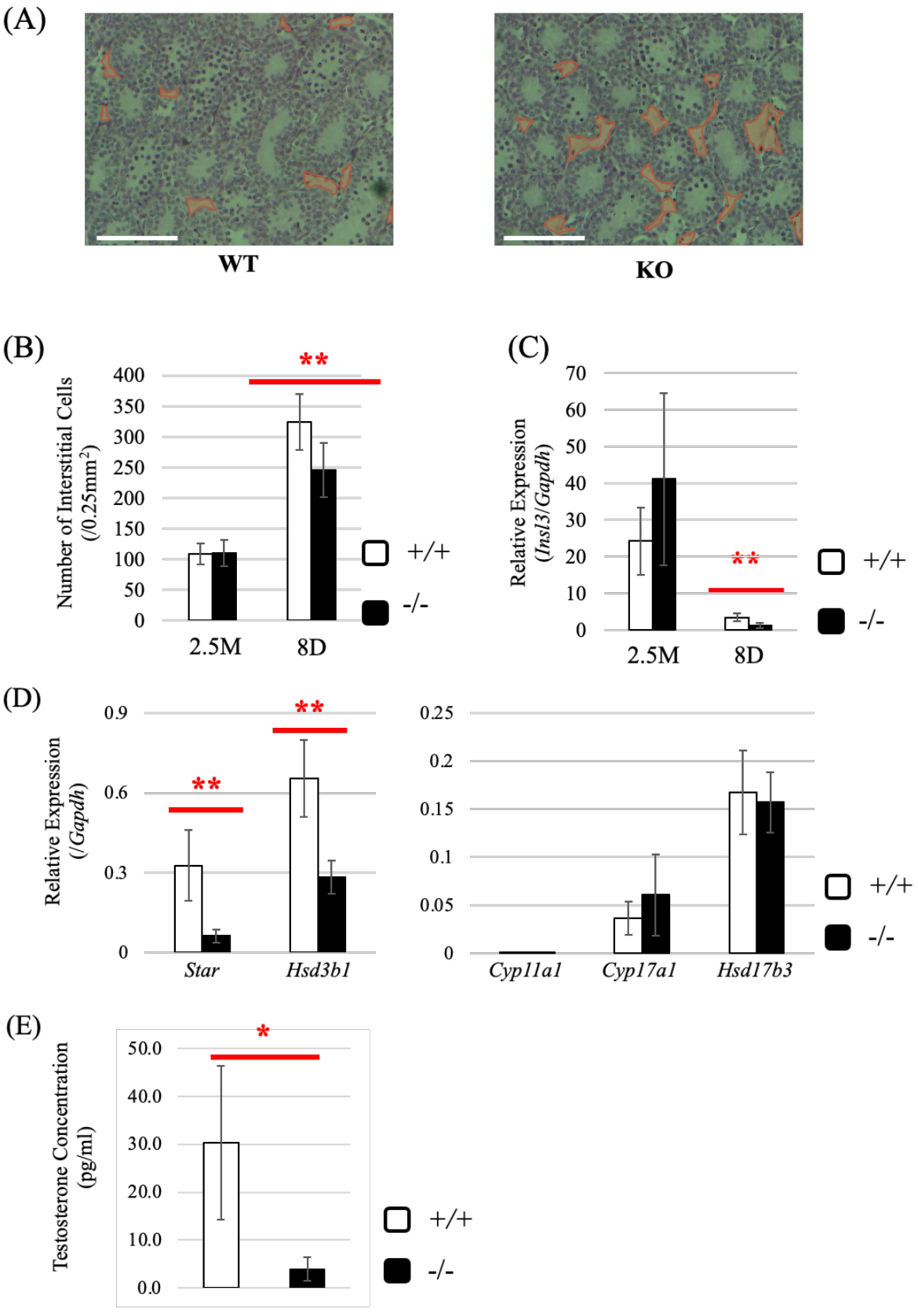

(A)
WT
KO
(B)
Number of Interstitial Cells (/0.25mm²)
400
350
300
250
200
150
100
50
0
**
2.5M
8D
+/+
-/-
(C)
Relative Expression (Insl3/Gapdh)
70
60
50
40
30
20
10
0
**
2.5M
8D
+/+
-/-
(D)
Relative Expression (/Gapdh)
0.9
0.6
0.3
0
**
**
Star
Hsd3b1
0.25
0.2
0.15
0.1
0.05
0
Cyp11a1
Cyp17a1
Hsd17b3
+/+
-/-
(E)
Testosterone Concentration (pg/ml)
50.0
40.0
30.0
20.0
10.0
0.0
*
+/+
-/-

Figure 1-7. Characterization of *Start*-KO mice at 8 dpp. (A) Testis section at 8 dpp (line #1). Testes from 8-day-old wild-type and *Start*-KO littermates were fixed with Bouin's solution, dehydrated, embedded in paraffin, cut into 7-μm-thick sections, and stained with hematoxylin and eosin. Interstitial regions containing few cells are encircled with red. Scale bar, 100 μm. (B) Numbers of interstitial cells at 8 dpp (line #1) and 2.5 months (line #2). The numbers of interstitial cells in three randomly selected 0.25-mm^2 squares were counted for each of the three mice. Data are presented as means ± S.D. from average values of three sets of wild-type and *Start*-KO littermates. Statistical significance was analyzed by Student's t-test. ** $P < 0.01$. (C) *Insl3* expression at 8 dpp (line #1) and 2.5 months (lines #1 and #2). qRT-PCR was performed using cDNAs from wild-type and *Start*-KO testes at the ages of 8 dpp and 2.5 months. Data are presented as means ± S.D. from three sets and four sets of wild-type and KO littermates at 8 dpp and 2.5 months, respectively. Statistical significance was analyzed by Student's t-test. ** $P < 0.01$. (D) Expression of steroidogenic genes at 8 dpp in the testis determined by qRT-PCR (line #1). Total RNAs were purified from 8-day-old wild-type and *Start*-KO testes and used for qRT-PCR. The *Gapdh* gene was used as an internal control to normalize the expression level of each gene. Data are presented as means ± S.D. from three sets of wild-type and KO littermates. Statistical significance was analyzed by Welch's t-test. ** $P < 0.01$. (E) Serum testosterone level at 8 dpp (lines #1 and #2). Serum was collected from 8-day-old wild-type and *Start*-KO littermates, and testosterone concentration (pg/ml) was measured by ELISA. Data are presented as means ± S.D. from three sets of littermates. Statistical significance was analyzed by Welch's t-test. * $P < 0.05$.

Figure 1-8

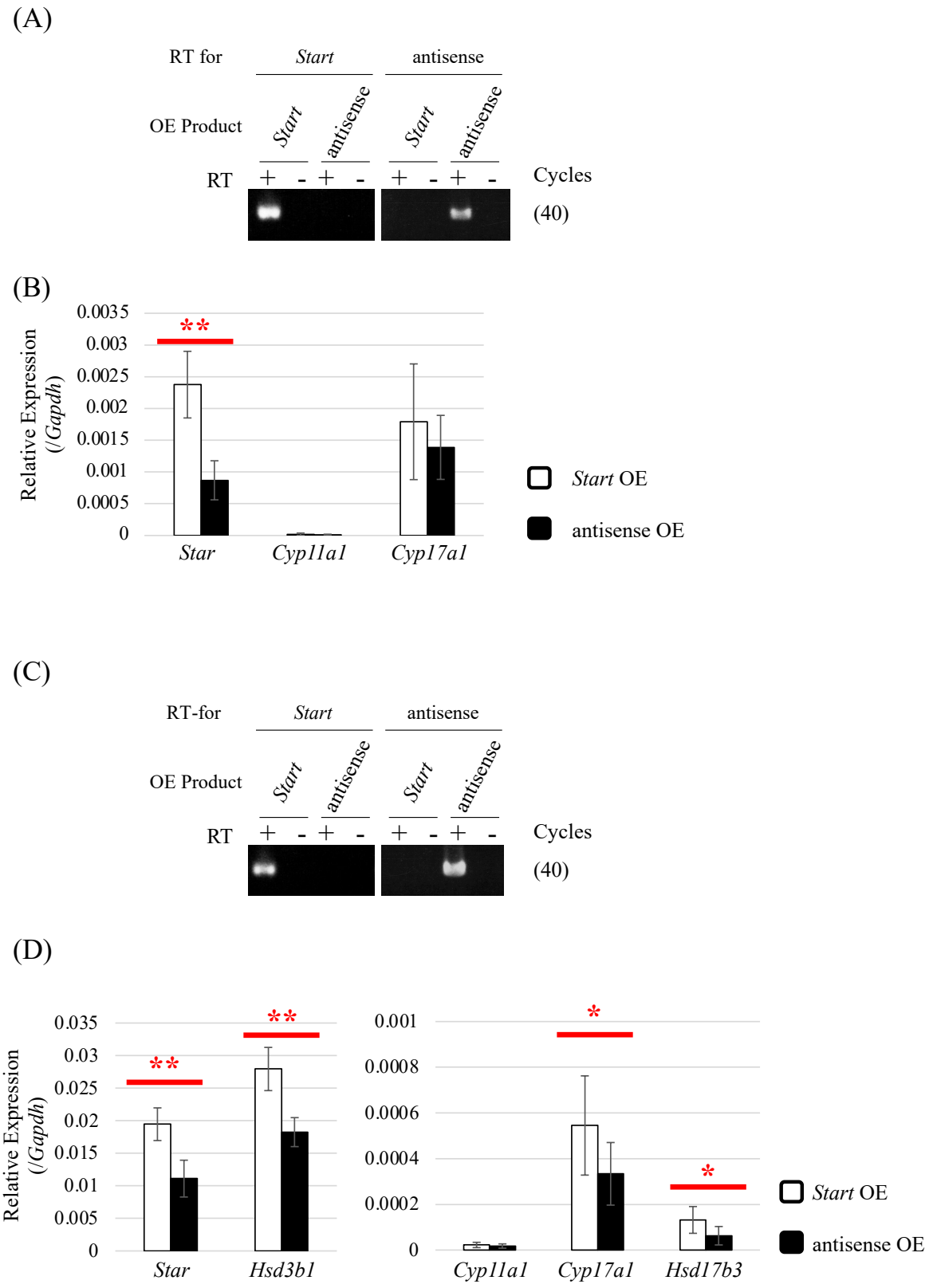

(A)
RT for
Start
antisense
OE Product
Start
antisense
Start
antisense
RT
+ - + - + - + -
Cycles
(40)
(B)
Relative Expression
(/Gapdh)
0.0035
0.003
0.0025
0.002
0.0015
0.001
0.0005
0
**
Star
Cyp11a1
Cyp17a1
Start OE
antisense OE
(C)
RT-for
Start
antisense
OE Product
Start
antisense
Start
antisense
RT
+ - + - + - + -
Cycles
(40)
(D)
Relative Expression
(/Gapdh)
0.035
0.03
0.025
0.02
0.015
0.01
0.005
0
**
**
Star
Hsd3b1
0.001
0.0008
0.0006
0.0004
0.0002
0
*
*
Cyp11a1
Cyp17a1
Hsd17b3
Start OE
antisense OE

Figure 1-8. Effect of *Start* OE in Leydig cell lines. (A) *Start* OE in TM3 cells by strand-specific RT-PCR. Total RNAs were purified from TM3 cells that had been transfected with vectors for OE of the sense or antisense strand of *Start*. RT-PCR was performed using reverse and forward primers of "*Start* full length" (Table 1-1) for specific reverse transcription of *Start* and its antisense transcript, respectively. 'RT for' shows the transcript to be detected by each RT-PCR, and 'OE Product' shows the transcript that was overexpressed in the cell. The cycle number of PCR is shown in parenthesis. (B) Expression of steroidogenic genes in TM3 cells overexpressing *Start*. Total RNAs purified in (A) were used for qRT-PCR using the oligo(dT) primer for reverse transcription. The *Gapdh* gene was used as an internal control to normalize the expression level of each gene. Data are presented as means ± S.D. from three independent experiments, and statistical significance was analyzed by Welch's t-test. ** $P < 0.01$. (C) *Start* OE in MA-10 cells by strand-specific RT-PCR. *Start* OE was performed in MA-10 cells. Strand-specific RT-PCR was performed and the results are indicated as above. (D) Expression of steroidogenic genes in MA-10 cells overexpressing *Start*. qRT-PCR was performed as in (B) and the results are shown as above. Data are presented as means ± S.D. from four independent experiments, and statistical significance was analyzed by Student's t-test. * $P < 0.05$, ** $P < 0.01$.

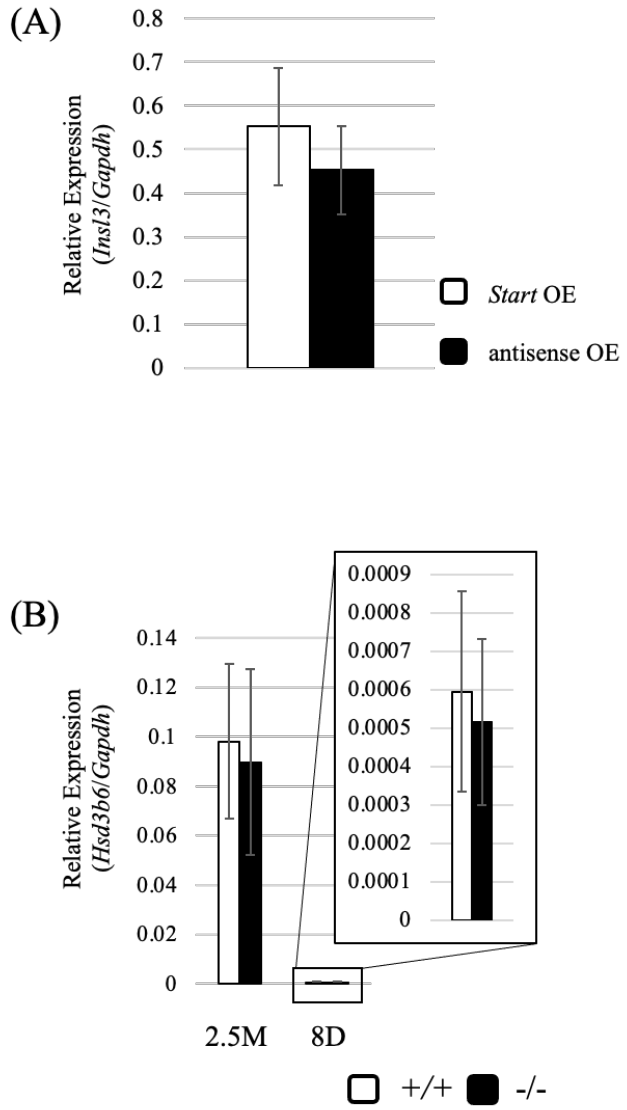


Figure 1-9. Expression of Leydig cell markers in the cultured cell MA-10 and the testis. (A) qRT-PCR was performed using RNA samples collected from MA-10 cells overexpressing *Start* and its antisense transcript. The *Gapdh* gene was used as an internal control. Data are presented as means ± S.D. from four independent experiments. Statistical significance was analyzed by Student's t-test, but no significance was detected. (B) *Hsd3b6* expression at 8 dpp (line #1) and 2.5 months (lines #1 and #2) in wild-type and *Start*-KO testes. qRT-PCR was performed by using total RNA samples from each testis. Data are presented as means ± S.D. from three sets and four sets of wild-type and KO littermates at 8 dpp and 2.5 months, respectively. Statistical significance was analyzed by Student's t-test. but no significant difference was detected.

Chapter 2

A mouse testis-specific lncRNA, *Start*, upregulates steroidogenic genes through the miRNA pathway

Abstract

An lncRNA, *Start*, dominantly localized in the cytosol of mouse Leydig cells, regulates steroidogenesis as shown in chapter 1, but the molecular mechanism of the regulation was unrevealed. Here, I attempted to reveal the molecular basis of *Start* function in Leydig cells. First, I performed reporter gene assay using the luciferase gene fused with the *Start* full-length sequence to assess whether *Start* is targeted by miRNAs. As a result, I observed significantly lower reporter activity in *Start*-fused group, and the reduction was recovered by *Start* OE. Such recovery of reporter activity was also observed by KD of *Ago2* and dicer1, ribonuclease type III (*Dicer1*), two major components in the miRNA pathway. Moreover, in a Leydig cell line, *Ago2*-KD resulted in significant upregulation of *Start*-target steroidogenic genes, while *Ago2*-OE downregulated them. The downregulation by *Ago2*-OE was reversed by co-OE of *Start*, which strongly suggests that *Start* regulates expression of steroidogenic genes via interacting with miRNAs. Indeed, miRNA pull-down assay using labelled *Start* identified miRNAs that potentially bound to *Start* in a sequence specific manner. These results supported my idea that *Start* acts as a decoy against miRNAs that target steroidogenic genes in Leydig cells.

Introduction

The testis consists of germ cells and somatic cells including Leydig cells, Sertoli cells, myoid cells, and small population of other cells [89,90]. Among those somatic cells, in adult males, only Leydig cells are responsible for steroid synthesis and produce testosterone, which is received by Sertoli cells as well as Leydig cells themselves for the complete progression of spermatogenesis [39]. According to previous studies, testosterone production ought to be tightly governed by two distinct pathways. One is the distal feedback loop involving the hypothalamus and pituitary [9-11]. Once

testosterone is released from Leydig cells, those two organs receive the signal and modulate GnRH and LH secretion according to the serum testosterone level. The LH ultimately affects testosterone production in Leydig cells, which completes the HPG_axis [10,11,38]. The other pathway is the proximal androgen-AR signaling pathway [85]. As evidenced by a previous study, AR-KO in Leydig cells disturbed expression of steroidogenic genes, suggesting the significance of autocrine regulation in steroid synthesis. While these distal and proximal control networks had been considered to play fundamental roles in steroidogenesis, I found a novel regulatory mechanism by which a testis-specific lncRNA controlled. To reach better unified understanding about regulatory mechanisms underlying endogenous steroidogenesis control, I decided to elucidate molecular basis of *Start* function in Leydig cells.

Given that *Lhb* expression in the pituitary and serum LH secretion in *Start*-KO male mice were not altered compared to wildtype, *Start* deficiency might not affect the HPG_axis. Instead, I speculated that *Start* is likely to control endogenous steroidogenesis in Leydig cells. As reviewed in a recent paper, lncRNAs are involved in gene regulation via various pathways [91]. Especially when they are localized in the cytosol, lncRNAs frequently interact with miRNAs, another class of noncoding RNAs, playing a role as post transcriptional regulators. Recently, such gene regulatory networks among mRNA-miRNA-lncRNA were termed as competing endogenous RNA (ceRNA) [70-72,92,93]. Because lncRNAs generally show higher tissue-specificity than mRNAs [94] and the testis expresses much more lncRNAs than other tissues, the ceRNA network ought to play important roles in testis-specific gene regulation. However, how the ceRNA network governs a regulatory network underlying steroidogenesis is mostly unknown.

In the chapter1, I found that *Start* was dominantly localized in the cytosol of Leydig cells and *Start* OE resulted in significant upregulation of steroidogenic gene. These results led me to hypothesize that the positive correlation between *Start* and its targets was mediated by miRNAs. To test this hypothesis, here, I utilized *in vitro* reporter gene assay and found the negative correlation of target steroidogenic genes with the *Ago2* gene, indicating the involvement of *Start* in the miRNA

pathway. In addition, miRNA pull-down assay confirmed physical binding of several miRNA species to *Star*t, emphasizing its possible function in the miRNA pathway. Thus, I concluded that *Start* directly upregulated its target genes by acting as a decoy against miRNAs in Leydig cells.

Materials and methods

Cell Culture

MA-10 cells were kindly provided from Dr. Takashi Yazawa at Asahikawa Medical University. GC-2spd(ts) cells (CRL-2196) were obtained from American Type Culture Collection. Hepa1-6 (RCB1638) cells were obtained from RIKEN Cell Bank (Tsukuba, Japan). MA-10 cells were cultured as described in chapter 1. One fiftieth of confluent cells in a 6-cm dish was spread into each well of 24-well plates one day before transfection. The next day, 5.0 µl PEI Max was mixed with 50 µl Opti-MEM and 1.5 µg DNA in that order. The mixture was added to each well after 20-min incubation. The other cells were cultured in DMEM containing 10% fetal bovine serum, 100 U/ml penicillin, 100 µg/ml streptomycin, and 292 µg/ml l-glutamine (Invitrogen, Carlsbad, CA). For transfection into GC-2 cells and Hepa1-6 cells, 1.6×10^5 cells were seeded in a 3.5-cm dish a day before transfection. Two micrograms of DNA constructs were mixed and incubated with 100 µl of Opti-MEM medium (Thermo fisher scientific) and 5.0 µl of GeneJuice (Novagen, Inc., Madison, WI) according to the manufacturer's instruction. For establishment of stable OE and Knock Down (KD) cells, selection was done with a medium containing 300 µg/ml of hygromycin for 10 days.

Plasmid Construction

The *Start* full length was cloned as described in chapter 1. To generate a construct for expression of a fusion RNA of the *Luciferase* gene and *Start*, I first inserted thymidine kinase promoter, which was isolated from the pEBMulti-Neo vector by digestion with *Bgl*II and *Hind*III, into

the *Bgl*II/*Hind*III site of the pGL3-Basic vector (TK-Luc-empty). Then, *Star*t full sequence was inserted at a blunted-*Xba*I site of TK-Luc-empty (TK-Luc-Start). At the same time, an inversely inserted construct was obtained (TK-Luc-Reverse).

The *Ago2* open reading frame was amplified by RT-PCR with a pair of primer shown in Table 2-1, total RNA purified from the mouse testis, and KOD Fx Neo (Toyobo). The product was inserted into the *Eco*RV site of a pcDNA3.1 (+) vector (Invitrogen), and its sequence was confirmed by DNA sequencing analysis. For co-OE, the open reading frame of the *Ago2* gene was digested with *Eco*RI/*Not*I and transferred to the *Eco*RI/*Not*I site of a pPBhCMV*-1-cHA-pA vector (Tet_Ago2). For *Start* OE experiment, pCAG-Start and pCAG-reverse vectors, which were generated as described in chapter 1, were used.

For KD experiment, short-hairpin RNA (shRNA) sequences against *Start, Ago2*, and *Dicer1* were designed by the BLOCK-iT RNAi Designer (https://rnaidesigner.thermofisher.com/rnaiexpress/), a web page supplied by Thermo Fisher Scientific, and were artificially synthesized (Table 2-1). Each sequence was inserted into the *Bam*HI/*Hind*III site of a pBAsi-mU6 Neo vector (Takara) that was modified to carry the hygromycin resistant gene at the blunted-*Eco*RI site.

Reporter Gene Assay

The constructs for reporter gene assay generated as above contained the firefly luciferase gene. I co-transfected them with a pRL-CMV vector (Promega, Madison, WI), by which the Renilla luciferase gene was driven by the CMV promoter, and I normalized firefly luciferase activity to Renilla luciferase activity to adjust transfection efficiency. The activity was further normalized to that of the cells transfected with a pGL3-Basic vector, and relative activity was calculated. The value from a pGL3-Basic vector was set to 1.0.

qRT-PCR

qRT-PCR for mRNAs and *Start* RNA was performed as described in chapter 1.

RT-PCR for miRNAs

For miRNA-specific purification, the testis and GC-2spd(ts) cells were collected with ISOGEN II reagent (Nippon Gene), and total RNAs were separated into two fractions, one for RNAs less than 200 nt (small RNA) and the other for longer RNAs, according to manufacturer's instruction. Small RNAs were then treated with TurboDNase (Thermo Fisher Scientific) to remove genome DNA completely and poly-adenylated by E. coli Poly (A) Polymerase (NEB), followed by reverse transcription using a 3'RACE adaptor primer (Table 2-1). After cDNA synthesis, PCR was performed with a 3'RACE outer primer and each miRNA-specific primer (Table 2-1) by KOD Fx Neo (Toyobo).

miRNA Pull-Down Assay

A 5-Bromo-2′-Uridine (BrU) -labelled *Start* RNA was synthesized by *in vitro* transcription with *Eco*RI-digested pBlue-Start (generated in chapter 1) and T3 RNA polymerase. The reverse sequence of *Start* RNA was also synthesized as a control with *Hind*III-digested pBlue-Start and T7 RNA polymerase. Each labeled RNA was mixed in TE buffer and incubated with small RNAs, which were purified from the mouse testis, to form hybridized double-strand RNAs. For this hybridization, RNAs were first kept at 94°C for 5 min, then slowly cooled to 22°C in 30 min. Then they were pulled-down by anti-BrdU antibody (MBL international, Woburn, MA, USA)-conjugated beads. The pull-down fraction was then treated with a DNase, a poly (A) polymerase, and a reverse transcriptase as described above, and was finally subjected to PCR with KOD Fx Neo (Toyobo).

Statistical analysis

Results are presented as the mean value ± S.D. of at least three independent experiments. The data were statistically analyzed by Student's t-test, Welch's t-test or one-way analysis of variance (ANOVA) followed by the Tukey HSD test. A *P* value less than 0.05 was considered statistically significant. All calculations were done by R software (Ver. 3.5.0; https://cran.ism.ac.jp/bin/windows/).

Results

Start can be targeted by the miRNA pathway

To investigate molecular mechanisms of a cytosolic lncRNA, *Start*, I examined whether *Start* could be targeted by the miRNA degradation pathway. To assess that, I connected the full length of *Start* to the 3'end of the *Luciferase* gene to express a fusion RNA composed of *Luciferase* coding sequence with *Start* RNA (Luc-Start). This and an empty construct were separately transfected into GC-2spd(ts) cells, and luciferase activity was measured as shown in Fig. 2-1A. Low activity was observed in the Luc-Start group compared to the control, whereas the activity was not decreased when the *Start* was placed in the reverse direction (Fig. 2-1A).

I then established stable *Start*-overexpressing GC-2spd(ts) cells (pCAG-Start) and performed a reporter gene assay using Luc-Start to examine whether the reduction in luciferase activity was caused in a sequence-specific manner or not. As a control, stable OE of the reverse sequence of *Start* (pCAG-reverse) was performed. As shown in Fig.2-1B, I could not find any reduction with pCAG-Start, while there was significant reduction with pCAG-reverse. Collectively, reduction of reporter activity was observed in a strand-specific manner, and that was recovered only by *Start* OE but not by reverse OE. These results implied that *Start* sequence was targeted by the miRNA pathway.

During miRNA biogenesis, the *Ago2* protein directly interacts with miRNAs, binds to their target mRNAs, and digests targets by its endonuclease activity [32-35], thus is known to be indispensable for endogenous miRNA networks. To assess whether *Start* is involved in the pathway, the *Ago2* gene was stably knocked down by shRNA transfection in GC-2spd(ts) cells (shAgo2). qRT-PCR was performed to check KD efficiency (Fig. 2-2A), and as expected, expression of the *Ago2* gene was successfully downregulated compared to an empty construct (shControl). Then, Luc-Start was transfected into these stable-KD cells to investigate its involvement in the miRNA pathway. As a

result, while luciferase activity was significantly decreased in shControl, such reduction was not observed in shAgo2 (Fig. 2-2B). This result showed that *Start* was targeted by the miRNA pathway, and such event was recovered by downregulation of components in the miRNA biogenesis.

Ago2 OE-induced downregulation of steroidogenic genes was recovered by *Start* OE

To assess whether steroidogenic genes were regulated by the miRNA pathway, I established stable *Ago2* KD cells by shRNA transfection into *Start* OE MA-10 cells that were used in chapter 1. I examined *Ago2* expression in these newly established cells, and confirmed successful decrease of the *Ago2* level (shAgo2_MA-10, Fig.2-3A). Then, qRT-PCR was performed to evaluate expression of steroidogenic genes, and the results revealed that *Star, Cyp17a1,* and *Hsd3b1* were significantly upregulated compared to a control group (Fig. 2-3A).

For further confirmation, I performed transient *Ago2* OE in MA-10 cells with the Tet_Ago2 vector. The *Ago2* gene was successfully and significantly overexpressed (Fig. 2-3B), and as expected, steroidogenic genes including *Star, Cyp11a1, Cyp17a1* and *Hsd3b1* were significantly downregulated. These results revealed that expression of *Start* targets, a subset of steroidogenic genes, was mediated by the miRNA pathway.

Based on the above results, *Start* and its target genes were found to be regulated by the *Ago2* gene, and *Start* OE resulted in significant increases of its targets. These findings led me to hypothesize that *Start* and its target genes were bound by common miRNAs. To assess this hypothesis, I performed co-OE of *Ago2* with *Start* in MA-10 cells. Because *Start* showed the sequence-dependent function, its reverse sequence was used as a control. Compared to the reverse sequence OE, *Start* OE significantly increased expression of steroidogenic genes that were downregulated by *Ago2* (Fig. 2-3C). Here, I also evaluated expression of the *Nr5a1* gene, an upstream transcription factor which regulates various steroidogenic genes including *Start* targets (reviewed in 95). As a result, *Nr5a1* gene expression was downregulated by *Ago2* OE but not affected by *Start* OE (Fig. 2-3B, C). This suggests that the *Nr5a1* gene is targeted by the miRNA pathway but not controlled by *Start*. These results supported my idea

that *Start* regulates its target steroidogenic genes by interacting with miRNAs, and the regulation was not mediated by an upstream factor, the *Nr5a1*gene.

Identification of miRNAs potentially interacting with *Start*

miRNAs can bind to their target mRNAs and/or lncRNAs in a sequence-dependent thermodynamics manner, and we can predict possible miRNAs that interact with a specific sequence. By submitting the *Start* full length to the RegRNA2.0 database (http://regrna2.mbc.nctu.edu.tw) [96], I obtained 23 miRNA candidates that might target *Start* RNA as listed in Table 2-1. To confirm whether these candidates could interact with *Start* in testicular cells or not, I first checked their expression in the mouse testis and GC-2spd(ts) cells by RT-PCR with small RNAs. As a result, out of 23 candidates, 13 miRNAs were consistently expressed in both the mouse testis and GC-2spd(ts) cells (Figs. 2-4A and B).

To identify miRNAs that can bind to the *Start* transcript, I performed a miRNA-pulldown assay using BrU-labelled *Start.* The reverse sequence of *Start* was also synthesized and used as a control. As shown in Fig.2-4C, I could successfully pull down *Start* and miRNAs in each fraction. Fig.2-4D represents the result of the first trial, in which I performed RT-PCR for all 13 candidates and detected 4 miRNA species, miR-326-3p, miR-383-3p, miR-705, and miR-1930-5p. Fig.2-4E shows the result of the second trial, in which I only checked those 4 miRNA species and detected miR-326-3p, miR-383-3p and miR-1930-5p.

Discussion

Previous studies have reported that the testis expresses much more lncRNAs than other tissues in a spatio-temporal manner [19,43], suggesting their significance in testis-specific functions; nonetheless, details of how they work was only poorly understood. Because *Start* was dominantly

localized at the cytosol in Leydig cells as shown in chapter 1, I hypothesized that *Start* regulated its target genes through the miRNA pathway. Here, by taking advantages of cultured cell lines and *in vitro* assay, I revealed a molecular mechanism underlying the *Start* function in Leydig cells. My data support my hypothesis and showed that *Start* could activate its target steroidogenic genes via the miRNA pathway and could interact with miRNA species including miR-326-5p, miR-383-3p and miR-1930-5p.

My current study demonstrated that *Start* could be regulated by the miRNA pathway and at the same time, a subset of steroidogenic genes, *Star, Cyp17a1, Hsd3b1* and *Hsd17b3*, were negatively correlated with the *Ago2* gene. These strongly suggests that both *Start* and its target genes are targeted by the miRNA pathway. Moreover, *Start* OE significantly recovered the reduction of steroidogenic genes including *Star,* and *Hsd3b1,* caused by *Ago2* OE. Therefore, I concluded that *Start* and its targets were downregulated by common miRNA sets, and indeed I identified miRNA candidates potentially interacting with *Start*. *Start* may play a role as a decoy against those miRNAs to recover expression of its target mRNAs, which leads to establishment of the ceRNA network in Leydig cells.

Previous studies have shown that cytosolic lncRNAs can rescue expression of their target mRNAs by acting as a decoy against miRNAs, and such a regulatory network is termed as ceRNA [93]. The physiological interaction among mRNAs-miRNAs-lncRNAs is believed to play a role in organizing more accurate gene expression [94,97]. Thus, ceRNAs are known to function in various biological processes including development and cancer formation, but the significance in male reproduction was still to be assessed [98-101]. A limited number of reports attempted to uncover roles of ceRNAs in the rodent testis but only under abnormal conditions such as induced hormone disturbance and cytoplasmic toxin treatment [102-104]. Therefore, further evaluation of how ceRNAs orchestrate spermatogenesis should be inspired, and in this chapter, I unraveled a potential molecular mechanism by which *Start* regulates expression of steroidogenic genes through its function as a ceRNA.

miRNAs have been found as regulators involved in steroidogenesis in Leydig cells. miR-214 is

predicted to target the *Srebp* the gene, which is indispensable for steroid transport, in mouse Leydig tumor cells [104]. miR-125a and miR-455 downregulates the *Scarb1* gene, which is required for steroidogenesis in Leydig tumor cells [105]. These examples demonstrated the functional interaction between miRNAs and their target mRNAs. With regard to the interaction between a miRNA and lncRNA, one study reported that a well-characterized lncRNA *H19* interacts with miRNA let-7 and regulates translational activity of the *Star* gene in a mouse Leydig cell line, MTLC-1 [106]. Thus, the significance of mRNA-miRNA and mRNA-lncRNA interaction in the testis has been separately reported, but how these two pathways are related for spermatogenesis and steroidogenesis was unclear. My data suggests that *Start* regulates steroidogenic genes by acting as a ceRNA in Leydig cells, which may fill a missing piece in the regulation of testis function

In this chapter, I identified three miRNA species, miR-326-3p, miR-383-3p and miR1930-5p, as candidates that physically interact with *Start* RNA. Based on the RegRNA2.0 database, these three miRNAs were predicted to bind throughout the *Start* sequence (Fig.2-4F), suggesting that the entire *Start* sequence is significant for the regulation of steroidogenesis. Of note, all the three miRNAs were reported by previous studies. miR-326-3p decreases *Phospholipase D1* expression in rat NRK-52E cells under the cadmium presence, resulting in an increase of apoptotic cells [107]. miR-383-3p interacts with the 3'untlanslated region (UTR) of IL2R2 to increase the cell availability in atherosclerosis rat [108] and is reported to function cooperatively with lncRNA HOXC-13AS in Nasopharyngeal carcinoma presumably as a part of a ceRNA network [109]. miR-1930-5p targets the *Mllt1* gene through a ceRNA network with an lncRNA, MEG3, in mouse primary cultured brain endothelial cells [110]. These findings demonstrated that the three miRNAs are physiologically functional and indicate the possibility that they can act in the mRNA-miRNA-lncRNA network for regulating the steroidogenic genes in the testis. Intriguingly, the webtool RegRNA2.0 suggested these three miRNAs have possible ability to bind to *Start* target genes, namely *Star* and *Hsd3b1* (Fig.2-4F). This support my idea of functional relevance between *Start* and its two target genes via miRNA pathway. Although further investigation is required, my data suggest that *Start* acts as a component of

the ceRNA system to activate steroidogenic genes in mouse Leydig cells.

Table 2-1. Oligo DNA sequence used in the chapter2

Name	Forward	Reverse
[Cloning]		
Ago2 ORF	ATGTACTCGGGAGCCGGCCCC GTTCTTG	TCAAGCAAAGTACATGGTGCGC AGTGTG
[shRNA]		
shAgo2	GATCCATCGAACATGAGACGT CTTTGCTGTGAAGCCACAGAT GGGCAAAGACGTCTCATGTTC GATTTTTTTA	AGCTTAAAAAAATCGAACATGA GACGTCTTTGCCCATCTGTGGCT TCACAGCAAAGACGTCTCATGTT CGATG
shDicer1	GATCCGCCGATGATGCAGCCT CTAATACTGTGAAGCCACAGA TGGGTATTAGAGGCTGCATCA TCGGCTTTTTTA	AGCTTAAAAAAGCCGATGATGC AGCCTCTAATACCCATCTGTGGC TTCACAGTATTAGAGGCTGCATC ATCGGCG
[RT-PCR]		
3’ RACE Adaptor		GCGAGCACAGAATTAATACGACT CACTATAGGTTTTTTTTTTTVN
3’ RACE outer primer		GCGAGCACAGAATTAATACGACT
miR-383-3p	CCACAGCACTGCCTGGTCAG	
miR-5113	ACAGAGGAGGAGAGAGATCC	
miR-326-3p	CCTCTGGGCCCTTCCTCCAG	
miR-344-5p	AGTCAGGCTCCTGGCTAGAT	
miR-351-5p	TCCCTGAGGAGCCCTTTGAG	
miR-468-3p	TATGACTGATGTGCGTGTGT	
miR-770-5p	AGCACCACGTGTCTGGGCCA	
miR-705	GGTGGGAGGTGGGGTGGGCA	
miR-742-3p	GAAAGCCACCATGCTGGGTA	
miR-466b-5p	TGATGTGTGTGTACATGTAC	
miR-466c-5p	TGATGTGTGTGTGCATGTAC	
miR-1930-5p	ACCTCCATAGTACCTGCAGC	
miR-1940	TATGGAGGACTGAGAAGGTG	
miR-432	TCTTGGAGTAGATCAGTGGG	
miR-767	TGCACCATGGTTGTCTGAGC	
miR-3085-5p	AGGTGCCATTCCGAGGGCCA	
miR-466o-5p	TGATGTGTGTGTACATGTAC	
miR-3097-5p	CACAGGTGGGAAGTGTGTGT	
miR-3473c	TCTCTCCAGCCCCCATAATA	

Table 2-1. (Continued)

Name	Forward	Reverse
miR-5128	CAATTGGGGCTGGCGAGATG	
miR-532-3p	CCTCCCACACCCAAGGCTTG	
miR-5107	TGGGCAGAGGAGGCAGGGAC	
miR-3473d	CCACTGAGCCACTTTCCAGC	
[qRT-PCR]		
Start	CCCACTCTTAGCCTCATGGT	CCATCACCCAGCCTGTTCGTT
Star	GGGTGGTAGTCAGGAGACAC	TTCACAGCTATGCAGTGGGA
Cyp11a1	ATGAGCCAGGAGGTCTAAGC	TCCACCCTATGGGTCCCTAA
Cyp17a1	CATGCATGAGAACGGCATCA	CATTCGAACAAGACCAGGGC
Hsd3b1	ATGAGCCACTTGTCAACTGGG AGG	TGCTGAAGCCTAAGAACTGAGA CTC
Hsd17b3	GTCACGATCGGAGCTGAATC	TCGTGTCAGGAGGAATCGTT
Nr5a1	AAGCCACTCTGTAGGACCAAG C	TGTAAATCTGACGCGAAAGCAG
Ago2	TGCCATACTGTGATCTGGGG	CCTCTCGGACGCTAGGATCT
Dicer1	ATGGGTTTAACCTGGAGCGG	AGCATCAGGGTACGTGCAAA
Ago2 open reading frame	TCACGTTCATCGTGGTGCAG	TCTTCGTGTCCACGGTTGTG
Gapdh	TGCACCACCAACTGCTTAGC	GGCATGGACTGTGGTCATGAG

Fig. 2-1

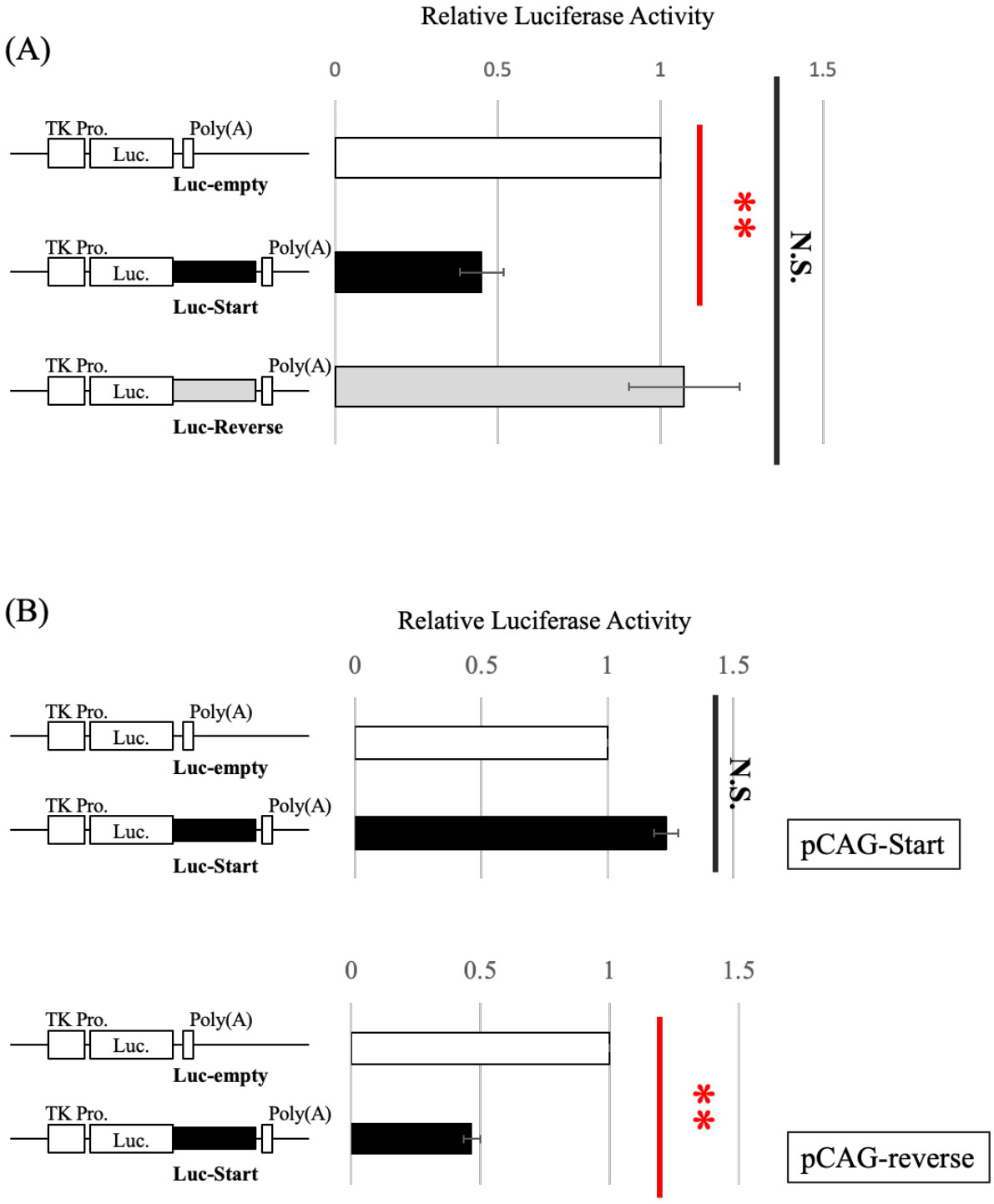

(A)
Relative Luciferase Activity
0
0.5
1
1.5
TK Pro.
Luc.
Poly(A)
Luc-empty
Luc-Start
Luc-Reverse
**
N.S.
(B)
Relative Luciferase Activity
pCAG-Start
pCAG-reverse

Figure 2-1. *Start*-linked reporter gene showed decreased activity. (A) Effect of *Start* sequence on reporter activity was examined by utilizing reporter gene assay system. The Luc-Start vector, which carries the *Luciferase* gene fused with *Start* sequence and driven by the TK promoter, was transfected into GC-2spd(ts) cells. Luc-Reverse vectors, which carries the *Luciferase* gene fused with the reverse sequence of *Start* and is driven by the TK promoter, and Luc-empty, which carries the *Luciferase* gene driven by the TK promoter, were used as control groups. Two days after transfection, cells were collected and firefly luciferase activity was measured. Each value was normalized to a value of Renilla luciferase activity. The data are presented as mean ± S.D. from five independent experiments. **: $p<0.01$. (B) Effect of *Start* sequence on reporter activity was assessed under *Start* OE. Constructs shown at the left side were transfected into pCAG-Start and pCAG-reverse cells. Reporter activity was measured as in (A). The data are presented as mean ± S.D. from three or five independent experiments in pCAG-Start and pCAG-reverse, respectively. **: $p<0.01$.

Fig. 2-2

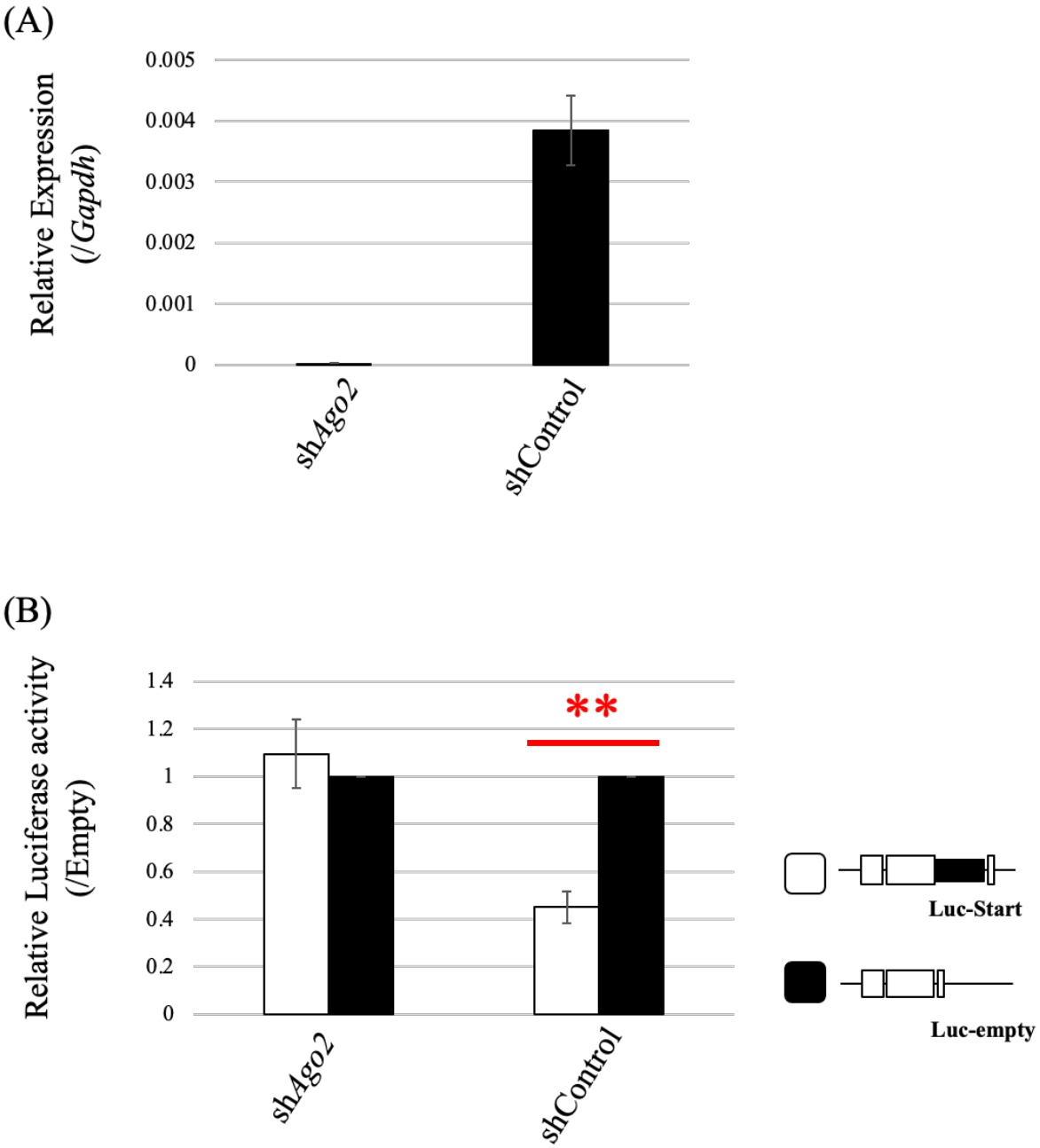

(A)
Relative Expression
(/Gapdh)
0.005
0.004
0.003
0.002
0.001
0
shAgo2
shControl
(B)
Relative Luciferase activity
(/Empty)
1.4
1.2
1
0.8
0.6
0.4
0.2
0
**
shAgo2
shControl
Luc-Start
Luc-empty

Figure 2-2. KD of miRNA machinery genes rescued a decrease in luciferase activity by *Start*. (A) KD efficiency was evaluated by qRT-PCR. shRNA vector against the *Ago2* gene was stably transfected into GC-2spd(ts) cells. After cell establishment, the expression level of *Ago2* was quantified by qRT-PCR. The data are presented as mean ± S.D. from three independent experiments. (B) Effect of *Start* sequence on reporter activity was assessed under KD of the *Ago2* gene. Constructs shown at the right side were transfected into each KD cell, separately. Luc-empty, shown in Fig. 2-1, was used as a control. Two days after transfection, cells were collected and firefly luciferase activity was measured. Each value was normalized to a value of Renilla luciferase activity. The value from Luc-empty was set to 1.0. The data are presented as mean ± S.D. from five independent experiments. **: $p<0.01$.

Fig. 2-3

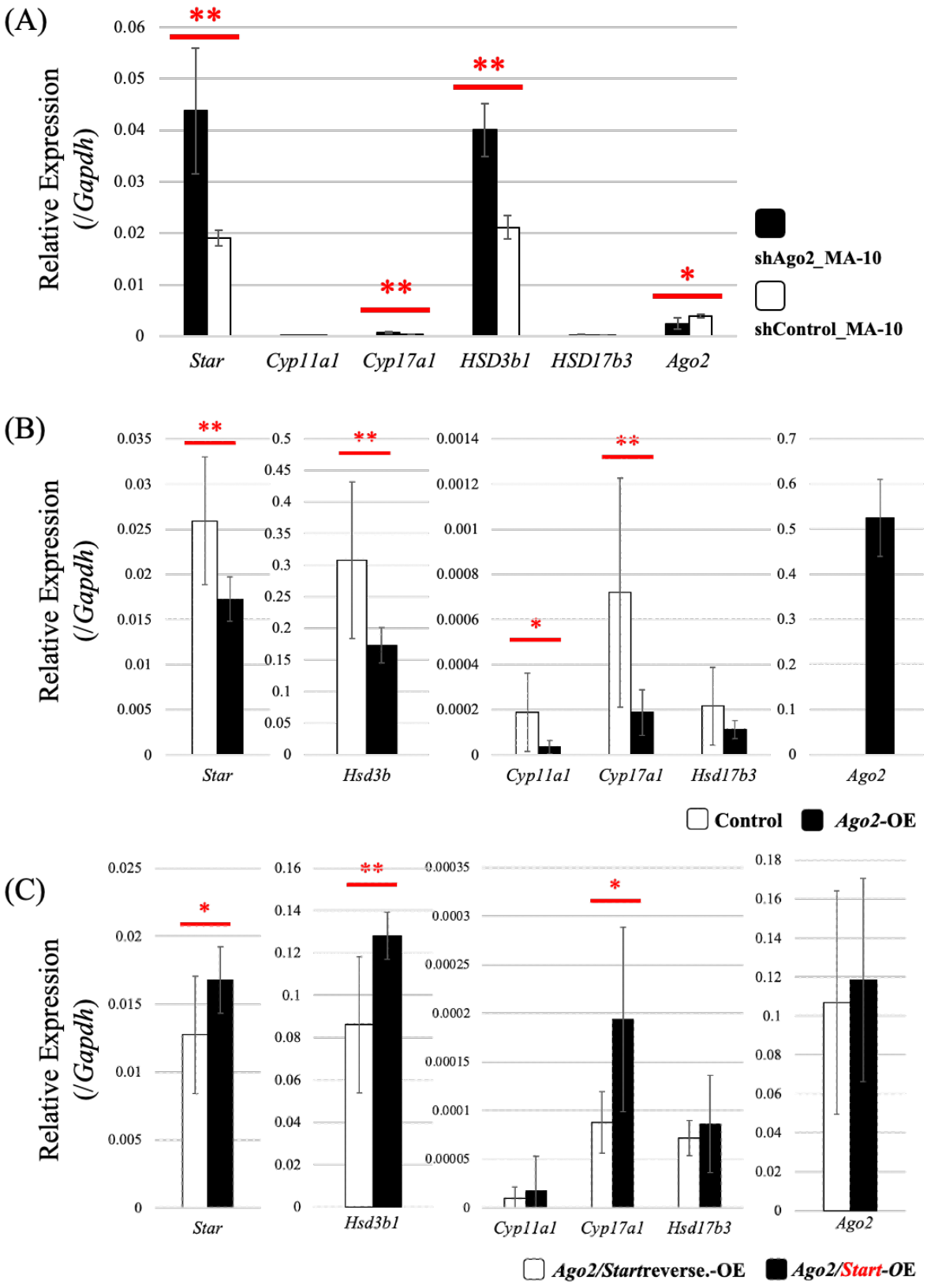
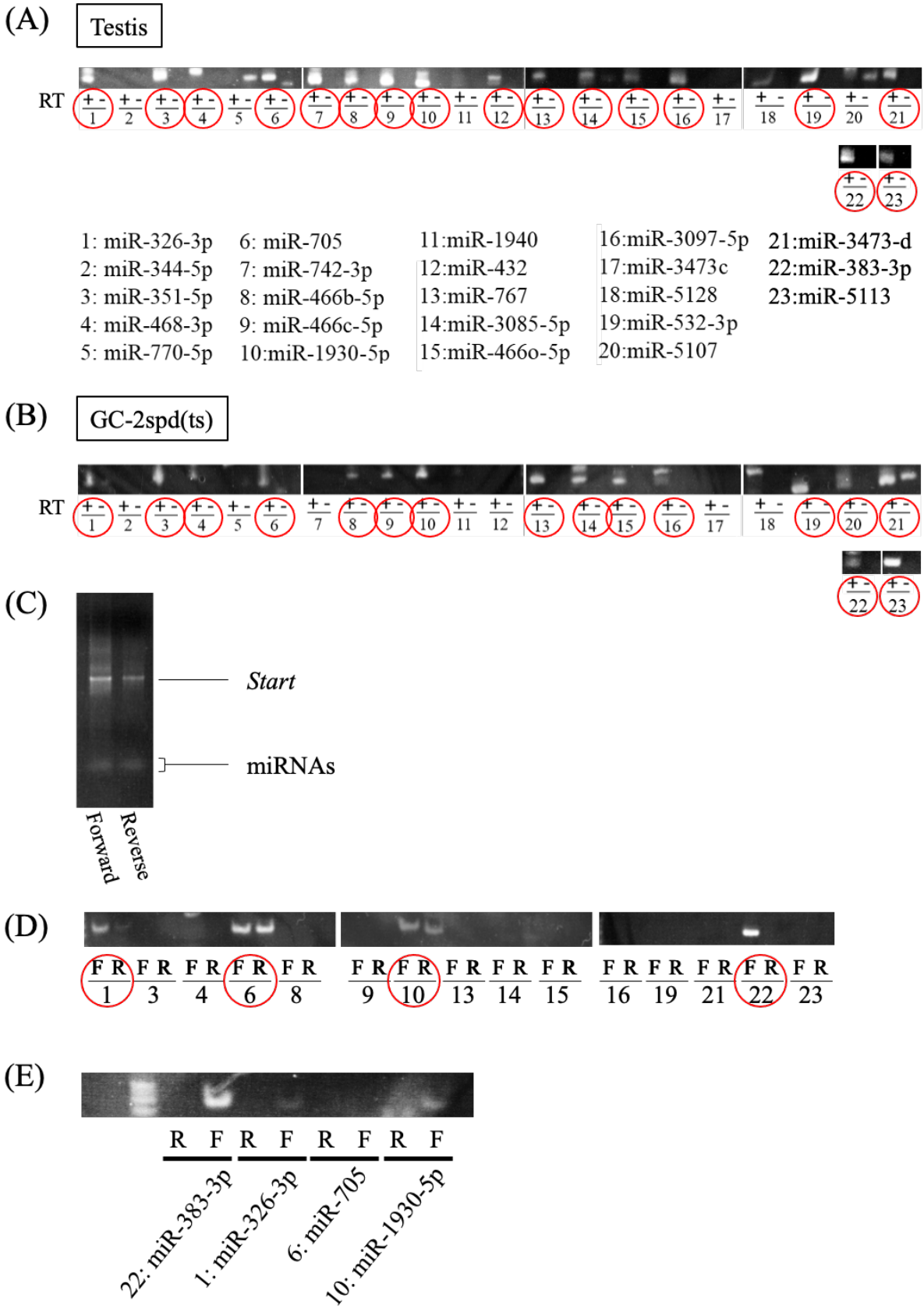

(A)
Relative Expression (/Gapdh)
0.06
0.05
0.04
0.03
0.02
0.01
0
**
**
**
*
Star
Cyp11a1
Cyp17a1
HSD3b1
HSD17b3
Ago2
shAgo2_MA-10
shControl_MA-10
(B)
Relative Expression (/Gapdh)
Star
Hsd3b
Cyp11a1
Cyp17a1
Hsd17b3
Ago2
Control
Ago2-OE
(C)
Relative Expression (/Gapdh)
Star
Hsd3b1
Cyp11a1
Cyp17a1
Hsd17b3
Ago2
Ago2/Startreverse.-OE
Ago2/Start-OE

Figure 2-3. *Start* and its target genes interact with common miRNAs. (A) The function of *Ago2* in expression of steroidogenic genes was assessed by KD experiment. The shRNA vector against the *Ago2* gene was stably transfected into Start-OE cells. After selection, expression of *Ago2* and a subset of steroidogenic genes were quantified by qRT-PCR. Each value was normalized to that for a housekeeping gene, *Gapdh*. The data are presented as mean ± S.D. from three independent experiments. *: $p<0.05$, **: $p<0.01$. shAgo2_MA-10; MA-10 cells transfected with the shAgo2 vector shControl_MA-10; MA-10 cells transfected with the pBAsi-mU6 Neo vector (B) Effects of *Ago2* OE on expression of steroidogenic genes. The Tet-Ago2 and pPBhCMV*-1-cHA-pA vector were transfected separately. Three days later, expression of *Ago2* and a subset of steroidogenic genes were quantified by qRT-PCR. Each value was normalized to that for a housekeeping gene, *Gapdh*. The data are presented as mean ± S.D. from four independent experiments. *: $p<0.05$, **: $p<0.01$ (C) Effect of co-OE of *Start* with *Ago2* OE on expression of steroidogenic genes. The Tet-Ago2 vector was co-transfected with pCAG-Start or pCAG-reverse. qRT-PCR was performed and the expression levels were calculated as in (B) The data are presented as mean ± S.D. from five independent experiments. *: $p<0.05$, **: $p<0.01$

Fig. 2-4


(A)
Testis
RT
1: miR-326-3p
2: miR-344-5p
3: miR-351-5p
4: miR-468-3p
5: miR-770-5p
6: miR-705
7: miR-742-3p
8: miR-466b-5p
9: miR-466c-5p
10:miR-1930-5p
11:miR-1940
12:miR-432
13:miR-767
14:miR-3085-5p
15:miR-466o-5p
16:miR-3097-5p
17:miR-3473c
18:miR-5128
19:miR-532-3p
20:miR-5107
21:miR-3473-d
22:miR-383-3p
23:miR-5113
(B)
GC-2spd(ts)
RT
(C)
Start
miRNAs
Forward
Reverse
(D)
(E)
22: miR-383-3p
1: miR-326-3p
6: miR-705
10: miR-1930-5p

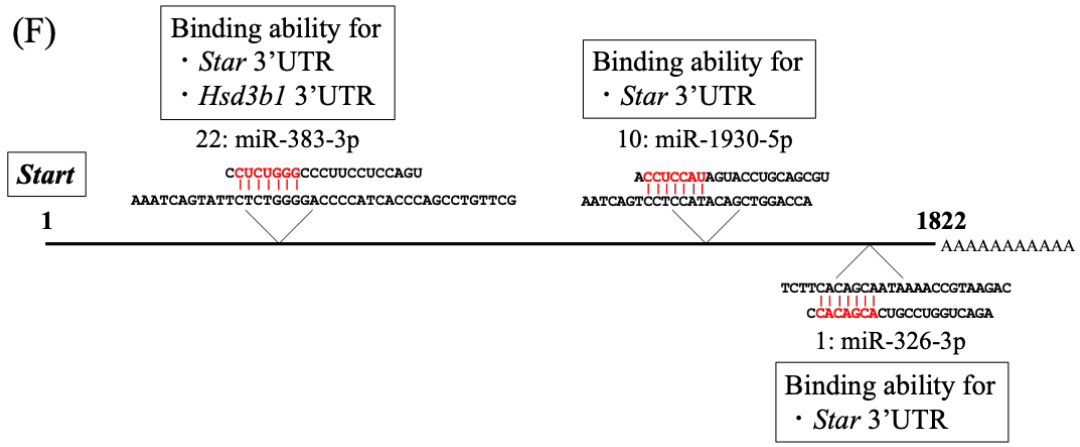


Figure 2-4. Identification of miRNAs potentially interacting with *Start*. (A) Expression of 23 candidate miRNAs was examined by RT-PCR. Small RNA fraction was purified from mouse testis. After DNase treatment, polyadenylation, and RT reaction, cDNAs were subjected to PCR. A result of 40 cycles reaction are presented. Each number represents each candidate miRNA as shown below. The numbers encircled by red are representing miRNAs which showed positive signals after reaction. (B) Expression of 23 candidate miRNAs in GC-2spd(ts) cells was examined by RT-PCR. small RNA fraction was purified from GC-2spd(ts) cells. RT-PCR was performed, and the results are shown as in (A). (C) Successful pull-down of *Start* or its reverse strand with miRNAs. Gel image represent a result of electrophoresis of RNAs in each pull-down fraction visualized by ethidium bromide staining. (D) Four miRNA candidates were identified by the first pull-down assay. miRNAs that can bind to *Start* sequence was pulled-down by using a BrdU -labeled *Start* RNA. A result of RT-PCR by 40 cycles reaction for 13 candidates are presented. F: Forward sequence of *Start*, R: Reverse sequence of *Start* (E) Three miRNA candidates were identified by the second pull-down assay. The miRNA pull-down and RT-PCR were performed as in (D). Only the four candidates in the first trial were examined in this second trial. (F) Schematic drawing of potential binding sites of the three miRNA candidates. Putative binding sites of each miRNA was simulated by the RegRNA2.0 database. The seed sequence of miRNAs is represented by red fonts. Binding ability of each miRNA for 3'UTR of two *Start* target genes were represented.

Chapter 3

Start transcription contributes to enhancer activity of a genome region encompassing it for two *Prss/Tessp* genes in mouse spermatocytes

Abstract

In previous chapters, I descrived the significance and molecular basis of *Start* function in Leydig cells. Interestingly, *Start* was also expressed in germ cells and localized in nuclei of pachytene spermatocytes, implying its function in transcriptional regulation during meiosis. Here, I investigated the function of nuclear *Start* in germ cells by focusing on its gene regulatory activity at the transcriptional level. The RNA-seq data and qRT-PCR results demonstrated that two genes, *Prss43/Tessp-3* and *Prss45*, linked to *Start* were significantly downregulated in the *Start*-KO testis. This result was consistent with reporter gene analyses that demonstrated enhancer activity of a 5.4-kb genome sequence encompassing *Start*. Moreover, induction of *Start* transcription from the 5.4-kb sequence by the Tet-on system increased its enhancer activity, and KD experiments by shRNAs exhibited significant reduction of enhancer activity. Collectively, transcriptional activity of *Start* was positively correlated with the enhancer activity served by the 5.4-kb sequence. Thus, I concluded that *Start* can play a role to activate adjacent *Prss/Tessp* genes by mediating enhancer activity of a genome region containing the *Start* sequence itself.

Introduction

Spermatogenesis is a highly complexed event which produces male haploid gametes, and can be divided into three processes including mitosis in spermatogonia, meiosis in spermatocytes, and spermiogenesis in spermatids through spermatozoa [1,2]. Throughout this process, gene expression patterns are dramatically changed in a genome-wide scale [60,111,112]. A number of genes involved in somatic cell functions are silenced at the beginning of meiosis, when meiotic genes transiently get activated. Those meiotic genes need to be tightly regulated for completion of meiosis and post meiotic events, but how they are transcriptionally activated is still to be elucidated.

During the transition from mitosis to meiosis, epigenetic regulation, especially histone modifications, plays important roles in transcriptional regulation. Histone modifications are regarded as possible markers for various types of genomic regulatory elements. For example, H3 lysine 4 mono-methylation (H3K4me1) and histone H3 lysine 27 acetylation (H3K27ac) are two major marks for active enhancers, H3 lysine 4 tri-methylation is a mark for active promoter, and H3 lysine 9 tri-methylation and H3 lysine 27 tri-methylation are present at silenced chromatin regions [113-117]. Among those elements, enhancer is broadly known as a tissue-specific regulatory element and enriched with histones carrying an acetyl group [118,119]. In fact, H3K27ac are broadly present at meiosis-specific gene loci and contribute to promoting late spermatogenetic gene expression profiles in male germ cells [112,120].

In addition to enhancers, lncRNAs also show transient appearance when spermatogonia differentiate into primary spermatocytes, and the temporal activation coincides with expression of mRNAs. Thus, lncRNAs have been presumed to play a role in transcriptional regulation during spermatogenesis. Indeed, some previous studies reported the function of lncRNAs during spermatogenesis. A mouse testis-specific lncRNA, *Tesra*, activates the *Prss42/Tessp-2* gene in primary spermatocytes, and another testis lncRNA, *Mrhl*, controls meiotic commitment in spermatogonial cells [20,28].

Moreover, recent studies uncovered the presence of lncRNAs that were transcribed from enhancer regions, termed as enhancer-derived RNAs or enhancer-RNAs (eRNAs) [121,122]. Once an eRNA is transcribed from an enhancer, it accelerates enhancer activity itself, providing the function as a transcriptional regulator. While these studies suggest the significance of lncRNAs or eRNAs in transcriptional regulation, only a limited number of studies have been reported about this issue, and the function of lncRNAs in gene regulation during spermatogenesis is still to be evaluated.

In the previous chapters, I reported the function and mechanism of *Start* in Leydig cells, but the *Start* transcript was also localized in nuclei of germ cells, primary spermatocytes at the pachytene stage, implying its contribution to transcriptional regulation. In this chapter, I attempted to investigate

a role of *Start* in germ cells and revealed that a genome sequence encompassing *Start* can act as an enhancer for linked *Prss/Tessp* genes. Thus, I concluded that this genome region would be a germline-specific enhancer for two *Prss/Tessp* genes and its activity could get activated when *Start* was transcribed.

Materials and Methods

RNA-seq analysis

RNA-seq analysis was performed as described in the chapter1. The expression level of each *Prss/Tessp* gene was calculated as gene-specific Reads Per Kilobase of exon per Million mapped reads (RPKM).

Plasmid Construction

To obtain *Start* and its flanking sequence, a bacterial artificial chromosome clone encompassing the *Prss/Tessp* gene cluster (B6Ng01-306O15, RIKEN Bioresource Center, Tsukuba, Japan) was digested with *Sac*II, and a 5.4-kb fragment was collected as BAC 5.4kb. This sequence was first cloned into a pBluescript II KS(+) vector (Novagen) (pBlue-BAC 5.4kb), then digested with *Not*I/*Sal*I, blunted, and inserted at the blunted *Bam*HI site of the TK-Luc-empty vector (TK-Luc-BAC 5.4kb). For Dox-dependent *Start* induction, a 459-bp hCMV*-1 promoter sequence was obtained by digestion of the pPBhCMV*1-cHA-pA plasmid with *Sac*II and *Acc*I. The hCMV*-1 promoter was then blunted and inserted at the *Eco*RV site of the TK-Luc-BAC 5.4kb vector (Start-OE). For generation of a Reverse-OE construct, the reverse sequence of *Start* was inserted at the blunted *Bgl*II site of the pPBhCMV*1-cHA-pA plasmid. It was digested with *Sal*I/*Mlu*I and blunted, then inserted at the *Eco*RI/*Eco*RV site of the pBlue-BAC 5.4kb plasmid. Subsequently, it was digested with *Not*I/*Sal*I and blunted, and inserted at the blunted *Bam*HI site of the TK-Luc-empty plasmid (Reverse-OE). For

generating a λ2.3kb-OE construct, a 2.3-kb λ*Hin*dIII fragment was inserted at the blunted *Bgl*II site of the pPBhCMV*1-cHA-pA plasmid. It was digested with *Sal*I/*Mlu*I and blunted, then inserted at the *Eco*RI/*Eco*RV site of the pBlue-BAC 5.4kb plasmid. Subsequently, it was digested with *Not*I/*Sal*I and blunted, and inserted at the blunted *Bam*HI site of the Luc-empty plasmid (λ2.3kb-OE).

For KD experiment, shRNA against *Start* was designed by the web-page BLOCK-iT RNAi Designer supplied by Thermo fisher scientific. Designed sequence (Table 3-1) was then inserted at the *Bam*HI/*Hin*dIII site of the pBAsi-mU6 Neo vector (Takara) that was modified to carry the hygromycin resistant gene at the blunted *Eco*RI site.

The promoter sequence of each *Prss/Tessp* gene was amplified by PCR with a pair of primers listed in Table 3-1. The promoter of each *Prss/Tessp* gene was inserted at the upstream of the *Luciferase* gene, and the BAC 5.4kb was inserted at the downstream region, resulting in reporter constructs that consisted of the *Luciferase* gene, which was driven by each *Prss/Tessp* promoter, and BAC 5.4kb. The length of each promoter was determined according to previous studies demonstrating that approximately 1.0-1.5 kb sequence was sufficient for spermatocyte-specific expression [123, 124].

Cell Culture and transfection

GC-2spd(ts) cells were cultured and used for transfection as shown in chapter 2. To establish stable “Start-OE”, “Reverse-OE” and “λ2.3kb-OE “, transfected cells were selected by 2.0 μg/ml puromycin for 10 days. For transient transfection, 2.0×10^4 cells were seeded in a 24 well-plate a day before transfection. Five hundred nanograms of DNA constructs were used for transfection with GeneJuice (Novagen) according to the manufacturer’s protocol.

Reporter Gene Assay

The constructs for reporter gene assay generated as above contained the firefly luciferase gene. In transient experiment, the pRL-CMV vector (Promega, Madison, WI), by which the Renilla

luciferase gene was driven by the CMV promoter, was co-transfected with experimental constructs. I normalized firefly luciferase activity to Renilla luciferase activity to adjust transfection efficiency.

For stable cells such as Start-OE, Reverse-OE and λ2.3kb-OE, the value of firefly luciferase was normalized by each protein amount which was measured by BCA Protein Assay Kit (Thermo fisher scientific). For transcriptional induction, cells were treated with 1 μg/ml Doxycycline (Dox) a day before reporter assay.

Statistical analysis

Results are presented as the mean value ± S.D. of at least three independent experiments. The data were statistically analyzed by Student's t-test, Welch's t-test or one-way analysis of variance (ANOVA) followed by the Tukey HSD test. A *P* value less than 0.05 was considered statistically significant. All statistical calculations were done by R software (Ver. 3.5.0; https://cran.ism.ac.jp/bin/windows/).

Results

A subset of *Prss/Tessp* genes were downregulated in *Start*-KO testes

Our group previously reported that *Tesra* and a flanking region of *lncRNA-HSVIII* can act as *cis*-regulators for the *Prss42/Tessp-2* gene in primary spermatocytes [27,28]. These studies suggested the significance of noncoding factors/elements at the locus in spermatogenesis. Therefore, I presumed that *Start* can act as a regulator of transcription of *Prss/Tessp* genes because it is localized in nuclei of primary spermatocytes (Fig. 1-4). To assess the possibility, I first calculated RPKM values of six *Prss/Tessp* genes by the RNA-seq data in *Start*-KO and wild-type testes. As a result, expression of *Prss43/Tessp-3* and *Prss45* were decreased to 17% and 47%, respectively, in Start-KO compared to wildtype (Fig. 3-1A). For further confirmation, I performed qRT-PCR using four sets of adult *Start*-

KO and wild-type testes, and revealed that *Prss43/Tessp-3* and *Prss45* were significantly downregulated to 8% and 64%, respectively, in *Start*-KO (Fig. 3-1B). These results implied a possible function of *Start* encoding sequence for regulation of these two genes.

Enhancer activity of a 5.4-kb sequence encompassing *Start*

To assess whether the *Start*-encoding region can act as a regulator at the transcriptional level, I performed a reporter gene assay using DNA constructs shown in Fig. 3-2A. This BAC 5.4kb sequence, which encompassed the full length of *Start* and its 2886-bp upstream and 702-bp downstream sequences, was inserted downstream of the *Luciferase* gene driven by the TK promoter. I separately transfected this and empty constructs into GC-2spd(ts) cells, a cell line derived from mouse spermatocytes, and measured luciferase activity (Fig. 3-2A). The result showed that BAC 5.4kb insertion clearly elevated TK promoter activity by more than 10 folds, suggesting its potential function as an enhancer, and I tentatively named its activity “Start-enhancer”.

To investigate its contribution to each *Prss/Tessp* gene, I performed a series of reporter assays using constructs that carried *Prss/Tessp* gene promoter sequences. The promoter of each *Prss/Tessp* gene was inserted at the upstream of the *Luciferase* gene, and BAC 5.4kb was inserted at the downstream region, resulting in reporter constructs that consisted of the *Luciferase* gene, which was driven by each *Prss/Tessp* promoter, and BAC 5.4kb. They were transfected independently into GC-2spd(ts) cells, and luciferase activity was measured 2 days later. As a result (Fig. 3-2B), the BAC 5.4kb sequence significantly enhanced a subset of promoters including *Prss42/Tessp-2, Prss44/Tessp-4*, *Prss45*, and *Prss50*, supporting its role as an enhancer for linked *Prss/Tessp* genes.

Positive correlation between enhancer activity of BAC 5.4kb and *Start* transcription

Interestingly, during this assay, I detected the *Start* transcript only in a BAC 5.4kb group while it was detected neither endogenously in GC-2spd(ts) cells nor in a control group. This led me to speculate that a promoter of *Start* is present within the 5.4kb sequence and is enough to drive *Start*

transcription, and such transcription contributes to enhancer function. To test whether *Start* transcription itself can accelerate enhancer activity or not, I decided to utilize the Tet-on system. The hCMV*-1 promoter, a modified promoter which is activated in the presence of Dox, was inserted 210 bp downstream of *Start* transcriptional start site to perform reporter assay with or without Dox. As control groups, two constructs encompassing the *Start* reverse sequence or a 2.3-kb sequence derived from lambda phage genome were generated ("Reverse-OE" and "λ2.3kb-OE"). I calculated a ratio of luciferase activity with Dox to that without Dox (Dox+/Dox-) to assess whether *Start* transcription contributed to Start-enhancer activity. As shown in Fig.3-3A, Start-OE by 24-hr Dox treatment elevated reporter activity by 8.2 folds whereas Reverse-OE and λ2.3kb-OE enhanced it by only 2.9 folds and 4.1 folds, respectively. Importantly, the fold increase by Start-OE was significantly high compared to that by Reverse-OE and λ2.3kb-OE, which suggested that transcription of *Start* could affect the Start-enhancer activity.

Next, to examine whether the *Start* transcript contributes to this Start-enhancer activation or not, I performed *Start* KD in *Start*-OE cells under the Dox-absent condition. I prepared three shRNA-*Start* constructs, targeting distinct sequences in *Start*, and first checked their KD efficiency (Fig. 3-3B). qRT-PCR results showed that approximately 40%, 90%, and 60% downregulation was observed by each shRNA. Then, I used all of them for measurement of luciferase activity and found that the activity was consistently and significantly reduced when *Start* was downregulated (Fig. 3-3C). This result clearly supported my hypothesis that BAC 5.4kb can act as an enhancer and its activity is positively correlated with the *Start* expression status.

Discussion

My data demonstrated that a 5.4kb genomic sequence encompassing *Start* enhanced activity of the TK promoter (Fig. 3-2A) and the potential enhancer activity could be for multiple targets including

Prss42/Tessp-2, *Prss44/Tessp-4*, *Prss45,* and *Prss50* (Fig. 3-2B). These are consistent with disturbed expression of *Prss45* in *Start*-KO testes but inconsistent with the dramatic reduction of *Prss43/Tessp-3* expression. This inconsistency might come from a partial insufficiency of the *Prss43/Tessp-3* promoter used for the reporter assay or a lack of components which drives the promoter in GC-2spd(ts) cells. In fact, public ChIP-seq data suggest broad enrichment with H3K4me1 and H3K27ac, epigenetic markers for enhancers, at the 5.4-kb region in spermatocytes but not in liver (Figs. 3-4A and B, GEO accession numbers: GSM1202711, GSM1202714, GSM4185611, and GSM4185612), which supports that the 5.4-kb region functions as an enhancer. In addition, the induction of *Start* transcription by the Tet-on system significantly increased the Start-enhancer activity, and KD of *Start* in the system downregulated the activity. Taken together, I conclude that Start-enhancer could activate transcription of *Prss43/Tessp-3* and *Prss45* genes and the activity is correlated with *Start* transcription.

An lncRNA transcribed at enhancer region is frequently termed as eRNA [121-125]. A pioneer study on eRNA revealed that the expression level of eRNA can be positively correlated with its target mRNA expression [126]. As evidenced by previous researches, transcription of RNAs that are coded for an enhancer region can accelerate its enhancer activity, supplying a novel concept of enhancer function [127,128]. Considering that *Start* was transcribed from an enhancer region and its transcriptional activity affected its enhancer activity, it can be classified as a kind of eRNA species. Given that the *Prss/Tessp* locus is considered to be indispensable for complete meiosis, *Start* transcription may mediate activity of Start-enhancer, resulting in spatio-temporal control of germline development [29-31].

In general, enhancers function in a cell type-specific manner to provide distinct transcriptome in various tissues or cells [129,130]. During spermatogenesis, spermatogenetic cell type-specific enhancers were found at each stage such as spermatocyte and round spermatid [24,131]. Moreover, a recent genome-wide study uncovered that a couple of enhancers, termed as a super enhancer, regulates hundreds of meiotic gene expression during early meiosis [120]. These findings indicate the significance of *cis*-regulating enhancers in sperm development. In case of Start-enhancer, because

Start transcription was significantly activated at 14 dpp (Fig. 1-3B), it may play a role in gene activation in early spermatogenesis.

At this point, the molecular mechanism by which Start-enhancer activates *Prss43/Tessp-3* and *Prss45* genes remains elusive, but some previous studies shed light on such a mysterious part. Previous studies have uncovered that eRNAs are supposed to enhance its target genes via mediating chromatin loop and recruiting partner proteins, at the target locus [127,128,132]. The *HOTTIP* lncRNA interacts with WDA5 and recruits it to a target locus, the *HOXA* cluster. This complex supports to form chromatin loop at the locus, resulting in increased transcription of *HOXA* cluster genes. The *p53* protein binds to the p53-bound enhancer regions and promotes transcription of eRNAs, which activates transcription of their interactive targets. The oestrogen receptor-dependent eRNAs also contribute to transcriptional activation by co-acting with an active form of estrogen receptor. Therefore, Start-enhancer may be involved in transcriptional activation of *Prss43/Tessp-3* and *Prss45* in a similar way. Further investigation to identify its partner protein and to determine whether the loop structure is formed at the locus specifically during spermatogenesis is strongly encouraged.

Table 3-1. Oligo DNA sequence used in the chapter 3

Name	Forward	Reverse
[Cloning]		
Prss45 Promoter	GCGATTGGCACCGTTTACTT	GCGCAATGACGTAGCCATAC
Prss46 Promoter	GCTCCTATCCTCCTGTCCCT	TCCACCGCCTTCCCATTTAC
Prss50 Promoter	GGTGTGCTTCAGTGACTCCA	CAGCGAGTCAGAGGTGGC
[shRNA]		
shStart-Ver.1	GATCCGGACAATCAGTTGTTCCT TTGCTGTGAAGCCACAGATGGG CAAAGGAACAACTGATTGTCCT TTTTTA	AGCTTAAAAAAGGACAATCTGTT GTTCCTTTGCCCATCTGTGGCTTC ACAGCAAAGGAACAACTGATTGT CCG
shStart-Ver.2	GATCCGCAGCTGAAAGAGACTC TAGTCTGTGAAGCCACAGATGG GACTAGAGTCTCTTTCAGCTGCT TTTTTA	AGCTTAAAAAAGCAGCTGAAAGA GACTCTAGTCCCATCTGTGGCTTC ACAGACTAGAGTCTCTTTCAGCT GC
shStart-Ver.3	GATCCGGATGAAGATTTCTAGCA AGTCTGTGAAGCCACAGATGGG ACTTGCTAGAAATCTAACATCCT TTTTTA	AGCTTAAAAAAGGATGAAGATTT CTAGCAAGTCCCATCTGTGGCTTC ACAGACTTGCTADAAATGTTCATC C
[qRT-PCR]		
Gapdh	TGCACCACCAACTGCTTAGC	GGCATGGACTGTGGTCATGAG
Prss42/Tessp-2		
Prss43/Tessp-3	GGTCTGCAAGACTCAGGACA	AGAGGACAGGGACTCCATTG
Prss44-Tessp-4	CAAGGACATCATGGGGAATA	CTACCTGCACCCACGTTTTA
Prss45	GGGAGGACTTGTGCTATGGA	ATGAGAATACCCCAGCCAGA
Prss46	TGGTTTGCCAGATGAACAAG	TGGTGTAGACGCTTGGGAAT
Prss50	CCACCGAACTCACAGACCAT	GTTGCTGGAATGAACCGTCT

Fig. 3-1

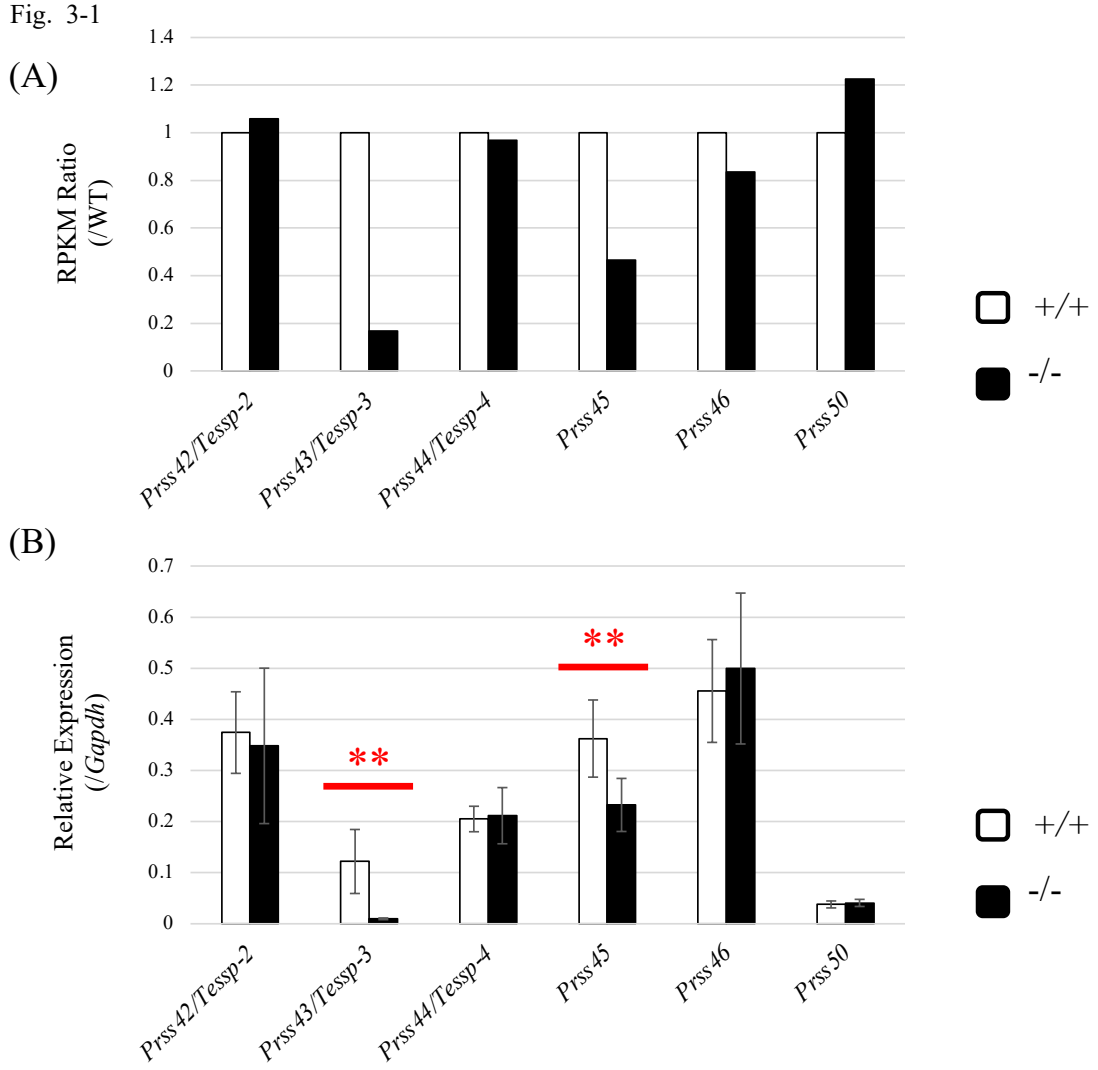


Figure 3-1. Expression of *Prss/Tessp* genes in *Start*-KO and wild-type testes. (A) Expression of the *Prss/Tessp* genes in the testis at 2.5 months (line #2) by RNA-seq. The ratios of RPKM values for *Prss42/Tessp-2, Prss43/Tessp-3, Prss44/Tessp-4, Prss45, Prss46,* and *Prss50* in a *Start*-KO testis to those in a 2.5-month-old wild-type testis were calculated. The expression level for each gene in the wild-type was set to 1 and fold changes in a KO mouse are presented. (B) Expression of the *Prss/Tessp* genes in the testis at 2.5 months (lines #1 and #2) determined by qRT-PCR. Total RNAs were purified from 2.5-month-old wild-type and *Start*-KO testes and used for qRT-PCR. The *Gapdh* gene was used as an internal control to normalize the expression level of each gene. Data are presented as means ± S.D. from four sets of wild-type and KO littermates. ** $P < 0.01$.

Fig. 3-2

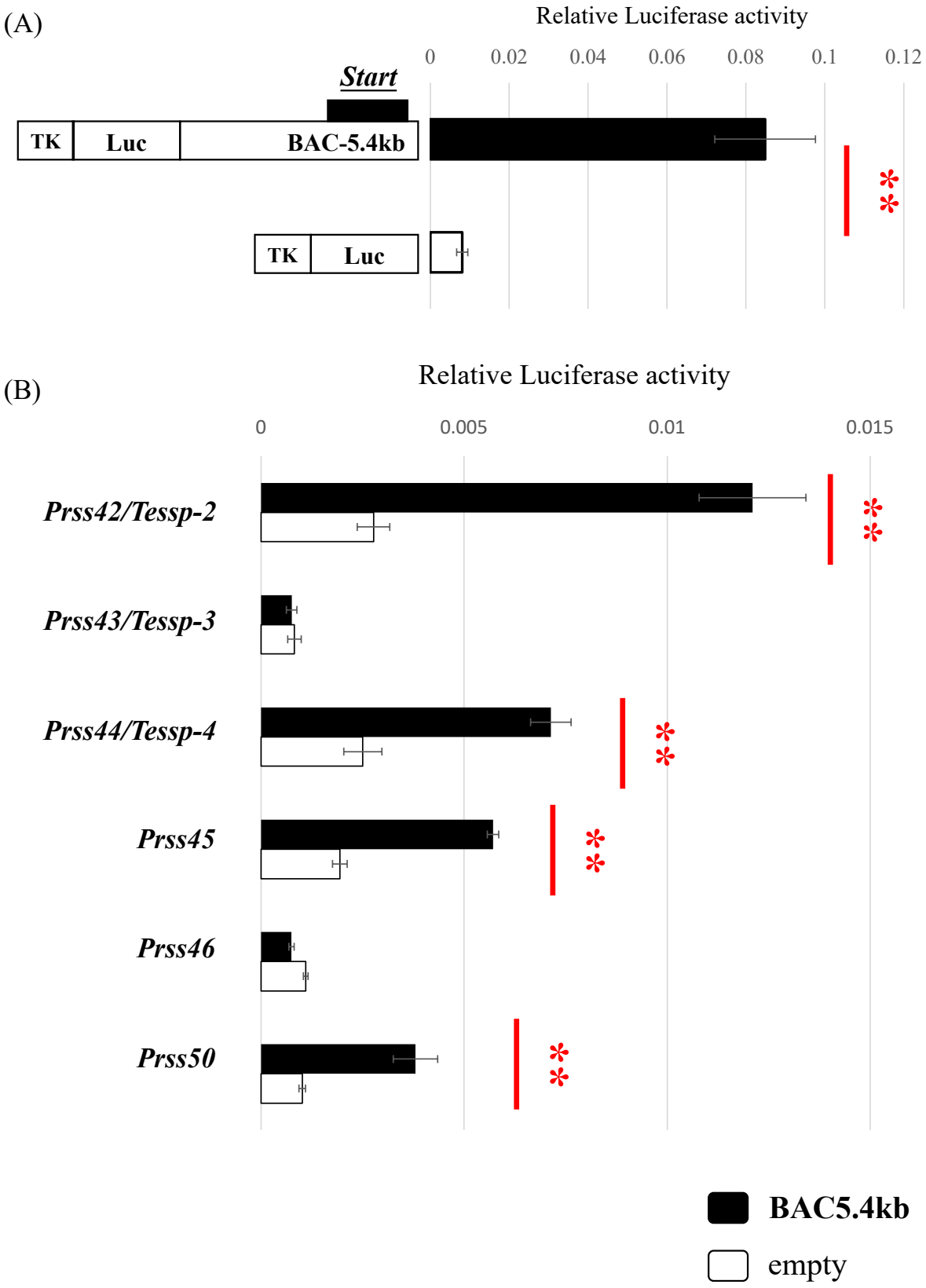
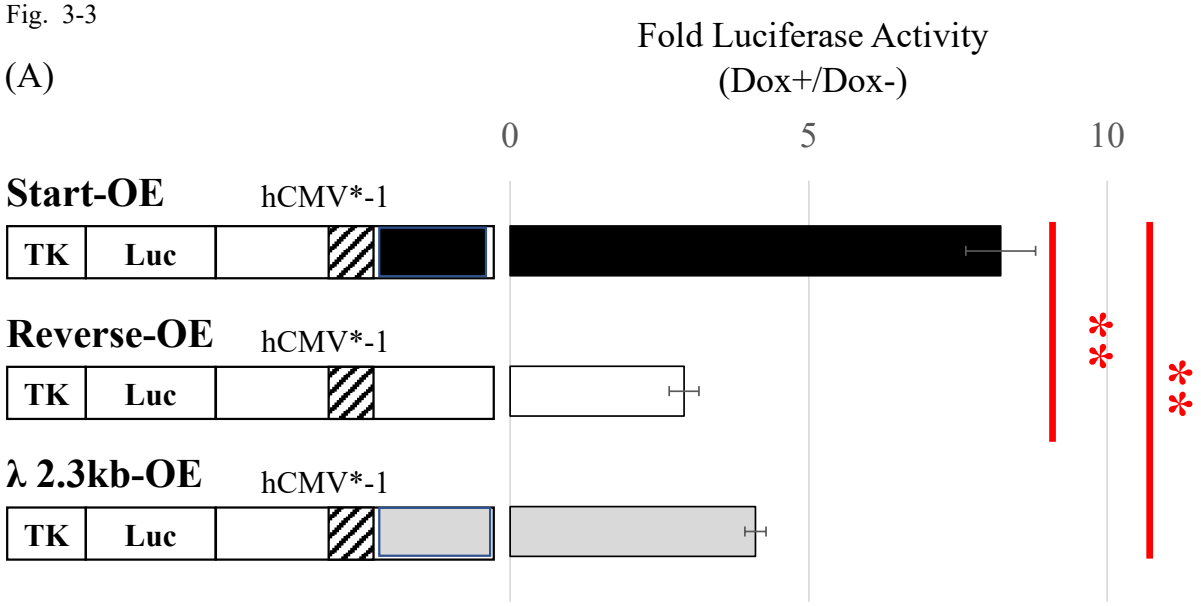
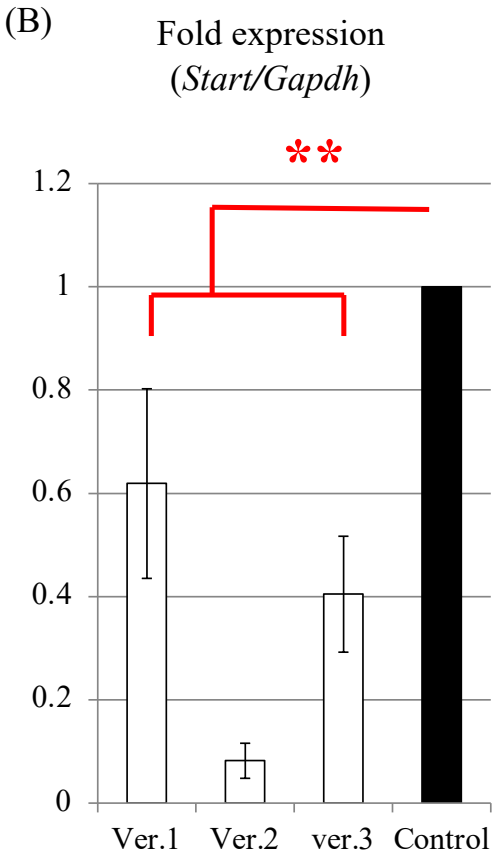

(A)
Relative Luciferase activity
0
0.02
0.04
0.06
0.08
0.1
0.12
Start
TK
Luc
BAC-5.4kb
TK
Luc
(B)
Relative Luciferase activity
0
0.005
0.01
0.015
Prss42/Tessp-2
Prss43/Tessp-3
Prss44/Tessp-4
Prss45
Prss46
Prss50
BAC5.4kb
empty

Figure 3-2. Enhancer activity of BAC 5.4kb encompassing *Start*. (A) Enhancer activity of a 5.4-kb genome sequence encompassing *Start* (BAC 5.4kb) was assessed by reporter gene assay. The BAC-derived sequence was inserted at the downstream of firefly luciferase gene as shown at the left side. This BAC-inserted vector was transfected into GC-2spd(ts) cells. The Luc-Start vector, which carries the *Luciferase* mRNA linked with *Start* sequence and driven by the TK promoter, was transfected into GC-2spd(ts) cells as a control. Two days later, cells were collected and firefly luciferase activity was measured. Each value was normalized to the value of Renilla luciferase activity. The data are presented as mean ± S.D. from three independent experiments. **: $p<0.01$. (B) Enhancer activity for *Prss/Tessp* promoters was examined by reporter gene assay. The promoter sequence of each *Prss/Tessp* gene was inserted at the upstream of the firefly luciferase gene. Then, BAC 5.4kb sequence was inserted at the downstream region. Each construct was transfected into GC-2spd(ts) cells, and 2 days after transfection, cells were collected and firefly luciferase activity was measured. Each value was normalized to the value of Renilla luciferase activity. The data are presented as mean ± S.D. from three independent experiments. **: $p<0.01$.

Fig. 3-3


(A)
Fold Luciferase Activity
(Dox+/Dox-)
0
5
10
Start-OE
hCMV*-1
TK
Luc
Reverse-OE
hCMV*-1
TK
Luc
λ 2.3kb-OE
hCMV*-1
TK
Luc
**
**


(B)
Fold expression
(Start/Gapdh)
**
1.2
1
0.8
0.6
0.4
0.2
0
Ver.1
Ver.2
ver.3
Control

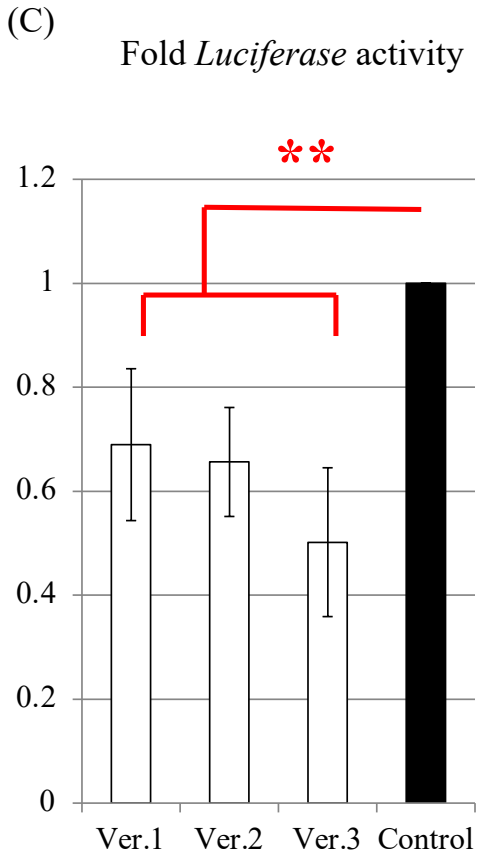

(C)
Fold Luciferase activity
**
1.2
1
0.8
0.6
0.4
0.2
0
Ver.1
Ver.2
Ver.3
Control

Figure 3-3. *Start* expression correlated with Start-enhancer activity. (A) Induction of *Start* transcription significantly upregulated enhancer activity. Constructs shown at the left side were transfected into GC-2spd(ts) cells. A day after transfection, Dox+ cells were treated with 1 μg/ml of Dox, while Dox- cells were treated with the same volume of Milli-Q water. A day after the Dox treatment, cells were collected and firefly luciferase activity was measured. Each value was then normalized to the amount of protein determined by the BCA assay. The ratio of the value in Dox+ to that in Dox- was calculated. The graph represents the ratio value in each sample. The data are presented as mean ± S.D. from five independent experiments. **: $p<0.01$. (B) KD efficiency of three shRNAs was evaluated by qRT-PCR. Each shRNA construct was separately and stably transfected into *Start*-OE cells. After establishment, total RNA was collected from each cell and used for qRT-PCR. The *Gapdh* gene was used as an internal control to normalize the expression level of each gene. Data are presented as means ± S.D. from four independent experiments. ** $P < 0.01$. (C) *Start*-KD effect on enhancer activity was evaluated by reporter gene assay. Transfected cells as in (B) were collected and used for reporter gene assay. The firefly luciferase activity was measured, and each value was normalized to the amount of protein determined by BCA assay. The value in Control was set to 1.0. The data are presented as mean ± S.D. from five independent experiments. **: $p<0.01$.

Fig. 3-4

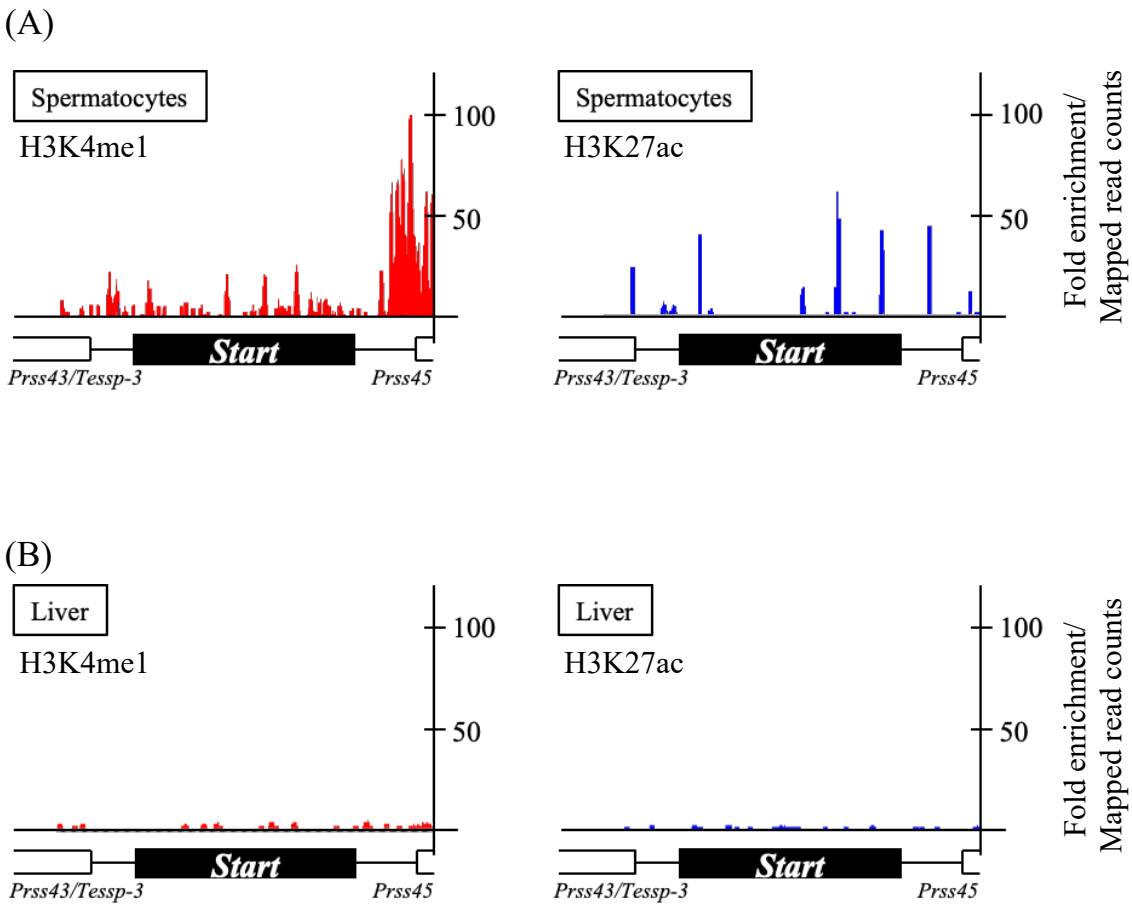


Figure 3-4. Enhancer marks at the BAC 5.4kb region encompassing *Start* in spermatocytes and liver. (A) The ChIP-seq data for two histone modification patterns in spermatocytes are shown. The epigenetic marks are H3K4me1 (left panel, red) and H3K27ac (right panel, blue). (B) The ChIP-seq data for two histone modification patterns in the liver are shown as in (A).

General Discussion

This study has attempted to reveal the function of a novel testis-specific lncRNA, *Start*, in mouse testicular germ cells and Leydig cells. Most notably, this study provided evidences of *Start* function in two distinct functions and cell types (Fig. 4). In germ cells, *Start* can act as an eRNA that accelerates transcription of linked *Prss43/Tessp-3* and *Prss45* genes. Given that *Start* expression is elevated at 14 dpp but its target genes are activated at a bit later stage during spermatogenesis, *Start* may first be transcribed and consequently activate Start-enhancer. According to previous studies, eRNAs are involved in gene regulation in a spatio-temporal manner similarly to canonical enhancers, resulting in cell-type specific gene expression profiles [133-135]. Therefore, this *Start* RNA may contribute to the transition of gene expression patterns from mitosis to meiosis during spermatogenesis. Particularly, one of its targets, *Prss43/Tessp-3*, is known to be essential for the progression of meiosis, as evidenced by an inhibitory experiment of PRSS43 protein in cultured testis pieces leading to increased number of apoptotic cells [29]. The other target, PRSS45 protein, was found in spermatids and mature sperm, suggesting its roles in sperm development or fertilization [30]. Thus, *Start* may control the cell availability and/or sperm quality in the testis. Seemingly consistent with this hypothesis, in 7-month-old *Start*-KO testes, the *Sycp2* gene, a marker for pachytene spermatocytes, tended to be decreased compared to wild-type, which implies that *Start* functions in the maintenance of spermatogenetic cells (data not shown because n=2).

On the other hand, in Leydig cells, *Start* ought to act as a decoy against miRNA species in the cytoplasm. To date, there have been only one study reporting the presence of ceRNA network which regulates steroidogenesis in Leydig cells [106]. Based on the study, an lncRNA, *H19,* one of the most characterized lncRNAs among tissues, interacts with let-7 family miRNAs and regulates *Star* expression in mouse Leydig cell line MLTC-1. Considering that *Start* targets multiple steroidogenic genes, it may act on steroidogenic regulation in a similar way. In addition, in chapter 2, three miRNA species, miR-326-3p, miR-383-3p and miR-1930-5p, were identified as they interacted with *Start* RNA in a sequence-dependent manner. Because I did not assess the direct interaction between *Start* and miRNAs in Leydig cells, it is not sure whether these miRNAs are truly involved in the regulation

of steroidogenesis via *Start*. Further investigation using miRNA mimics or agonists is needed to determine their significance on expression of steroidogenic genes.

Collectively, *Start* has functions in both spermatogenesis and steroidogenesis, and therefore it is regarded as a multi-functional lncRNA: the transcriptional activation in germ cells and the upregulation of steroidogenesis in Leydig cells through the miRNA pathway. Today, there are several studies that indicated multiple roles of lncRNAs. As examples, *H19* plays a role in dosage compensation in nuclei and acts as a decoy against miRNAs in the cytosol [106,136]. lncRNA *Gas5* also interacts with miRNAs in the cytosol, provides small nucleolar RNAs, antagonizes the glucocorticoid receptor, and binds to polycomb repressive complex 2 to recruit it at the *Irf4* locus for gene silencing [137-140]. However, there are still no findings of eRNA which also acts as a component of ceRNA involved in testis-specific function. Therefore, this report is the first example of a multi-functional tissue-specific lncRNA in the testis, suggesting the novel significance of a noncoding element/factor which precisely finetunes the male reproductive trail.

Currently, our group has revealed three distinct testis-specific lncRNAs, *lncRNA-HSVIII, Tesra* and *Start*, at the mouse *Prss/Tessp* gene locus. Interestingly, all three lncRNAs are transcribed both in Leydig cells and in germ cells. Recently developed single cell analyses revealed significant difference in gene expression profiles between germ cells and somatic cells in the testis [141,142]. Those study suggested that gene expression profiles are totally different not only between germ cells and somatic cells, but also even among somatic cells. In contrast to those findings, our group found the common presence of lncRNAs that are transcribed specifically in Leydig cells and germ cells from the same locus. This suggests the presence of unknown but universal transcriptional regulatory mechanisms underlying different cell types to govern tissue-specific function.

In this study, I have identified a novel testis-specific lncRNA and revealed its function both in steroidogenesis in Leydig cells and spermatogenesis in germ cells. For decades, transcriptomic studies have implied the presence and significance of lncRNAs in the testis, but only few studies have discovered the detail of each lncRNA. How lncRNAs regulate gene expression is still mostly

unknown, and the functional investigation on testis lncRNAs had been profoundly awaited. My study provided evidences that clarified the physiological importance of *Start* in two distinct pathways in the testis, solving the challenging problems in the reproductive science field.

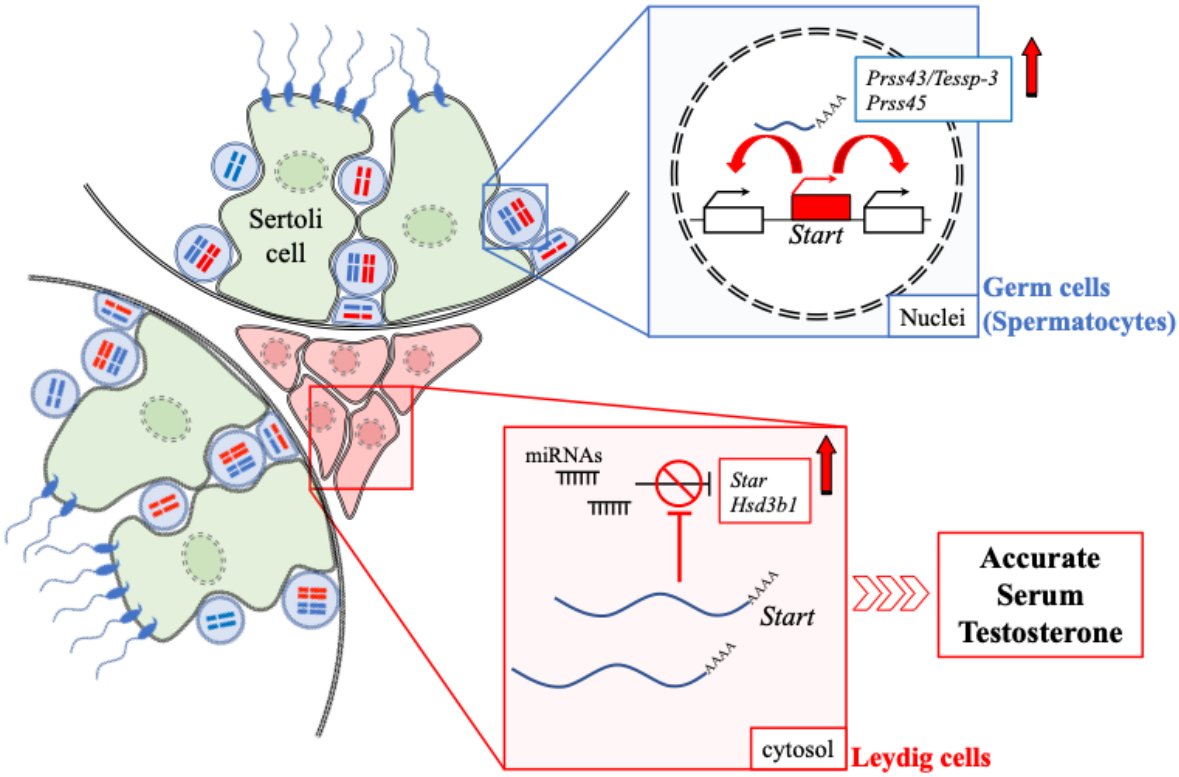


Figure 4. A schematic drawing of *Start* multiple-function in the testis. Germ cells, Leydig cells, and Sertoli cells were colored with blue, red and green, respectively. *Start* expresses both in germ cells and Leydig cells, and functions in two distinct pathways. In Leydig cells, as shown in the chapter1 and chapter2, *Start* acts as a decoy against miRNAs in the cytosol, and eventually upregulates its target steroidogenic genes. This is consistent with a significant reduction of serum testosterone level observed in *Start*-KO male. On the other hand, in germ cells, a genomic sequence encompassing *Start* can act as an enhancer against linked *Prss43/Tessp-3* and *Prss45,* as shown in the chapter3. Moreover, its enhancer activity exhibited positive correlation with *Start* transcription.

Acknowledgement

I wish to express my grateful acknowledgement to Associate Professor Atsushi P. Kimura for his kind and earnest instruction, positive encouragements, and really meaningful discussion throughout this study. I am deeply grateful to Professor Yoshinao Katsu, Professor Asato Kuroiwa, and Associate Professor Tomoya Kotani for their various comments, advices, discussion, and encouragements. I express deep gratitude to Professor Honoo Satake, Dr Akira Shiraishi, and Dr Shin Matsubara in the Suntory Foundation for Life Sciences for their great instruction on deep-sequencing analysis and positive advices on research progression. Ms. Miho Terao and Dr. Shuji Takada in the National Center for Child Health and Development for their outstanding techniques to generate KO mice used in chapter 1 and chapter 3, Dr. Takashi Yazawa for kindly producing two Leydig cell-derived cell lines, TM3 cells and MA-10 cells, used in chapter 1 and chapter 2, and Associate Professor Tomoya Kotani and Ms. Natsumi Takei for their powerful expertise of *in situ* hybridization. I particularly would like to thank Associate Professor Katsueki Ogiwara, Dr. Yui Satoh and Dr. Yuki Maruyama for their technical help and positive advices. Finally, I am pleased to thank every members belonging to the reproduction and developmental course for their technical help, great discussion, daily talk, and deep kindness in my laboratory life.

References

1. Jan, S. Z., Hamer, G., Repping, S., de Rooij, D. G., van Pelt, A. M., & Vormer, T. L. (2012). Molecular control of rodent spermatogenesis. Biochimica et biophysica acta, 1822(12), 1838–1850. https://doi.org/10.1016/j.bbadis.2012.02.008
2. Hecht N. B. (1998). Molecular mechanisms of male germ cell differentiation. BioEssays : news and reviews in molecular, cellular and developmental biology, 20(7), 555–561. https://doi.org/10.1002/(SICI)1521-1878(199807)20:7<555::AID-BIES6>3.0.CO;2-J
3. Kopera, I. A., Bilinska, B., Cheng, C. Y., & Mruk, D. D. (2010). Sertoli-germ cell junctions in the testis: a review of recent data. Philosophical transactions of the Royal Society of London. Series B, Biological sciences, 365(1546), 1593–1605. https://doi.org/10.1098/rstb.2009.0251
4. Meng, X., Lindahl, M., Hyvönen, M. E., Parvinen, M., de Rooij, D. G., Hess, M. W., Raatikainen-Ahokas, A., Sainio, K., Rauvala, H., Lakso, M., Pichel, J. G., Westphal, H., Saarma, M., & Sariola, H. (2000). Regulation of cell fate decision of undifferentiated spermatogonia by GDNF. Science, 287(5457), 1489–1493. https://doi.org/10.1126/science.287.5457.1489
5. Mark, M., Jacobs, H., Oulad-Abdelghani, M., Dennefeld, C., Féret, B., Vernet, N., Codreanu, C. A., Chambon, P., & Ghyselinck, N. B. (2008). STRA8-deficient spermatocytes initiate, but fail to complete, meiosis and undergo premature chromosome condensation. Journal of cell science, 121(Pt 19), 3233–3242. https://doi.org/10.1242/jcs.035071
6. Chen, H., Ge, R. S., & Zirkin, B. R. (2009). Leydig cells: From stem cells to aging. Molecular and cellular endocrinology, 306(1-2), 9–16. https://doi.org/10.1016/j.mce.2009.01.023
7. Zirkin, B. R., & Papadopoulos, V. (2018). Leydig cells: formation, function, and regulation. Biology of reproduction, 99(1), 101–111. https://doi.org/10.1093/biolre/ioy059
8. Meng, J., Holdcraft, R. W., Shima, J. E., Griswold, M. D., & Braun, R. E. (2005). Androgens regulate the permeability of the blood-testis barrier. Proceedings of the National Academy of Sciences of the United States of America, 102(46), 16696–16700. https://doi.org/10.1073/pnas.0506084102

9. Kaprara, A., & Huhtaniemi, I. T. (2018). The hypothalamus-pituitary-gonad axis: Tales of mice and men. Metabolism: clinical and experimental, 86, 3–17. https://doi.org/10.1016/j.metabol.2017.11.018
10. Jin, J. M., & Yang, W. X. (2014). Molecular regulation of hypothalamus-pituitary-gonads axis in males. Gene, 551(1), 15–25. https://doi.org/10.1016/j.gene.2014.08.048
11. Harter, C., Kavanagh, G. S., & Smith, J. T. (2018). The role of kisspeptin neurons in reproduction and metabolism. The Journal of endocrinology, 238(3), R173–R183. https://doi.org/10.1530/JOE-18-0108
12. Heinrich, A., & DeFalco, T. (2020). Essential roles of interstitial cells in testicular development and function. Andrology, 8(4), 903–914. https://doi.org/10.1111/andr.12703
13. Umehara, T., Kawashima, I., Kawai, T., Hoshino, Y., Morohashi, K. I., Shima, Y., Zeng, W., Richards, J. S., & Shimada, M. (2016). Neuregulin 1 Regulates Proliferation of Leydig Cells to Support Spermatogenesis and Sexual Behavior in Adult Mice. Endocrinology, 157(12), 4899–4913. https://doi.org/10.1210/en.2016-1478
14. Kapranov, P., Cheng, J., Dike, S., Nix, D. A., Duttagupta, R., Willingham, A. T., Stadler, P. F., Hertel, J., Hackermüller, J., Hofacker, I. L., Bell, I., Cheung, E., Drenkow, J., Dumais, E., Patel, S., Helt, G., Ganesh, M., Ghosh, S., Piccolboni, A., Sementchenko, V., … Gingeras, T. R. (2007). RNA maps reveal new RNA classes and a possible function for pervasive transcription. Science (New York, N.Y.), 316(5830), 1484–1488. https://doi.org/10.1126/science.1138341
15. Esteller M. (2011). Non-coding RNAs in human disease. Nature reviews. Genetics, 12(12), 861–874. https://doi.org/10.1038/nrg3074
16. Wang, J., Liu, X., Wu, H., Ni, P., Gu, Z., Qiao, Y., Chen, N., Sun, F., & Fan, Q. (2010). CREB up-regulates long non-coding RNA, HULC expression through interaction with microRNA-372 in liver cancer. Nucleic acids research, 38(16), 5366–5383. https://doi.org/10.1093/nar/gkq285
17. Gong, C., & Maquat, L. E. (2011). "Alu"strious long ncRNAs and their role in shortening mRNA half-lives. Cell cycle (Georgetown, Tex.), 10(12), 1882–1883.

https://doi.org/10.4161/cc.10.12.15589

18. Brown, C. J., Ballabio, A., Rupert, J. L., Lafreniere, R. G., Grompe, M., Tonlorenzi, R., & Willard, H. F. (1991). A gene from the region of the human X inactivation centre is expressed exclusively from the inactive X chromosome. Nature, 349(6304), 38–44. https://doi.org/10.1038/349038a0
19. Necsulea, A., Soumillon, M., Warnefors, M., Liechti, A., Daish, T., Zeller, U., Baker, J. C., Grützner, F., & Kaessmann, H. (2014). The evolution of lncRNA repertoires and expression patterns in tetrapods. Nature, 505(7485), 635–640. https://doi.org/10.1038/nature12943
20. Kataruka, S., Akhade, V. S., Kayyar, B., & Rao, M. (2017). Mrhl Long Noncoding RNA Mediates Meiotic Commitment of Mouse Spermatogonial Cells by Regulating Sox8 Expression. Molecular and cellular biology, 37(14), e00632-16. https://doi.org/10.1128/MCB.00632-16
21. Arun, G., Akhade, V. S., Donakonda, S., & Rao, M. R. (2012). mrhl RNA, a long noncoding RNA, negatively regulates Wnt signaling through its protein partner Ddx5/p68 in mouse spermatogonial cells. Molecular and cellular biology, 32(15), 3140–3152. https://doi.org/10.1128/MCB.00006-12
22. Nakajima, R., Sato, T., Ogawa, T., Okano, H., & Noce, T. (2017). A noncoding RNA containing a SINE-B1 motif associates with meiotic metaphase chromatin and has an indispensable function during spermatogenesis. PloS one, 12(6), e0179585. https://doi.org/10.1371/journal.pone.0179585
23. Kurihara, M., Otsuka, K., Matsubara, S., Shiraishi, A., Satake, H., & Kimura, A. P. (2017). A Testis-Specific Long Non-Coding RNA, lncRNA-Tcam1, Regulates Immune-Related Genes in Mouse Male Germ Cells. Frontiers in endocrinology, 8, 299. https://doi.org/10.3389/fendo.2017.00299
24. Yang, H., Wang, F., Li, F., Ren, C., Pang, J., Wan, Y., Wang, Z., Feng, X., & Zhang, Y. (2018). Comprehensive analysis of long noncoding RNA and mRNA expression patterns in sheep testicular maturation. Biology of reproduction, 99(3), 650–661.

https://doi.org/10.1093/biolre/ioy088

25. Gao Y., Li S., Lai Z., Zhou Z., Wu F., Huang Y., Lan X., Lei C., Chen H., & Dang R. (2019). Analysis of long non-coding RNA and mRNA expression profiling in immature and mature bovine (Bos taurus) testes. Frontiers in genetics, 10, 646. https://doi.org/10.3389/fgene.2019.00646
26. Kimura, A. P., Yoneda, R., Kurihara, M., Mayama, S., & Matsubara, S. (2017). A Long Noncoding RNA, lncRNA-Amhr2, plays a role in Amhr2 gene activation in mouse ovarian granulosa cells. Endocrinology, 158(11), 4105–4121. https://doi.org/10.1210/en.2017-00619
27. Yoneda, R., Satoh, Y., Yoshida, I., Kawamura, S., Kotani, T., & Kimura, A. P. (2016). A genomic region transcribed into a long noncoding RNA interacts with the Prss42/Tessp-2 promoter in spermatocytes during mouse spermatogenesis, and its flanking sequences can function as enhancers. Molecular reproduction and development, 83(6), 541–557. https://doi.org/10.1002/mrd.22650
28. Satoh, Y., Takei, N., Kawamura, S., Takahashi, N., Kotani, T., & Kimura, A. P. (2019). A novel testis-specific long noncoding RNA, Tesra, activates the Prss42/Tessp-2 gene during mouse spermatogenesis†. Biology of reproduction, 100(3), 833–848. https://doi.org/10.1093/biolre/ioy230
29. Yoneda, R., Takahashi, T., Matsui, H., Takano, N., Hasebe, Y., Ogiwara, K., & Kimura, A. P. (2013). Three testis-specific paralogous serine proteases play different roles in murine spermatogenesis and are involved in germ cell survival during meiosis. Biology of reproduction, 88(5), 118. https://doi.org/10.1095/biolreprod.112.106328
30. Ou, C. M., Lin, S. R., Lin, H. J., Luo, C. W., & Chen, Y. H. (2010). Exclusive expression of a membrane-bound Spink3-interacting serine protease-like protein TESPL in mouse testis. Journal of cellular biochemistry, 110(3), 620–629. https://doi.org/10.1002/jcb.22571
31. Holcomb, R. J., Oura, S., Nozawa, K., Kent, K., Yu, Z., Robertson, M. J., Coarfa, C., Matzuk, M. M., Ikawa, M., & Garcia, T. X. (2020). The testis-specific serine proteases PRSS44, PRSS46, and

PRSS54 are dispensable for male mouse fertility†. Biology of reproduction, 102(1), 84–91. https://doi.org/10.1093/biolre/ioz158

32. Hutvágner, G., McLachlan, J., Pasquinelli, A. E., Bálint, E., Tuschl, T., & Zamore, P. D. (2001). A cellular function for the RNA-interference enzyme Dicer in the maturation of the let-7 small temporal RNA. Science, 293(5531), 834–838. https://doi.org/10.1126/science.1062961
33. Ketting, R. F., Fischer, S. E., Bernstein, E., Sijen, T., Hannon, G. J., & Plasterk, R. H. (2001). Dicer functions in RNA interference and in synthesis of small RNA involved in developmental timing in C. elegans. Genes & development, 15(20), 2654–2659. https://doi.org/10.1101/gad.927801
34. Matranga, C., Tomari, Y., Shin, C., Bartel, D. P., & Zamore, P. D. (2005). Passenger-strand cleavage facilitates assembly of siRNA into Ago2-containing RNAi enzyme complexes. Cell, 123(4), 607–620. https://doi.org/10.1016/j.cell.2005.08.044
35. Chendrimada, T. P., Gregory, R. I., Kumaraswamy, E., Norman, J., Cooch, N., Nishikura, K., & Shiekhattar, R. (2005). TRBP recruits the Dicer complex to Ago2 for microRNA processing and gene silencing. Nature, 436(7051), 740–744. https://doi.org/10.1038/nature03868
36. O'Hara, L., & Smith, L. B. (2015). Androgen receptor roles in spermatogenesis and infertility. Best practice & research. Clinical endocrinology & metabolism, 29(4), 595–605. https://doi.org/10.1016/j.beem.2015.04.006
37. Smith, L. B., & Walker, W. H. (2014). The regulation of spermatogenesis by androgens. Seminars in cell & developmental biology, 30, 2–13. https://doi.org/10.1016/j.semcdb.2014.02.012
38. Ramaswamy, S., & Weinbauer, G. F. (2015). Endocrine control of spermatogenesis: Role of FSH and LH/ testosterone. Spermatogenesis, 4(2), e996025. https://doi.org/10.1080/21565562.2014.996025
39. Le Roy, C., Lejeune, H., Chuzel, F., Saez, J. M., & Langlois, D. (1999). Autocrine regulation of Leydig cell differentiated functions by insulin-like growth factor I and transforming growth factor beta. The Journal of steroid biochemistry and molecular biology, 69(1-6), 379–384.

https://doi.org/10.1016/s0960-0760(99)00075-8

40. Roser J. F. (2008). Regulation of testicular function in the stallion: an intricate network of endocrine, paracrine and autocrine systems. Animal reproduction science, 107(3-4), 179–196. https://doi.org/10.1016/j.anireprosci.2008.05.004

41. Lim, S., Luo, M., Koh, M., Yang, M., bin Abdul Kadir, M. N., Tan, J. H., Ye, Z., Wang, W., & Melamed, P. (2007). Distinct mechanisms involving diverse histone deacetylases repress expression of the two gonadotropin beta-subunit genes in immature gonadotropes, and their actions are overcome by gonadotropin-releasing hormone. Molecular and cellular biology, 27(11), 4105–4120. https://doi.org/10.1128/MCB.00248-07

42. Tsuchiya, M., Inoue, K., Matsuda, H., Nakamura, K., Mizutani, T., Miyamoto, K., & Minegishi, T. (2003). Expression of steroidogenic acute regulatory protein (StAR) and LH receptor in MA-10 cells. Life sciences, 73(22), 2855–2863. https://doi.org/10.1016/s0024-3205(03)00698-2

43. Washietl, S., Kellis, M., & Garber, M. (2014). Evolutionary dynamics and tissue specificity of human long noncoding RNAs in six mammals. Genome research, 24(4), 616–628. https://doi.org/10.1101/gr.165035.113

44. Sun, J., Lin, Y., & Wu, J. (2013). Long non-coding RNA expression profiling of mouse testis during postnatal development. PloS one, 8(10), e75750. https://doi.org/10.1371/journal.pone.0075750

45. Liang, M., Li, W., Tian, H., Hu, T., Wang, L., Lin, Y., Li, Y., Huang, H., & Sun, F. (2014). Sequential expression of long noncoding RNA as mRNA gene expression in specific stages of mouse spermatogenesis. Scientific reports, 4, 5966. https://doi.org/10.1038/srep05966

46. Zhao, Z., Qiao, L., Dai, Z., He, Q., Lan, X., Huang, S., & He, L. (2020). LncNONO-AS regulates AR expression by mediating NONO. Theriogenology, 145, 198–206. https://doi.org/10.1016/j.theriogenology.2019.10.025

47. Major, A. T., Hogarth, C. A., Young, J. C., Kurihara, Y., Jans, D. A., & Loveland, K. L. (2019). Dynamic paraspeckle component localisation during spermatogenesis. Reproduction (Cambridge,

England), 158(3), 267–280. https://doi.org/10.1530/REP-19-0139

48. Kurihara, M., Shiraishi, A., Satake, H., & Kimura, A. P. (2014). A conserved noncoding sequence can function as a spermatocyte-specific enhancer and a bidirectional promoter for a ubiquitously expressed gene and a testis-specific long noncoding RNA. Journal of molecular biology, 426(17), 3069–3093. https://doi.org/10.1016/j.jmb.2014.06.018
49. Yoneda, R., & Kimura, A. P. (2013). A testis-specific serine protease, Prss41/Tessp-1, is necessary for the progression of meiosis during murine in vitro spermatogenesis. Biochemical and biophysical research communications, 441(1), 120–125. https://doi.org/10.1016/j.bbrc.2013.10.028
50. Matsubara, S., Kurihara, M., & Kimura, A. P. (2014). A long non-coding RNA transcribed from conserved non-coding sequences contributes to the mouse prolyl oligopeptidase gene activation. Journal of biochemistry, 155(4), 243–256. https://doi.org/10.1093/jb/mvt113
51. Takei, N., Nakamura, T., Kawamura, S., Takada, Y., Satoh, Y., Kimura, A. P., & Kotani, T. (2018). High-Sensitivity and High-Resolution In Situ Hybridization of Coding and Long Non-coding RNAs in Vertebrate Ovaries and Testes. Biological procedures online, 20, 6. https://doi.org/10.1186/s12575-018-0071-z
52. Naito, Y., Hino, K., Bono, H., & Ui-Tei, K. (2015). CRISPRdirect: software for designing CRISPR/Cas guide RNA with reduced off-target sites. Bioinformatics (Oxford, England), 31(7), 1120–1123. https://doi.org/10.1093/bioinformatics/btu743
53. Hogan, B., Beddington, R., Costantini, F & Lacy, E. Manipulating the Mouse Embryo (A Laboratory Manual, 2nd ed. Plainview, NY: Cold Spring Harbor Laboratory Press, 1994)
54. Matsubara, S., Shiraishi, A., Osugi, T., Kawada, T., & Satake, H. (2019). The regulation of oocyte maturation and ovulation in the closest sister group of vertebrates. eLife, 8, e49062. https://doi.org/10.7554/eLife.49062
55. Wu, X., Wan, S., & Lee, M. M. (2007). Key factors in the regulation of fetal and postnatal Leydig cell development. Journal of cellular physiology, 213(2), 429–433.

https://doi.org/10.1002/jcp.21231

56. Seminara, S. B., Messager, S., Chatzidaki, E. E., Thresher, R. R., Acierno, J. S., Jr, Shagoury, J. K., Bo-Abbas, Y., Kuohung, W., Schwinof, K. M., Hendrick, A. G., Zahn, D., Dixon, J., Kaiser, U. B., Slaugenhaupt, S. A., Gusella, J. F., O'Rahilly, S., Carlton, M. B., Crowley, W. F., Jr, Aparicio, S. A., & Colledge, W. H. (2003). The GPR54 gene as a regulator of puberty. The New England journal of medicine, 349(17), 1614–1627. https://doi.org/10.1056/NEJMoa035322
57. Chen, H., Wang, Y., Ge, R., & Zirkin, B. R. (2017). Leydig cell stem cells: Identification, proliferation and differentiation. Molecular and cellular endocrinology, 445, 65–73. https://doi.org/10.1016/j.mce.2016.10.010
58. Potter, S. J., & DeFalco, T. (2017). Role of the testis interstitial compartment in spermatogonial stem cell function. Reproduction (Cambridge, England), 153(4), R151–R162. https://doi.org/10.1530/REP-16-0588
59. Shami, A. N., Zheng, X., Munyoki, S. K., Ma, Q., Manske, G. L., Green, C. D., Sukhwani, M., Orwig, K. E., Li, J. Z., & Hammoud, S. S. (2020). Single-Cell RNA Sequencing of Human, Macaque, and Mouse Testes Uncovers Conserved and Divergent Features of Mammalian Spermatogenesis. Developmental cell, 54(4), 529–547.e12. https://doi.org/10.1016/j.devcel.2020.05.010
60. Ivell, R., Wade, J. D., & Anand-Ivell, R. (2013). INSL3 as a biomarker of Leydig cell functionality. Biology of reproduction, 88(6), 147. https://doi.org/10.1095/biolreprod.113.108969
61. Strong, M. E., Burd, M. A., & Peterson, D. G. (2019). Evaluation of the MA-10 cell line as a model of insl3 regulation and Leydig cell function. Animal reproduction science, 208, 106116. https://doi.org/10.1016/j.anireprosci.2019.106116
62. Mather J. P. (1980). Establishment and characterization of two distinct mouse testicular epithelial cell lines. Biology of reproduction, 23(1), 243–252. https://doi.org/10.1095/biolreprod23.1.243
63. Ascoli M. (1981). Characterization of several clonal lines of cultured Leydig tumor cells: gonadotropin receptors and steroidogenic responses. Endocrinology, 108(1), 88–95.

https://doi.org/10.1210/endo-108-1-88

64. Chen, Y., Zheng, Y., Gao, Y., Lin, Z., Yang, S., Wang, T., Wang, Q., Xie, N., Hua, R., Liu, M., Sha, J., Griswold, M. D., Li, J., Tang, F., & Tong, M. H. (2018). Single-cell RNA-seq uncovers dynamic processes and critical regulators in mouse spermatogenesis. Cell research, 28(9), 879–896. https://doi.org/10.1038/s41422-018-0074-y

65. Anguera, M. C., Ma, W., Clift, D., Namekawa, S., Kelleher, R. J., 3rd, & Lee, J. T. (2011). Tsx produces a long noncoding RNA and has general functions in the germline, stem cells, and brain. PLoS genetics, 7(9), e1002248. https://doi.org/10.1371/journal.pgen.1002248

66. Wichman, L., Somasundaram, S., Breindel, C., Valerio, D. M., McCarrey, J. R., Hodges, C. A., & Khalil, A. M. (2017). Dynamic expression of long noncoding RNAs reveals their potential roles in spermatogenesis and fertility. Biology of reproduction, 97(2), 313–323. https://doi.org/10.1093/biolre/iox084

67. Li, C., Shen, C., Shang, X., Tang, L., Xiong, W., Ge, H., Zhang, H., Lu, S., Shen, Y., Wang, J., Fei, J., & Wang, Z. (2020). Two novel testis-specific long noncoding RNAs produced by 1700121C10Rik are dispensable for male fertility in mice. The Journal of reproduction and development, 66(1), 57–65. https://doi.org/10.1262/jrd.2019-104

68. Marchese, F. P., Raimondi, I., & Huarte, M. (2017). The multidimensional mechanisms of long noncoding RNA function. Genome biology, 18(1), 206. https://doi.org/10.1186/s13059-017-1348-2

69. Noh, J. H., Kim, K. M., McClusky, W. G., Abdelmohsen, K., & Gorospe, M. (2018). Cytoplasmic functions of long noncoding RNAs. Wiley interdisciplinary reviews. RNA, 9(3), e1471. https://doi.org/10.1002/wrna.1471

70. Hitachi, K., Nakatani, M., Takasaki, A., Ouchi, Y., Uezumi, A., Ageta, H., Inagaki, H., Kurahashi, H., & Tsuchida, K. (2019). Myogenin promoter-associated lncRNA Myoparr is essential for myogenic differentiation. EMBO reports, 20(3), e47468. https://doi.org/10.15252/embr.201847468

71. Gupta, R. A., Shah, N., Wang, K. C., Kim, J., Horlings, H. M., Wong, D. J., Tsai, M. C., Hung, T., Argani, P., Rinn, J. L., Wang, Y., Brzoska, P., Kong, B., Li, R., West, R. B., van de Vijver, M. J., Sukumar, S., & Chang, H. Y. (2010). Long non-coding RNA HOTAIR reprograms chromatin state to promote cancer metastasis. Nature, 464(7291), 1071–1076. https://doi.org/10.1038/nature08975

72. Wang, K. C., Yang, Y. W., Liu, B., Sanyal, A., Corces-Zimmerman, R., Chen, Y., Lajoie, B. R., Protacio, A., Flynn, R. A., Gupta, R. A., Wysocka, J., Lei, M., Dekker, J., Helms, J. A., & Chang, H. Y. (2011). A long noncoding RNA maintains active chromatin to coordinate homeotic gene expression. Nature, 472(7341), 120–124. https://doi.org/10.1038/nature09819

73. Gong, C., & Maquat, L. E. (2011). lncRNAs transactivate STAU1-mediated mRNA decay by duplexing with 3' UTRs via Alu elements. Nature, 470(7333), 284–288. https://doi.org/10.1038/nature09701

74. Lee, S., Kopp, F., Chang, T. C., Sataluri, A., Chen, B., Sivakumar, S., Yu, H., Xie, Y., & Mendell, J. T. (2016). Noncoding RNA NORAD Regulates Genomic Stability by Sequestering PUMILIO Proteins. Cell, 164(1-2), 69–80. https://doi.org/10.1016/j.cell.2015.12.017

75. Carrieri, C., Cimatti, L., Biagioli, M., Beugnet, A., Zucchelli, S., Fedele, S., Pesce, E., Ferrer, I., Collavin, L., Santoro, C., Forrest, A. R., Carninci, P., Biffo, S., Stupka, E., & Gustincich, S. (2012). Long non-coding antisense RNA controls Uchl1 translation through an embedded SINEB2 repeat. Nature, 491(7424), 454–457. https://doi.org/10.1038/nature11508

76. Kallen, A. N., Zhou, X. B., Xu, J., Qiao, C., Ma, J., Yan, L., Lu, L., Liu, C., Yi, J. S., Zhang, H., Min, W., Bennett, A. M., Gregory, R. I., Ding, Y., & Huang, Y. (2013). The imprinted H19 lncRNA antagonizes let-7 microRNAs. Molecular cell, 52(1), 101–112. https://doi.org/10.1016/j.molcel.2013.08.027

77. Liu, A. N., Qu, H. J., Gong, W. J., Xiang, J. Y., Yang, M. M., & Zhang, W. (2019). LncRNA AWPPH and miRNA-21 regulates cancer cell proliferation and chemosensitivity in triple-negative breast cancer by interacting with each other. Journal of cellular biochemistry, 120(9),

14860–14866. https://doi.org/10.1002/jcb.28747

78. Ye, Z. M., Yang, S., Xia, Y. P., Hu, R. T., Chen, S., Li, B. W., Chen, S. L., Luo, X. Y., Mao, L., Li, Y., Jin, H., Qin, C., & Hu, B. (2019). LncRNA MIAT sponges miR-149-5p to inhibit efferocytosis in advanced atherosclerosis through CD47 upregulation. Cell death & disease, 10(2), 138. https://doi.org/10.1038/s41419-019-1409-4
79. ROOSEN-RUNGE, E. C., & ANDERSON, D. (1959). The development of the interstitial cells in the testis of the albino rat. Acta anatomica, 37, 125–137. https://doi.org/10.1159/000141460
80. Shima Y. (2019). Development of fetal and adult Leydig cells. Reproductive medicine and biology, 18(4), 323–330. https://doi.org/10.1002/rmb2.12287
81. Yokoyama, C., Chigi, Y., Baba, T., Ohshitanai, A., Harada, Y., Takahashi, F., & Morohashi, K. I. (2019). Three populations of adult Leydig cells in mouse testes revealed by a novel mouse HSD3B1-specific rat monoclonal antibody. Biochemical and biophysical research communications, 511(4), 916–920. https://doi.org/10.1016/j.bbrc.2019.02.100
82. Vergouwen, R. P., Jacobs, S. G., Huiskamp, R., Davids, J. A., & de Rooij, D. G. (1991). Proliferative activity of gonocytes, Sertoli cells and interstitial cells during testicular development in mice. Journal of reproduction and fertility, 93(1), 233–243. https://doi.org/10.1530/jrf.0.0930233
83. Habert, R., Lejeune, H., & Saez, J. M. (2001). Origin, differentiation and regulation of fetal and adult Leydig cells. Molecular and cellular endocrinology, 179(1-2), 47–74. https://doi.org/10.1016/s0303-7207(01)00461-0
84. Kumar, R. C., & Thakur, M. K. (2004). Androgen receptor mRNA is inversely regulated by testosterone and estradiol in adult mouse brain. Neurobiology of aging, 25(7), 925–933. https://doi.org/10.1016/j.neurobiolaging.2003.10.011
85. O'Hara, L., McInnes, K., Simitsidellis, I., Morgan, S., Atanassova, N., Slowikowska-Hilczer, J., Kula, K., Szarras-Czapnik, M., Milne, L., Mitchell, R. T., & Smith, L. B. (2015). Autocrine androgen action is essential for Leydig cell maturation and function, and protects against late-

onset Leydig cell apoptosis in both mice and men. FASEB journal : official publication of the Federation of American Societies for Experimental Biology, 29(3), 894–910. https://doi.org/10.1096/fj.14-255729

86. Hu, K., Li, L., Liao, Y., & Liang, M. (2018). LncRNA Gm2044 highly expresses in spermatocyte and inhibits Utf1 translation by interacting with Utf1 mRNA. Genes & genomics, 40(7), 781–787. https://doi.org/10.1007/s13258-018-0690-4
87. Gao, Y., Li, S., Lai, Z., Zhou, Z., Wu, F., Huang, Y., Lan, X., Lei, C., Chen, H., & Dang, R. (2019). Analysis of Long Non-Coding RNA and mRNA Expression Profiling in Immature and Mature Bovine (Bos taurus) Testes. Frontiers in genetics, 10, 646. https://doi.org/10.3389/fgene.2019.00646
88. Yang, H., Wang, F., Li, F., Ren, C., Pang, J., Wan, Y., Wang, Z., Feng, X., & Zhang, Y. (2018). Comprehensive analysis of long noncoding RNA and mRNA expression patterns in sheep testicular maturation. Biology of reproduction, 99(3), 650–661. https://doi.org/10.1093/biolre/ioy088
89. Potter, S. J., & DeFalco, T. (2017). Role of the testis interstitial compartment in spermatogonial stem cell function. Reproduction, 153(4), R151–R162. https://doi.org/10.1530/REP-16-0588
90. Shami, A. N., Zheng, X., Munyoki, S. K., Ma, Q., Manske, G. L., Green, C. D., Sukhwani, M., Orwig, K. E., Li, J. Z., & Hammoud, S. S. (2020). Single-Cell RNA Sequencing of Human, Macaque, and Mouse Testes Uncovers Conserved and Divergent Features of Mammalian Spermatogenesis. Developmental cell, 54(4), 529–547.e12. https://doi.org/10.1016/j.devcel.2020.05.010
91. Panni, S., Lovering, R. C., Porras, P., & Orchard, S. (2020). Non-coding RNA regulatory networks. Biochimica et biophysica acta. Gene regulatory mechanisms, 1863(6), 194417. https://doi.org/10.1016/j.bbagrm.2019.194417
92. Salmena, L., Poliseno, L., Tay, Y., Kats, L., & Pandolfi, P. P. (2011). A ceRNA hypothesis: the Rosetta Stone of a hidden RNA language?. Cell, 146(3), 353–358.

https://doi.org/10.1016/j.cell.2011.07.014

93. Tay, Y., Rinn, J., & Pandolfi, P. P. (2014). The multilayered complexity of ceRNA crosstalk and competition. Nature, 505(7483), 344–352. https://doi.org/10.1038/nature12986

94. Ransohoff, J. D., Wei, Y., & Khavari, P. A. (2018). The functions and unique features of long intergenic non-coding RNA. Nature reviews. Molecular cell biology, 19(3), 143–157. https://doi.org/10.1038/nrm.2017.104

95. Hoivik, E. A., Lewis, A. E., Aumo, L., & Bakke, M. (2010). Molecular aspects of steroidogenic factor 1 (SF-1). Molecular and cellular endocrinology, 315(1-2), 27–39. https://doi.org/10.1016/j.mce.2009.07.003

96. Chang, T. H., Huang, H. Y., Hsu, J. B., Weng, S. L., Horng, J. T., & Huang, H. D. (2013). An enhanced computational platform for investigating the roles of regulatory RNA and for identifying functional RNA motifs. BMC bioinformatics, 14 Suppl 2(Suppl 2), S4. https://doi.org/10.1186/1471-2105-14-S2-S4

97. Abdollahzadeh, R., Daraei, A., Mansoori, Y., Sepahvand, M., Amoli, M. M., & Tavakkoly-Bazzaz, J. (2019). Competing endogenous RNA (ceRNA) cross talk and language in ceRNA regulatory networks: A new look at hallmarks of breast cancer. Journal of cellular physiology, 234(7), 10080–10100. https://doi.org/10.1002/jcp.27941

98. Quan, X., Zhao, M., Yang, X., Zhu, Y., & Tian, X. (2019). AP2γ mediated downregulation of lncRNA LINC00511 as a ceRNA suppresses trophoblast invasion by regulating miR-29b-3p/Cyr61 axis. Biomedicine & pharmacotherapy = Biomedecine & pharmacotherapie, 120, 109269. https://doi.org/10.1016/j.biopha.2019.109269

99. Xu, J., Feng, L., Han, Z., Li, Y., Wu, A., Shao, T., Ding, N., Li, L., Deng, W., Di, X., Wang, J., Zhang, L., Li, X., Zhang, K., & Cheng, S. (2016). Extensive ceRNA-ceRNA interaction networks mediated by miRNAs regulate development in multiple rhesus tissues. Nucleic acids research, 44(19), 9438–9451. https://doi.org/10.1093/nar/gkw587

100. Wang, H., Huo, X., Yang, X. R., He, J., Cheng, L., Wang, N., Deng, X., Jin, H., Wang, N., Wang,

C., Zhao, F., Fang, J., Yao, M., Fan, J., & Qin, W. (2017). STAT3-mediated upregulation of lncRNA HOXD-AS1 as a ceRNA facilitates liver cancer metastasis by regulating SOX4. Molecular cancer, 16(1), 136. https://doi.org/10.1186/s12943-017-0680-1

101. Yang, X. Z., Cheng, T. T., He, Q. J., Lei, Z. Y., Chi, J., Tang, Z., Liao, Q. X., Zhang, H., Zeng, L. S., & Cui, S. Z. (2018). LINC01133 as ceRNA inhibits gastric cancer progression by sponging miR-106a-3p to regulate APC expression and the Wnt/β-catenin pathway. Molecular cancer, 17(1), 126. https://doi.org/10.1186/s12943-018-0874-1
102. E, Q., Wang, C., Gu, X., Gan, X., Zhang, X., Wang, S., Ma, J., Zhang, L., Zhang, R., & Su, L. (2020). Competitive endogenous RNA (ceRNA) regulation network of lncRNA-miRNA-mRNA during the process of the nickel-induced steroidogenesis disturbance in rat Leydig cells. Toxicology in vitro : an international journal published in association with BIBRA, 63, 104721. https://doi.org/10.1016/j.tiv.2019.104721
103. Meng, X., Peng, H., Ding, Y., Zhang, L., Yang, J., & Han, X. (2019). A transcriptomic regulatory network among miRNAs, piRNAs, circRNAs, lncRNAs and mRNAs regulates microcystin-leucine arginine (MC-LR)-induced male reproductive toxicity. The Science of the total environment, 667, 563–577. https://doi.org/10.1016/j.scitotenv.2019.02.393
104. Hu, Z., Shen, W. J., Cortez, Y., Tang, X., Liu, L. F., Kraemer, F. B., & Azhar, S. (2013). Hormonal regulation of microRNA expression in steroid producing cells of the ovary, testis and adrenal gland. PloS one, 8(10), e78040. https://doi.org/10.1371/journal.pone.0078040
105. Hu, Z., Shen, W. J., Kraemer, F. B., & Azhar, S. (2012). MicroRNAs 125a and 455 repress lipoprotein-supported steroidogenesis by targeting scavenger receptor class B type I in steroidogenic cells. Molecular and cellular biology, 32(24), 5035–5045. https://doi.org/10.1128/MCB.01002-12
106. Men, Y., Fan, Y., Shen, Y., Lu, L., & Kallen, A. N. (2017). The Steroidogenic Acute Regulatory Protein (StAR) Is Regulated by the H19/let-7 Axis. Endocrinology, 158(2), 402–409. https://doi.org/10.1210/en.2016-1340

107. Yuan, W., Liang, L., Huang, K., Deng, Y., Dong, M., Wang, G., & Zou, F. (2020). MiR-122-5p and miR-326-3p promote cadmium-induced NRK-52E cell apoptosis by downregulating PLD1. Environmental toxicology, 35(12), 1334–1342. https://doi.org/10.1002/tox.22998

108. Lian, Z., Lv, F. F., Yu, J., & Wang, J. W. (2018). The anti-inflammatory effect of microRNA-383-3p interacting with IL1R2 against homocysteine-induced endothelial injury in rat coronary arteries. Journal of cellular biochemistry, 119(8), 6684–6694. https://doi.org/10.1002/jcb.26854

109. Gao, C., Lu, W., Lou, W., Wang, L., & Xu, Q. (2019). Long noncoding RNA HOXC13-AS positively affects cell proliferation and invasion in nasopharyngeal carcinoma via modulating miR-383-3p/HMGA2 axis. Journal of cellular physiology, 234(8), 12809–12820. https://doi.org/10.1002/jcp.27915

110. Li, Z., Han, L., Liang, Q., & Huang, Z. (2020). Long noncoding RNA MEG3 contributes to dysfunction of brain microvascular endothelial cells after intracerebral hemorrhage by regulating the miR-1930-5p/Mllt1 axis. Brain research bulletin, 166, 1–11. Advance online publication. https://doi.org/10.1016/j.brainresbull.2020.10.002

111. Shima, J. E., McLean, D. J., McCarrey, J. R., & Griswold, M. D. (2004). The murine testicular transcriptome: characterizing gene expression in the testis during the progression of spermatogenesis. Biology of reproduction, 71(1), 319–330. https://doi.org/10.1095/biolreprod.103.026880 PMID: 15028632

112. Sin, H. S., Kartashov, A. V., Hasegawa, K., Barski, A., & Namekawa, S. H. (2015). Poised chromatin and bivalent domains facilitate the mitosis-to-meiosis transition in the male germline. BMC biology, 13, 53. https://doi.org/10.1186/s12915-015-0159-8 PMID:26198001

113. Local, A., Huang, H., Albuquerque, C. P., Singh, N., Lee, A. Y., Wang, W., Wang, C., Hsia, J. E., Shiau, A. K., Ge, K., Corbett, K. D., Wang, D., Zhou, H., & Ren, B. (2018). Identification of H3K4me1-associated proteins at mammalian enhancers. Nature genetics, 50(1), 73–82. https://doi.org/10.1038/s41588-017-0015-6

114. Zhang, B., Zheng, H., Huang, B., Li, W., Xiang, Y., Peng, X., Ming, J., Wu, X., Zhang, Y., Xu, Q.,

Liu, W., Kou, X., Zhao, Y., He, W., Li, C., Chen, B., Li, Y., Wang, Q., Ma, J., Yin, Q., Xie, W. (2016). Allelic reprogramming of the histone modification H3K4me3 in early mammalian development. Nature, 537(7621), 553–557. https://doi.org/10.1038/nature19361

115. Liu, Y., Zhang, Y., Yin, J., Gao, Y., Li, Y., Bai, D., He, W., Li, X., Zhang, P., Li, R., Zhang, L., Jia, Y., Zhang, Y., Lin, J., Zheng, Y., Wang, H., Gao, S., Zeng, W., & Liu, W. (2019). Distinct H3K9me3 and DNA methylation modifications during mouse spermatogenesis. The Journal of biological chemistry, 294(49), 18714–18725. https://doi.org/10.1074/jbc.RA119.010496
116. Creyghton, M. P., Cheng, A. W., Welstead, G. G., Kooistra, T., Carey, B. W., Steine, E. J., Hanna, J., Lodato, M. A., Frampton, G. M., Sharp, P. A., Boyer, L. A., Young, R. A., & Jaenisch, R. (2010). Histone H3K27ac separates active from poised enhancers and predicts developmental state. Proceedings of the National Academy of Sciences of the United States of America, 107(50), 21931–21936. https://doi.org/10.1073/pnas.1016071107
117. Rada-Iglesias, A., Bajpai, R., Swigut, T., Brugmann, S. A., Flynn, R. A., & Wysocka, J. (2011). A unique chromatin signature uncovers early developmental enhancers in humans. Nature, 470(7333), 279–283. https://doi.org/10.1038/nature09692
118. Fox, S., Myers, J. A., Davidson, C., Getman, M., Kingsley, P. D., Frankiewicz, N., & Bulger, M. (2020). Hyperacetylated chromatin domains mark cell type-specific genes and suggest distinct modes of enhancer function. Nature communications, 11(1), 4544. https://doi.org/10.1038/s41467-020-18303-0
119. Dao, L., Galindo-Albarrán, A. O., Castro-Mondragon, J. A., Andrieu-Soler, C., Medina-Rivera, A., Souaid, C., Charbonnier, G., Griffon, A., Vanhille, L., Stephen, T., Alomairi, J., Martin, D., Torres, M., Fernandez, N., Soler, E., van Helden, J., Puthier, D., & Spicuglia, S. (2017). Genome-wide characterization of mammalian promoters with distal enhancer functions. Nature genetics, 49(7), 1073–1081. https://doi.org/10.1038/ng.3884
120. Maezawa, S., Sakashita, A., Yukawa, M., Chen, X., Takahashi, K., Alavattam, K. G., Nakata, I., Weirauch, M. T., Barski, A., & Namekawa, S. H. (2020). Super-enhancer switching drives a burst

in gene expression at the mitosis-to-meiosis transition. Nature structural & molecular biology, 27(10), 978–988. https://doi.org/10.1038/s41594-020-0488-3

121. Liu F. (2017). Enhancer-derived RNA: A Primer. Genomics, proteomics & bioinformatics, 15(3), 196–200. https://doi.org/10.1016/j.gpb.2016.12.006

122. Rothschild, G., & Basu, U. (2017). Lingering Questions about Enhancer RNA and Enhancer Transcription-Coupled Genomic Instability. Trends in genetics : TIG, 33(2), 143–154. https://doi.org/10.1016/j.tig.2016.12.002

123. Sakatani, S., Takahashi, R., Okuda, Y., Aizawa, A., Otsuka, A., Komatsu, A., & Ono, M. (2000). Structure, expression, and conserved physical linkage of mouse testicular cell adhesion molecule-1 (TCAM-1) gene. Genome, 43(6), 957–962. https://doi.org/10.1139/g00-071

124. Gautier, A., Goupil, A. S., Le Gac, F., & Lareyre, J. J. (2013). A promoter fragment of the sycp1 gene is sufficient to drive transgene expression in male and female meiotic germ cells in zebrafish. Biology of reproduction, 89(4), 89. https://doi.org/10.1095/biolreprod.113.107706

125. Ntini, E., & Marsico, A. (2019). Functional impacts of non-coding RNA processing on enhancer activity and target gene expression. Journal of molecular cell biology, 11(10), 868–879. https://doi.org/10.1093/jmcb/mjz047

126. Ørom, U. A., Derrien, T., Beringer, M., Gumireddy, K., Gardini, A., Bussotti, G., Lai, F., Zytnicki, M., Notredame, C., Huang, Q., Guigo, R., & Shiekhattar, R. (2010). Long noncoding RNAs with enhancer-like function in human cells. Cell, 143(1), 46–58. https://doi.org/10.1016/j.cell.2010.09.001

127. Fu, Z., Chen, C., Zhou, Q., Wang, Y., Zhao, Y., Zhao, X., Li, W., Zheng, S., Ye, H., Wang, L., He, Z., Lin, Q., Li, Z., & Chen, R. (2017). LncRNA HOTTIP modulates cancer stem cell properties in human pancreatic cancer by regulating HOXA9. Cancer letters, 410, 68–81. https://doi.org/10.1016/j.canlet.2017.09.019

128. Li, W., Notani, D., Ma, Q., Tanasa, B., Nunez, E., Chen, A. Y., Merkurjev, D., Zhang, J., Ohgi, K., Song, X., Oh, S., Kim, H. S., Glass, C. K., & Rosenfeld, M. G. (2013). Functional roles of

enhancer RNAs for oestrogen-dependent transcriptional activation. Nature, 498(7455), 516–520. https://doi.org/10.1038/nature12210

129. Shlyueva, D., Stampfel, G., & Stark, A. (2014). Transcriptional enhancers: from properties to genome-wide predictions. Nature reviews. Genetics, 15(4), 272–286. https://doi.org/10.1038/nrg3682

130. Heinz, S., Romanoski, C. E., Benner, C., & Glass, C. K. (2015). The selection and function of cell type-specific enhancers. Nature reviews. Molecular cell biology, 16(3), 144–154. https://doi.org/10.1038/nrm3949

131. Urekar, C., Acharya, K. K., Chhabra, P., & Reddi, P. P. (2019). A 50-bp enhancer of the mouse acrosomal vesicle protein 1 gene activates round spermatid-specific transcription in vivo†. Biology of reproduction, 101(4), 842–853. https://doi.org/10.1093/biolre/ioz115

132. Melo, C. A., Drost, J., Wijchers, P. J., van de Werken, H., de Wit, E., Oude Vrielink, J. A., Elkon, R., Melo, S. A., Léveillé, N., Kalluri, R., de Laat, W., & Agami, R. (2013). eRNAs are required for p53-dependent enhancer activity and gene transcription. Molecular cell, 49(3), 524–535. https://doi.org/10.1016/j.molcel.2012.11.021

133. Cichewicz, M. A., Kiran, M., Przanowska, R. K., Sobierajska, E., Shibata, Y., & Dutta, A. (2018). MUNC, an Enhancer RNA Upstream from the MYOD Gene, Induces a Subgroup of Myogenic Transcripts in trans Independently of MyoD. Molecular and cellular biology, 38(20), e00655-17. https://doi.org/10.1128/MCB.00655-17

134. Zhao, Y., Zhou, J., He, L., Li, Y., Yuan, J., Sun, K., Chen, X., Bao, X., Esteban, M. A., Sun, H., & Wang, H. (2019). MyoD induced enhancer RNA interacts with hnRNPL to activate target gene transcription during myogenic differentiation. Nature communications, 10(1), 5787. https://doi.org/10.1038/s41467-019-13598-0

135. Pnueli, L., Rudnizky, S., Yosefzon, Y., & Melamed, P. (2015). RNA transcribed from a distal enhancer is required for activating the chromatin at the promoter of the gonadotropin α-subunit gene. Proceedings of the National Academy of Sciences of the United States of America, 112(14),

4369–4374. https://doi.org/10.1073/pnas.1414841112

136. Pfeifer, K., Leighton, P. A., & Tilghman, S. M. (1996). The structural H19 gene is required for transgene imprinting. Proceedings of the National Academy of Sciences of the United States of America, 93(24), 13876–13883. https://doi.org/10.1073/pnas.93.24.13876

137. Li, Y., Gu, J., & Lu, H. (2017). The GAS5/miR-222 Axis Regulates Proliferation of Gastric Cancer Cells Through the PTEN/Akt/mTOR Pathway. Digestive diseases and sciences, 62(12), 3426–3437. https://doi.org/10.1007/s10620-017-4831-4

138. Smith, C. M., & Steitz, J. A. (1998). Classification of gas5 as a multi-small-nucleolar-RNA (snoRNA) host gene and a member of the 5'-terminal oligopyrimidine gene family reveals common features of snoRNA host genes. Molecular and cellular biology, 18(12), 6897–6909. https://doi.org/10.1128/mcb.18.12.6897

139. Kino, T., Hurt, D. E., Ichijo, T., Nader, N., & Chrousos, G. P. (2010). Noncoding RNA gas5 is a growth arrest- and starvation-associated repressor of the glucocorticoid receptor. Science signaling, 3(107), ra8. https://doi.org/10.1126/scisignal.2000568

140. Sun, D., Yu, Z., Fang, X., Liu, M., Pu, Y., Shao, Q., Wang, D., Zhao, X., Huang, A., Xiang, Z., Zhao, C., Franklin, R. J., Cao, L., & He, C. (2017). LncRNA GAS5 inhibits microglial M2 polarization and exacerbates demyelination. EMBO reports, 18(10), 1801–1816. https://doi.org/10.15252/embr.201643668

141. Tan, K., Song, H. W., & Wilkinson, M. F. (2020). Single-cell RNAseq analysis of testicular germ and somatic cell development during the perinatal period. Development (Cambridge, England), 147(3), dev183251. https://doi.org/10.1242/dev.183251

142. Shami, A. N., Zheng, X., Munyoki, S. K., Ma, Q., Manske, G. L., Green, C. D., Sukhwani, M., Orwig, K. E., Li, J. Z., & Hammoud, S. S. (2020). Single-Cell RNA Sequencing of Human, Macaque, and Mouse Testes Uncovers Conserved and Divergent Features of Mammalian Spermatogenesis. Developmental cell, 54(4), 529–547.e12. https://doi.org/10.1016/j.devcel.2020.05.010